

A low-angle photograph of a forest with snow-covered trees against a clear blue sky. The trees are covered in a thick layer of snow, and the sky is a vibrant blue. The perspective is looking up from the forest floor, creating a sense of height and depth.

# Descriptor variables of the root zone storage capacity in Canada

Leon van Voorst



# Descriptor variables of the root zone storage capacity in Canada

by

Leon van Voorst

to obtain the degree of Master of Science  
at the Delft University of Technology,  
to be defended publicly on Friday July 10, 2020 at 11:00 AM.

Student number: 4373936  
Project duration: September 1, 2019 – July 10, 2020  
Thesis committee: Dr. M. Hrachowitz, TU Delft, chair  
Dr. ir. R.J. van der Ent, TU Delft  
Dr. ir. O. Morales Napoles, TU Delft

An electronic version of this thesis is available at <http://repository.tudelft.nl/>.

Picture cover page: BeWilder (2014)



# Preface

This thesis on the descriptor variables of the root zone storage capacity in Canada concludes my 6 year lasting journey on the TU Delft, which has been an incredible experience. Here, I would like to take the opportunity to thank everybody who was part of and contributed to this important phase of my life.

Choosing has always been a major difficulty in my life, which particularly complicated study selection right after high school graduation. Although being a tough decision, I have never regretted my choice for Civil Engineering. Not only did I learn how to contribute to society using technology, but it also made me meet a lot of amazing people whom I share great memories with.

I met some of these people on day one of my student life during the COW introduction weekend and we have been friends ever since. I enjoyed sitting together during lectures and working together in many projects, but I particularly appreciate all the memories we share outside university: the countless times we cooked the most delicious wraps, the trips to Groningen and Utrecht and the holidays to Berlin and Seville. Thank you guys for these amazing memories and I hope to keep making these memories together in the future.

Besides, what partly started as an initial project group during the first year of my Bachelor eventually evolved into a very strong group of friends, whom I have shared many great experiences with. Not only did we help each other with exercises, I also enjoyed the fun we had outside university. I know I was not always there, but hereby I promise to be present as often as possible in the future and I look forward to join during the young but amazing tradition in the last weekend of August and potentially start a new tradition on ski's and snowboards. Thank you guys for the great times and experiences during the last few years and good luck with the home stretch of your time on the TU Delft.

The choice of Master after three years of Bachelor was again not an easy decision. Eventually I decided to choose the Water Management track, combined with several Hydraulic Engineering courses. Again, this choice turned out well, as I enjoyed a large majority of the courses I took during my Master and additionally made new friends from all over the world, who made studying a lot more pleasant.

After two years of courses and an internship it was finally time to start working towards an end and begin with my Master thesis. Ironically, the choice for a thesis topic was one of the easiest decisions I have made during my student life. Main reason for this is the infectious enthusiasm with which Markus talked about hydrology during the course Hydrological Modelling and several exploratory talks on potential thesis topics. This way I got lured into a 10-months during journey exploring the root zone of Canada, which eventually resulted in this thesis. I am very grateful to Markus, Ruud and Oswaldo for their consistent help and input during the process of thesis writing and their inspiring enthusiasm.

Furthermore, I would like to thank 'het hokje' for being a large source of motivation during the thesis process. Without the coffee breaks, card games, table tennis sessions, friday afternoon drinks and Skype calls my last year as student would have been a lot duller. I look forward to see you guys graduate too.

Lastly, I owe a big thank you to my family who have been very supportive throughout the thesis writing process and were a great source of motivation during my life at university.

Now here I am, finished with my Master and therefore on the verge of a new choice in my life. At this moment I am not sure yet what the future will bring, but I am well prepared due to what I have learned on the TU Delft. And if university has taught me one thing it is that it does not matter what choices you make, as long as you share your experiences with amazing people. Enjoy reading.

*Leon van Voorst  
Delft, July 2020*



# Summary

The root zone storage capacity is a critical determinant in hydrology, playing a major role in the partitioning of precipitation into evaporation and runoff. Besides, it is an important parameter in climatological and hydrological models. Understanding of the root zone storage capacity and its major determining processes is therefore fundamental in environmental sciences. Several studies have investigated root zone storage capacity magnitude and its descriptor variables, but mainly in snow absent regions. Computation and analysis of root zone storage capacities in snow dominant regions is therefore underexposed. The studies that do consider snow dynamics are limited to a small number of catchments or a region with few spatial variation and therefore narrow spread in climate, topography and land-use parameters. This may complicate visualisation of the relationship of some potential descriptors with the root zone storage capacity. As such, additional understanding of the major descriptor variables of the root zone storage capacity in boreal regions with large spatial variation and in particular the influence of snow on the root zone storage capacity is desired.

The aim of this study is therefore to quantify catchment average root zone storage capacities, identify its main descriptor variables and their regional variability and determine the influence of snow on root zone storage capacities in a boreal region. To achieve this, an area with large variety in climate and landscape is required, with additional variation in snow dynamics. Due to its large spatial extent, Canada matches these requirements and is therefore used as study area.

Catchment average root zone storage capacities were computed for 230 Canadian catchments using a simple water balance approach with additional snow module and were found to be normally distributed with mean magnitude of 183 mm and a standard deviation of 70 mm. Individual correlation of climate, discharge and landscape variables showed most relevant relationship between root zone storage capacities and yearly potential evaporation, runoff coefficient and seasonality index, although with considerable variance.

Subsequent investigation on the mutual effect of several variables showed that the aridity index, runoff coefficient and seasonality timing index are major descriptor variables of the root zone storage capacity, by how they indicate the allocation of water for transpiration in a catchment and describe the degree of synchronisation between liquid input and atmospheric water demand. The earlier derived individual descriptors of the root zone storage capacity are encapsulated in these three main descriptor variables. Application of a multiple linear regression model using the aridity index, runoff coefficient and seasonality timing index showed these variables can be used to predict root zone storage capacities in Canada with an  $R^2$  of 0.72. Subsequent tests of the predictive capability of this model in distinct boreal region Finland resulted in an  $R^2$  of 0.62.

The influence of snow on the root zone storage capacity in Canada was identified by comparing its magnitude computed with and without a snow module. This analysis showed that whenever significantly present, snow effects lead to a decrease in root zone storage capacity magnitude, caused by increased overlap between liquid input and transpiration output in a catchment. These effects are encapsulated by the seasonality timing index.

To determine the regional variability of root zone storage capacity descriptors in Canada, catchments were clustered based on similar functioning. The results indicated that different variables have an effect on the root zone storage capacity in different functionally comparable regions and that a large part of the functional behaviour of the clusters can be explained by the geographical location of their catchments. The influence of these regionally dependent variables on the root zone storage capacity is encapsulated in the earlier defined main descriptor variables aridity index, runoff coefficient and seasonality timing index.



# Contents

List of Symbols	viii
List of Figures	xi
List of Tables	xiii
1 Introduction	1
1.1 Problem statement . . . . .	2
1.2 Research objective . . . . .	2
1.3 Relevance . . . . .	3
2 Methodology	5
2.1 Study area. . . . .	5
2.2 Data sources and correction . . . . .	6
2.2.1 Hydrometric data . . . . .	6
2.2.2 Meteorological data . . . . .	7
2.2.3 Snow cover data . . . . .	9
2.2.4 Elevation data . . . . .	10
2.2.5 Land cover data . . . . .	10
2.2.6 Catchment selection . . . . .	10
2.3 Approach for root zone storage capacity computation . . . . .	11
2.3.1 Snow module . . . . .	12
2.3.2 Effective precipitation . . . . .	14
2.3.3 Transpiration . . . . .	15
2.3.4 Storage Deficits . . . . .	15
2.3.5 Catchment selection . . . . .	16
2.4 Descriptor variables. . . . .	16
2.4.1 Climate variables . . . . .	16
2.4.2 Landscape variables . . . . .	18
2.4.3 Discharge variables . . . . .	19
2.4.4 Runoff coefficient or evaporative index . . . . .	19
2.5 Assessment strategies. . . . .	19
2.5.1 Individual relationships . . . . .	19
2.5.2 Combined relationships . . . . .	19
2.5.3 Snow influence. . . . .	20
2.5.4 Regional variability of descriptor variables. . . . .	21
3 Results	23
3.1 Root zone storage capacity magnitudes. . . . .	23
3.2 Individual effects of descriptor variables . . . . .	24
3.2.1 Climate variables . . . . .	24
3.2.2 Runoff coefficient . . . . .	26
3.2.3 Landscape variables . . . . .	26
3.2.4 Discharge variables . . . . .	28
3.3 Combined effects of descriptor variables . . . . .	29
3.3.1 Budyko framework. . . . .	29
3.3.2 Seasonality and timing effects . . . . .	31
3.3.3 Multiple linear regression . . . . .	32
3.4 Influence of snow on root zone storage capacity . . . . .	36
3.5 Regional variability of descriptor variables . . . . .	39

4	Discussion	43
4.1	Study area	43
4.2	Data	44
4.3	Approach	45
4.3.1	Uncertainties in transpiration estimate	46
4.3.2	Static root zone	46
4.3.3	Alternative water sources for vegetation	47
4.3.4	Direct infiltration estimate	47
4.3.5	Choice of return period	47
4.3.6	Choice of maximum interception capacity	48
4.3.7	Snow module assumptions	49
4.3.8	Other methods that describe correlation	49
4.3.9	Model bias	49
4.4	Wider application	50
5	Conclusion	51
	References	53
A	Land cover distribution in classes	57
B	Calibration and validation overview	59
C	Overview of descriptor variables	69
C.1	Climate variables	69
C.2	Landscape variables	70
C.3	Discharge variables	71
D	Python code	73
E	Overview root zone storage capacities	75
F	Correlation of all test variables and $S_r$	77
F.1	Climate variables	77
F.2	Landscape variables	81
F.3	Discharge variables	82
G	Feature selection parameter set	85
H	Snow influence on change in $S_r$	87

# List of Symbols

## Symbols

A	Area	[L <sup>2</sup> ]
CE	Catch efficiency	[-]
$E_a$	Actual evaporation	[LT <sup>-1</sup> ]
$E_i$	Interception evaporation	[LT <sup>-1</sup> ]
$E_p$	Potential evaporation	[LT <sup>-1</sup> ]
$E_t$	Transpiration	[LT <sup>-1</sup> ]
H	Elevation	[L]
$I_{max}$	Maximum interception capacity	[L]
LR	Lapse rate	[ $\Theta$ L <sup>-1</sup> ]
P	Precipitation/Liquid input	[LT <sup>-1</sup> ]
$P_e$	Effective precipitation	[LT <sup>-1</sup> ]
$P_l$	Liquid precipitation	[LT <sup>-1</sup> ]
$P_{liq}$	Total liquid input	[LT <sup>-1</sup> ]
$P_s$	Solid precipitation	[LT <sup>-1</sup> ]
Q	Discharge	[LT <sup>-1</sup> ]
$Q_m$	Snow melt	[LT <sup>-1</sup> ]
$R_e$	Top of atmosphere radiation	[MT <sup>-3</sup> ]
SD	Storage deficit	[L]
$S_i$	Interception storage	[L]
$S_r$	Root zone storage capacity	[L]
$S_s$	Snow storage	[L]
$T_a$	Air temperature	[ $\Theta$ ]
$T_{av}$	Average temperature	[ $\Theta$ ]
$T_{max}$	Maximum temperature	[ $\Theta$ ]
$T_{min}$	Minimum temperature	[ $\Theta$ ]
U	Wind speed	[LT <sup>-1</sup> ]
$\lambda$	Latent heat of evaporation	[ML <sup>2</sup> T <sup>-2</sup> ]

## Abbreviations

CANOPEX	Canadian Model Parameter Experiment	
DEM	Digital elevation model	
HBV	Hydrologiska Byrans Vattenbalansavdelning	
HYDAT	Hydrometric data portal from Environment Canada	
MCT	Mass Curve Technique	
MF	Melt factor/Degree day factor	[L $\Theta^{-1}$ T <sup>-1</sup> ]
$M_n$	Model without snow	
$M_s$	Snow model	
NDSI	Normalised difference snow index	[-]
NRCan	Natural Resources Canada	
PCA	Principal component analysis	
RP	Return period	[T]
SBE	Sequential backward elimination	
SFS	Sequential forward selection	
SWE	Snow water equivalent	[L]
TT	Threshold temperature	[ $\Theta$ ]

**Descriptor variables**

AI	Aridity index	[-]
EI	Evaporative index	[-]
ID	Interstorm duration	[T]
$P_b$	Fractional bare cover	[-]
$P_c$	Fractional cropland cover	[-]
$P_f$	Fractional forest cover	[-]
$P_s$	Fractional shrubland/herbaceous cover	[-]
$P_{s,rel}$	Ratio of solid precipitation	[-]
$Q_{var,inter}$	Interannual variability of discharge	[-]
RC	Runoff coefficient	[-]
REI	Relative evaporative index	[-]
SI	Seasonality index	[-]
ST	Seasonality timing index	[-]
$\phi$	Phase difference	[T]

# List of Figures

2.1	Geospatial variation of the study catchments and annual precipitation in Canada. . . . .	5
2.2	(a) Example of the linear reservoir interpolation technique during winter recession periods with no data and (b) example of the linking year procedure before and after a period of no data. Note that only years with approximately the same discharge threshold are linked (0.2 mm/day difference) . . . . .	7
2.3	(a) The corrected dataset presented in the Budyko framework and (b) the dataset presented in the Budyko framework before correction. The dataset after correction shows a better fit. Catchments within the interval of (a) are used in this study. . . . .	10
2.4	A schematic overview of the procedure applied to determine root zone storage capacities. Precipitation is distributed into solid or liquid precipitation per elevation zone. Solid precipitation is stored in the snow storage reservoir of an elevation zone and released whenever a melt threshold is exceeded. The total liquid precipitation is passed through an interception reservoir, which releases effective precipitation. The storage deficits are then defined using fluxes of snow melt, effective precipitation and transpiration. Root zone storage capacities are obtained from these storage deficits. . . . .	11
2.5	Comparison of the presence of snow between (a) elevation zones and (b) MODIS snow cover data in catchment 22. Clear distinction in snow cover between different elevation zones can be identified. . . . .	13
2.6	Graphical representation of the cumulative storage deficits for catchment 22. . . . .	16
3.1	Distribution of root zone storage capacities in the study catchments. High magnitudes occur in the south east and centre of Canada. Low magnitudes are found in the north western regions. . . . .	23
3.2	Relationships between $S_r$ and climate indices (a) aridity index, (b) yearly potential evaporation, (c) seasonality index and (d) phase lag between maximum melt input and potential evaporation output. Colours indicate percentage solid precipitation. Titles show Pearson's r and statistical p-values. . . . .	24
3.3	Relationships between $S_r$ and landscape indices (a) runoff coefficient, (b) fractional forest cover, (c) fractional crop cover, (d) fractional shrub/herbaceous cover, (e) fractional bare cover and (f) maximum elevation difference. Titles show Pearson's r and statistical p-values. . . . .	27
3.4	Relationships between $S_r$ and the phase lag between discharge and potential evaporation. The title shows Pearson's r and statistical p-value. . . . .	28
3.5	Variation of $S_r$ in the Budyko framework. A strong relationship of AI and EI on $S_r$ can be observed. Colours indicate the magnitude of $S_r$ . . . . .	29
3.6	Correlation between AI and (a) yearly average precipitation and (b) yearly average potential evaporation. The figures indicate that change in AI is largely dominated by yearly average precipitation. . . . .	30
3.7	Relationship between $S_r$ and (a) the relative evaporative index and (b) the seasonality timing index, where colours indicate REI. The titles show Pearson's r and statistical p-values. . . . .	31
3.8	How the combined effect of seasonality and timing may influence the period of overlap between liquid input due to precipitation or snow melt and the liquid output due to evaporation. . . . .	32
3.9	The results of (a) sequential forward selection and (b) sequential backwards elimination based on a linear regression model. Variables that are not defined in the text are $Liq_{norm}$ and $SI_{melt}$ , which respectively are the ratio between the 90 percentile liquid input and the mean liquid input and the seasonality index of snow melt. Note that $R^2$ can become negative for the cross-validated model performance, whenever prediction by the regression model is worse than the mean of the cross-validation sets. A more detailed description of the coefficient of determination ( $R^2$ ) is provided in Section 2.5.2. . . . .	33
3.10	Relationship between yearly potential evaporation and seasonality timing index. . . . .	34

3.11	Relationship between modelled $S_r$ and predicted $S_r$ using a linear regression model with parameters AI, RC and ST in (a) Canada and (b) Finland. $R^2$ -predicted is provided in the title as a measure for the performance of the prediction. . . . .	35
3.12	Histogram of the change in $S_r$ between a model run with and without snow module where (a) shows the relative difference and (b) shows the total difference. An increase in $\Delta S_r$ indicates a larger root zone storage capacity occurs in $M_n$ . . . . .	37
3.13	The relationship between the relative difference in $S_r$ computed by the two different models and (a) the percentage of solid precipitation and (b) the difference in onset of storage deficit between the two models. The titles show Pearson's r and statistical p-values. . . . .	37
3.14	The relationship between the relative difference in $S_r$ computed by the two different models and the difference in the seasonality timing index between the two models. A negative ST difference indicates a decrease in the ST component for $M_n$ . . . . .	38
3.15	(a) 5 catchment clusters of similar functioning shown in a principal component analysis. (b) Boxplot showing the distribution of $S_r$ within each cluster. . . . .	39
3.16	Geospatial distribution of functional catchment clusters in Canada. . . . .	40
4.1	Comparison between modelled $S_r$ and predicted $S_r$ for catchments that were not considered in this study for falling outside several selection criteria. . . . .	44
4.2	Standard deviation of coverage percentage to show land cover change over time for (a) bare cover, (b) grass or crop cover, (c) shrubland or herbaceous cover (d) forest cover. The results indicate that there is little land cover change throughout the study period. . . . .	46
4.3	Sensitivity analysis on the influence of choosing a parameter set for (a) Return Period and (b) Maximum Interception Capacity. Deviation from the diagonal line indicates a larger difference between $S_r$ for the set used in this study and the comparison set. Parameter sets for the model set are RP[undefined,2,5,20] and $I_{max}$ [0,1,2,3]. High parameter sets are RP[undefined,5,10,40] and $I_{max}$ [0,2,3,4]. Low parameter sets are RP[undefined,2,5,20] and $I_{max}$ [0,0,1,2]. All for respectively bare cover, grass or crop cover, shrubland or herbaceous cover and forest cover. . . . .	48
E1	Relationship between $S_r$ and the first 15 climate variables. The numbers in the plot refer to the numbers in Appendix C.1. . . . .	78
E2	Relationship between $S_r$ and the second 15 climate variables. The numbers in the plot refer to the numbers in Appendix C.1. . . . .	79
E3	Relationship between $S_r$ and the last climate variables. The numbers in the plot refer to the numbers in Appendix C.1. . . . .	80
E4	Relationship between $S_r$ and the first 15 landscape variables. The numbers in the plot refer to the numbers in Appendix C.2. . . . .	81
E5	Relationship between $S_r$ and the last landscape variables. The numbers in the plot refer to the numbers in Appendix C.2. . . . .	82
E6	Relationship between $S_r$ and the first 15 discharge variables. The numbers in the plot refer to the numbers in Appendix C.3. . . . .	83
E7	Relationship between $S_r$ and the last discharge variables. The numbers in the plot refer to the numbers in Appendix C.3. . . . .	84
H.1	Relationship between several snow parameters and the change in $S_r$ . The numbers in the plot refer to the numbers in Appendix C. . . . .	87

# List of Tables

2.1	Fit parameters and max wind speed used for precipitation correction . . . . .	9
2.2	Land cover classes used in this study and their corresponding return periods. . . . .	16
4.1	Overview of the different return periods and maximum interception capacities used in the sensitivity analysis of their influence on $S_r$ . . . . .	48
A.1	Distribution of the ESA-CCI land cover classes into 5 classes of approximately equal behaviour regarding $I_{max}$ and RP. . . . .	57
B.1	Overview of the values used for the calibration parameters and the calibration and validation performance per catchment. The performance of the calibration and validation is based on the percentage of matches between the MODIS snow cover dataset and the snow reservoir in all elevation zones in a catchment for all days on which the MODIS dataset does not provide NAN-data. . . . .	67
E.1	Root zone storage capacity magnitude for every study catchment . . . . .	76



# 1

## Introduction

Vegetation has shown to be a critical determinant in the hydrological cycle. It is an important steering factor in the partitioning of precipitation into evaporation and runoff (e.g. Milly, 1994), due its ability to extract water stored in the unsaturated zone between field capacity and wilting point with its root system. The total volume of water per unit area that is stored in range of the root structure, therefore available for transpiration, is called the root zone storage capacity ( $S_r$ ). This root zone storage capacity is thus an important descriptor of hydrological functioning in catchments, directly affecting transpiration (Milly and Dunne, 1994) and runoff fluxes (Donohue et al., 2012) and therefore an important component in hydrological models (e.g. Fenicia et al., 2011). Besides,  $S_r$  directly influences land surface temperatures (e.g. Kleidon and Heimann, 1998b) as transpiration largely contributes to latent heat fluxes and is therefore also a key parameter in climate modelling (Kleidon and Heimann, 2000). Understanding of the root zone storage capacity is therefore critical in environmental studies. Such better insight can be achieved by identification of the main processes that describe  $S_r$ . Moreover, comprehension of these determining processes can lead to better understanding on the response of the root zone storage capacity in a system of constant change due to e.g. climate change and anthropogenic influences on land-use.

Theoretically, root zone storage capacities can be obtained from multiplication of root depth with subsurface pore volumes. However, both root depth observations (e.g Schenk and Jackson, 2002) and soil data are very scarcely available, complicating  $S_r$  computation using this approach. Besides, observations on the local scale are difficult to integrate to the catchment scale due to the heterogeneous nature of catchments (Crow et al., 2012) and therefore prone to location bias. As such, alternative methods for determining catchment average root zone storage capacities are required. In hydrological modelling, root zone storage capacities are often calibrated. However, calibration does not always provide a physical representation of  $S_r$  due to its subjectivity to parameter equifinality (Beven, 2006). Another approach that is commonly applied in literature is the estimation of root zone storage capacities based on a look-up table (Wang-Erlandsson et al., 2014), where  $S_r$  is estimated based on mean biome rooting depth and soil texture data derived from literature. However, this method fails to account for climatic conditions, although identical vegetation types have shown to develop different root zone storage capacities in regions with varying climates and landscapes (e.g. Collins and Bras, 2007). There is evidence that trees invest in root growth to reduce negative carbon assimilation effects during periods of water stress (Porporato et al., 2004). They do this by evolutionarily optimising their root system to environmental conditions in such a way that there is enough moisture to meet the evaporative water demand for above-ground growth, while minimising the total carbon invested in root growth and maintenance (Guswa, 2008, Kleidon, 2004). Therefore it is important to consider climatic conditions when determining the root zone storage capacity (Gentine et al., 2012, Kleidon and Heimann, 1998a).

This theory of optimisation was used by Gao et al. (2014) to design a Mass Curve Technique (MCT) allowing computation of  $S_r$  based on merely climate parameters. It was used to estimate root zone storage capacities in 300 U.S. catchments, after which the findings were compared with their hydrological model equivalent. The results indicated that ecosystems indeed develop root zone storage capacity by optimising to environmental conditions and they do so by developing a root system to overcome droughts with an explicit return period. Building on this approach, Wang-Erlandsson et al. (2016) derived a global estimate for  $S_r$  based on

remote sensing climate data and subsequently linked land cover types to the corresponding drought return periods their root zones adjust to. Furthermore, Nijzink et al. (2016) and De Boer-Euser et al. (2016) used a slightly different water balance approach based on annual storage deficits derived by accumulating daily differences between precipitation and evaporation to respectively test  $S_r$  dynamics in deforested catchments and prove climate-derived  $S_r$  on balance outperform soil-derived values.

Although the technique to derive  $S_r$  based on climatic conditions has thus proven to be a rather effective way to estimate root zone storage capacities in the previously mentioned studies, its use in climates with significant snow influence is underexposed. This whilst snow cover, by its delaying effect on liquid input, has large potential of influencing annual storage deficits and therefore  $S_r$ . Zhao et al. (2016) introduced a snow module to the MCT approach based on an estimation of snow water equivalent from snow depth and carried out a sensitivity analysis for  $S_r$  dynamics in snowfall-dominated climates, proving it to be a powerful tool for estimation of root zone storage capacities in different climates in China. de Boer-Euser et al. (2019) later used a comparable snow procedure to compute  $S_r$  in different boreal regions in Finland and analysed its controls, proving snow dynamics is important to consider for analysis of  $S_r$  in these regions. Both, de Boer-Euser et al. (2019) and Zhao et al. (2016) advise to extend research on  $S_r$  descriptors in boreal and temperate regions.

### 1.1. Problem statement

$S_r$  has proven to be a critical determinant in hydrology and climatology and has major influence on modelling studies. Additional knowledge on its major descriptor variables is therefore desired and can be used to increase understanding of root zone storage capacity response to a changing system. Estimation of  $S_r$  based on scarcely available field observations and calibration has shown to be difficult for different reasons, which has led to the development of a simple water balance approach for  $S_r$  computation. Several studies have applied different alternatives of this approach to compute root zone storage capacities and identify climatic descriptor variables, but mainly in snow absent regions. Computation and analysis of  $S_r$  in snow dominant regions is therefore underexposed. The existing studies that do consider snow are either limited to a small region with few variation in climate, topography and land use or only consider a small number of catchments. This may complicate visualisation of the relationship of some potential descriptors with the root zone storage capacity. As such, additional understanding of the major descriptor variables of the root zone storage capacity in boreal regions with large spatial variation and in particular the influence of snow on the root zone storage capacity is desired.

### 1.2. Research objective

Tackling this problem requires a boreal area with large variety in climate and landscape variables and varying snow dynamics, to accentuate their relevance in describing  $S_r$ . Due to its large spatial extent, Canada matches these requirements and is therefore used as study area. As such, this exploratory study aims to quantify catchment average root zone storage capacities, identify its main descriptor variables and their regional variability and determine the influence of snow on root zone storage capacities in Canada. This results in the following research question:

*What are the major descriptor variables of Canadian catchment average root zone storage capacity, do they vary between different functionally comparable regions and how does the root zone storage capacity depend on snow in Canada?*

Answering this question is based on comparison of catchment average, water balance derived  $S_r$  with its potential descriptor variables, existing of climate, landscape and discharge parameters. Both the individual as well as the combined effect of these variables on the root zone storage capacity will be investigated. The individual influence of snow on the root zone storage capacity will subsequently be analysed by comparing water balance derived  $S_r$  computed with and without snow module. The main determining parameters that are found using this approach are lastly distributed in clusters of similar functioning, which will be used to identify how distinct combinations of variables describe  $S_r$  in different functional catchment clusters and how they vary spatially in Canada.

### **1.3. Relevance**

The main objective of this research is thus to find several main descriptors of  $S_r$ . Whenever the descriptive capability of these variables is significant they may have the potential to be used as predictors towards a simplified estimation of  $S_r$ . This may possibly lead to increased applicability in ungauged basins, or basins with limited data availability. Furthermore, such estimations increase the potential of simplified  $S_r$  application in climate- and hydrological models, or could help in constraining the  $S_r$  parameter in calibration of hydrological models.



# 2

## Methodology

This chapter provides a description of the resources and strategies used to find the major descriptor variables of the root zone storage capacity in Canada and to test the influence snow has on  $S_r$  magnitude. First, the main characteristics of the study catchments are provided in Section 2.1, succeeded by an explanation of the data sources and corrections in Section 2.2. Subsequently, Section 2.3 describes the method used to compute  $S_r$ . Finally, Section 2.4 summarises and explains the main variables considered in this study and Section 2.5 gives an overview of the assessment strategies that are used to determine which of these parameters describes the root zone storage capacity best and identify the influence snow has on  $S_r$ .

### 2.1. Study area

This study uses 230 drainage basins located in Canada, well distributed over the Southern half of the country as shown in Figure 2.1. These catchments were all selected from a larger dataset based on data availability and reliability, as explained in Section 2.2. Like shown in Figure 2.1, computed by data derived from a Canadian hydrometeorological watershed database CANOPEX (Arsenault et al., 2016), the spatial variability of annual precipitation totals is large in Canada (460-2700 mm/year). Besides, temperature signals (mean annual averages between -5 and 8.5 °C) also differ greatly in different regions in the country. The large spatial climatic variability induces diversity in climate parameters that are considered in this study, leading to a greater distinction in their potential influence on  $S_r$ . This way, the large climatic variability in Canada helps accentuate the main climate parameters that describe the root zone storage capacity.

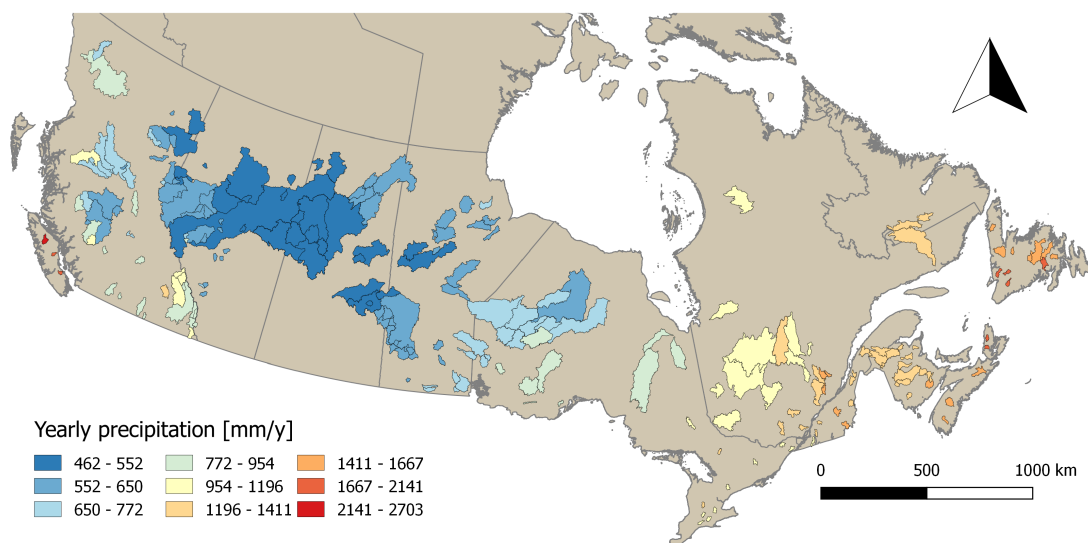


Figure 2.1: Geospatial variation of the study catchments and annual precipitation in Canada.

Furthermore, the large spatial extent of river catchments in Canada leads to a significant spread in landscape parameters. Catchments located in the Rocky Mountains and its foothills in Western Canada have topographic variables contrasting with the flatter Eastern catchments. In general, catchment average elevation ranges between 50 and 2000 m, whereas the elevation difference in a catchment varies between 60 and 3200 m. Besides, although being predominantly forested (with an average cover of 70%), catchment land cover exists of agricultural cropland, shrubs and herbaceous vegetation and bare soil, providing potential of analysing variance in  $S_r$  with land cover. As such, there is also adequate variance in landscape parameters between Canadian catchments to test their potential influence on root zone storage capacity magnitude.

Lastly, the Northern geographical location of Canada causes presence of snow during winter. However, the spatial variation in precipitation timing and winter temperature leads to distinct snow dynamics in many catchments, making this region an excellent study site for analysing the influence of snow dynamics on  $S_r$ .

## 2.2. Data sources and correction

The datasets used in this study are collected for two different purposes. Firstly, hydrometric, meteorological, snow cover and elevation data are required to compute root zone storage capacities with a water balance method and to define several climate and discharge descriptor variables. Secondly, elevation data and land cover data are used to determine landscape descriptor variables. In this section the origin of all datasets that are used in this study is discussed and the required processing and correction steps are explained.

### 2.2.1. Hydrometric data

The hydrometric dataset that is used in this study consists of discharge records for 698 river catchments in Canada, derived by the Canadian Model Parameter Experiment (CANOPEX) (Arsenault et al., 2016). These records were collected from Environment Canada's hydrometric data portal (HYDAT) (Government of Canada, 2018). The available time period of the discharge observations differs per catchment. A large number of catchment records contain missing data, which complicates use of a large number of catchments in this study. In general, any data gaps of 2 days or less have been linearly interpolated. For the many records that contain larger data voids (varying from several weeks to years), such simple interpolation is not possible. However, in this study it is essential that  $S_r$  is computed for a considerable number of catchments, to have enough possibilities of comparing  $S_r$  between catchments. To do this, at least several years of discharge records without data voids is required to determine a long term average discharge component, which is used to compute root zone storage capacities as described in section 2.3.3. Therefore, to increase the number of catchments available for analysis, a physically based interpolation method is applied in this study to fill data voids in several discharge records, as explained below.

A large number of streamflow records with data voids particularly miss data during winter months (November to February), which is caused by budget limitations for provincial gauge operators. In general, most precipitation during this period will fall in solid state and will therefore not have a large contribution on streamflow until the start of the melting period, which starts after February in the vast majority of the catchments. This means that the fast hydrological processes will cease and the hydrograph is particularly dominated by depletion of the groundwater reservoir during this period of the year. As previous studies have shown (e.g. Fenicia et al., 2006, Savenije, 2018), during such period of water recession, the groundwater reservoir will contribute to catchment drainage following the theory of a linear reservoir, which results in an exponential decrease of streamflow. Therefore, in this study, data voids during the winter period are filled by using an exponentially decaying function between the last and the first recorded measurement before and after the period of missing data (Figure 2.2a).

To keep the analysis as physically-based as possible, such interpolation was only carried out whenever the recorded temperatures in the data void periods were below zero, to increase the likeliness that reservoirs are indeed dominated by groundwater reservoir depletion. Additionally, to prevent the interpolation to have too much influence on the total discharge, it was only applied when contribution of the interpolated discharge was smaller than 10% of the total discharge.

A considerable number of catchment discharge records also contains missing data outside the winter periods. In many cases, this can be resolved by taking the hydrological years which contains data voids from the analysis and as such not considering these years in the determination of catchment long term average discharge. Note that in this study, hydrological years are split after October, as snow starts accumulating during this period and thus all snow dynamics is approximately caught within a single hydrological year. To

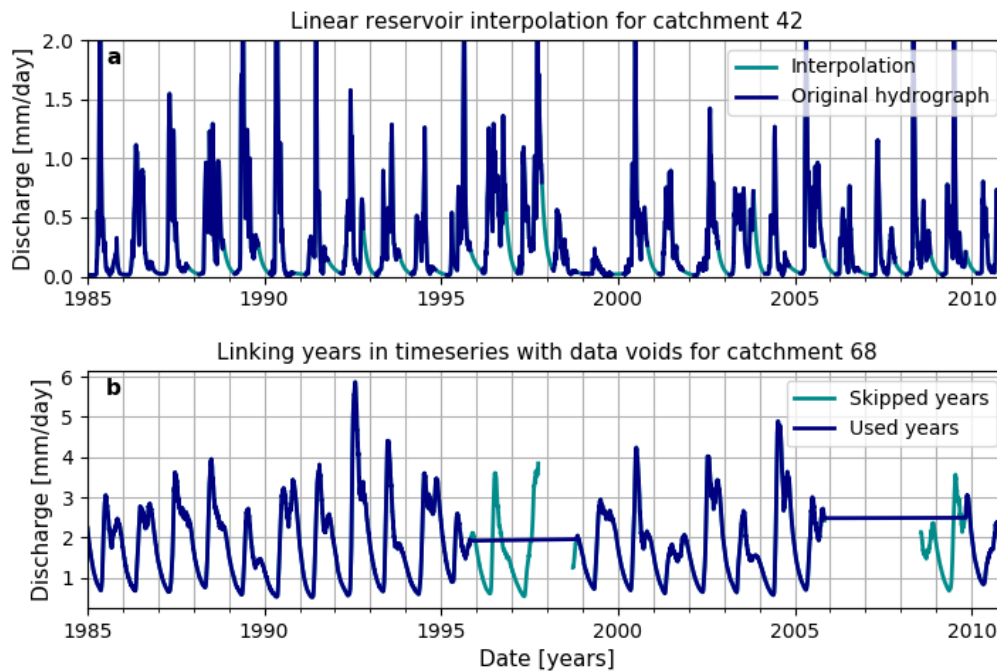


Figure 2.2: (a) Example of the linear reservoir interpolation technique during winter recession periods with no data and (b) example of the linking year procedure before and after a period of no data. Note that only years with approximately the same discharge threshold are linked (0.2 mm/day difference)

secure a certain continuity between precipitation and discharge response when skipping a hydrological year, it is important that the hydrological years before and after a skipped year show approximately identical behaviour. This means that the streamflow just before the skipped period must be approximately equal to the streamflow just after (Figure 2.2b). To account for this, all years before and after a skipped hydrological year are checked on their matching discharge. The years before and after a skipped year that have the least time between them and have a smaller difference in discharge than 0.2 mm/day were linked to each other. All years in between are not considered in the analysis and therefore not used to determine catchment long term average discharge.

Although the number of useful catchments significantly improves after the corrections, not all catchments have a data record with enough full years to construct a long term average discharge value. Therefore, not all of the CANOPEX catchments can be used in this study. Elaboration on the selection of catchments is given in Section 2.2.6.

### 2.2.2. Meteorological data

The meteorological quantities used in this study are precipitation, potential evaporation and temperature. This subsection describes the type of data used, the processing and corrections steps required and the origin of the datasets.

#### Potential evaporation and temperature

Direct potential evaporation ( $E_p$ ) data are scarce and not available for the Canadian catchments. However, CANOPEX (Arsenault et al., 2016) provides temperature data for all 698 considered Canadian catchments which can be used to estimate  $E_p$ . For the CANOPEX dataset, a 300 arc second gridded data climate product, provided by Natural Resources of Canada (NRCan), was averaged for every catchment to retrieve daily maximum and minimum temperature data (Hutchinson et al., 2009). The NRCan product was created by application of thin-plate smoothing splines to interpolate between raw meteorological data from observation stations across Canada as a function of longitude, latitude and elevation. Any missing temperature observations were estimated using interpolation, resulting in a dataset without missing data over the period of 1950-2010.

In this study, the average of daily maximum and minimum temperature data derived from the CANOPEX dataset are used to obtain catchment average daily temperatures. All three of these temperature variables are subsequently used to obtain an estimate of the daily potential evaporation, using the Hargreaves and Samani equation as described in Equation 2.1 (Hargreaves and Samani, 1985).

$$\lambda E_p = \alpha R_e (T_a \nu + 17.8) \sqrt{T_{max} - T_{min}} \quad (2.1)$$

where:

- $\lambda$  = Latent heat of evaporation
- $E_p$  = Potential evaporation
- $R_e$  = Top of atmosphere radiation
- $T_a \nu$  = Average temperature
- $T_{max}$  = Maximum temperature
- $T_{min}$  = Minimum temperature

The constant  $\alpha$  is generally set at 0.0023 (Maes et al., 2019), whereas  $\lambda$  is set equal to 2.26 kJ/kg. Furthermore, daily catchment average  $R_e$  data were obtained from global data series on 30 arc-second resolution provided by Mines Paris Tech (Mines ParisTech, 2014). Due to the cold winters in Canada, application of Equation 2.1 can lead to negative daily  $E_p$ . Whenever this occurs,  $E_p$  is set to 0 mm/day.

### Precipitation

The catchment average precipitation data used in this study are also obtained from the Canadian Model Parameter Experiment (CANOPEX) database (Arsenault et al., 2016). Like the temperature data, daily catchment average precipitation data were derived from the NRCan gridded product, which is based on the same interpolation technique (Hutchinson et al., 2009). As for temperature, the daily catchment average dataset from CANOPEX consists of no missing precipitation data for the period 1950-2010.

Canadian winter precipitation is generally dominated by snowfall, which complicates precipitation observations. Conversion of snow records to their snow water equivalent (SWE) for all Canadian gauges operated by Environment and Climate Change Canada happens by either using gauges filled with antifreeze or by assuming 1 cm of snow is equivalent to 1 mm of rain (B. Duguay, personal communication, October 10, 2019).

Additionally, winter precipitation may affect catch accuracy. In general, precipitation can be underestimated due to wind induced turbulence around rain gauges (Sevruk, 1982). This underestimation is significantly larger in snow-dominant regions like Canada with a large fraction of solid precipitation (e.g. Wolff et al., 2015), and is therefore expectedly also present in the precipitation dataset from CANOPEX. However, there are several ways to account for this underestimation by scaling the original data with a correction factor that describes precipitation catch efficiency (CE). Functions that determine such a catch efficiency are called transfer functions and they depend on the combined effect of wind speed (e.g. Yang et al., 1999) and temperature (e.g. Wolff et al., 2015). The transfer function used in this study to account for precipitation undercatch has been defined by Kochendorfer et al. (2017) and is provided in Equation 2.2.

$$CE = \exp(-aU(1 - \arctan(bT_a) + c)) \quad (2.2)$$

where:

- $CE$  = Catch efficiency
- $U$  = 10-Meter wind speed
- $T_a$  = Air temperature

Furthermore, parameters  $a$ ,  $b$  and  $c$  are coefficients that have been fitted based on a comparison between precipitation data from a reference gauge in Norway and the USA and normal gauges with different types of gauge shields.

It should be noted that the transfer function is originally intended for application on the point scale, whereas the data used in this study are based on an interpolated gridded product, with no information on the location of the observation stations used to create this product. As a result, the only opportunity is to use catchment average wind and temperature data to determine a daily catch efficiency per catchment (note that it is likely that these data are based on the same weather stations as used in the interpolated, gridded precipitation product). The daily catchment average air temperature data that are applied in equation 2.2

are obtained from CANOPEX (Arsenault et al., 2016). The daily catchment average wind data that are used as input in this equation are computed using a vector combination of the 0.75 degree gridded average  $U_{10}$  and  $V_{10}$  components obtained from the global reanalysis ERA-Interim (Dee et al., 2011).

Parameters  $a$ ,  $b$  and  $c$  from Equation 2.2 are taken from Kochendorfer et al. (2017), where they are fitted based on data from the USA and Norway, in which CE has been defined by comparing a reference gauge with several different other gauges (amongst others a Single Alter shielded gauge). Because the Single Alter shielded rain gauge is the most frequently used gauge in Canada (A. Cyr, personal communication, November 6, 2019), the fitted parameter values belonging to this gauge are expected to compute the most accurate catch efficiency, which is why they are used in this study. Lastly, the maximum wind speed that can be used to determine the catch efficiency by application of Equation 2.2 is 12 m/s. An overview of the parameters to determine a catchment average daily CE is presented in Table 2.1.

Table 2.1: Fit parameters and max wind speed used for precipitation correction

<b>a</b>	<b>b</b>	<b>c</b>	<b>Max U [m/s]</b>
0.03	1.04	0.66	12

After computing CE for every catchment, the corrected daily precipitation was obtained by division of the original CANOPEX precipitation value by CE. The corrected precipitation values have been used as description of precipitation throughout this study.

The effect of the undercatch correction for precipitation in the Canadian catchments can be tested by using the Budyko framework (Budyko et al., 1974). This is a commonly used framework in hydrology which describes the catchment long term average water balance. The position of a catchment in this framework describes the long term average distribution of water between runoff and actual evaporation, as a function of the atmospheric conditions in a catchment. Two examples of the Budyko framework are shown in Figure 2.3. The aridity index (AI) occupies the horizontal axis of the framework and gives a description of the dryness of a catchment by relating the catchment average liquid input ( $P$ ) and atmospheric demand ( $E_p$ ). The evaporative index (EI) covers the vertical axis and determines what part of the total liquid input is evaporated ( $E_a/P$ ). Theoretically, the framework is limited by a water limit for  $E_p > P$  (or  $AI > 1$ ), where evaporation is bound by the liquid input in a catchment, and an energy limit for  $E_p < P$  (or  $AI < 1$ ), where evaporation is bound by atmospheric energy demands. Budyko et al. (1974) defined a curve for the expected catchment EI for a given AI, which has proven to be followed rather accurately by catchments worldwide (e.g. Budyko et al., 1974, Gentile et al., 2012, Ye et al., 2015).

Since precipitation is describing both AI and EI, a change in precipitation will lead to a change in the position of a catchment on the Budyko framework. This is why the correction of precipitation has led to a changed position of the catchments (see Figure 2.3a and b). After the correction, the catchments plot significantly closer to the Budyko curve, which suggests a better reliability of the data. As such, it seems that the application of the local catch efficiency function by Kochendorfer et al. (2017) on a global dataset works well and it is likely that correction of the precipitation dataset has led to a better representation of reality.

### 2.2.3. Snow cover data

As snow dynamics plays an important role in the hydrological system in Canada and since it is a goal of this study to investigate the influence of snowfall on  $S_r$ , computation of  $S_r$  requires a description of snow melt. In general, snow depth or snow water equivalent (SWE) data are only provided on the point scale and are unreliable to determine a catchment average snow description. Besides, no snow depth or SWE data are available for all study catchments. Therefore, snow melt is modelled using a snow module in this study (see Section 2.3.1). This snow module consists of two model parameters, which are calibrated by comparing the presence of snow in a certain elevation zone of a catchment with satellite snow cover data for this particular area. For this, MODIS/Terra snow cover data are used (Hall and Riggs, 2016b), which is a gridded dataset providing Normalised Difference Snow Index (NDSI) with a 500 m resolution from the year 2000 onwards. Commonly, an NDSI threshold of 0.4 is used to indicate presence of snow cover (e.g. Dozier, 1989, Hall and Riggs, 2007, Sankey et al., 2015) and Härer et al. (2018) showed that this is indeed a valid threshold for products with a resolution of 500 m and more. Consistent with other studies, the NDSI threshold of 0.4 is also used in this study.

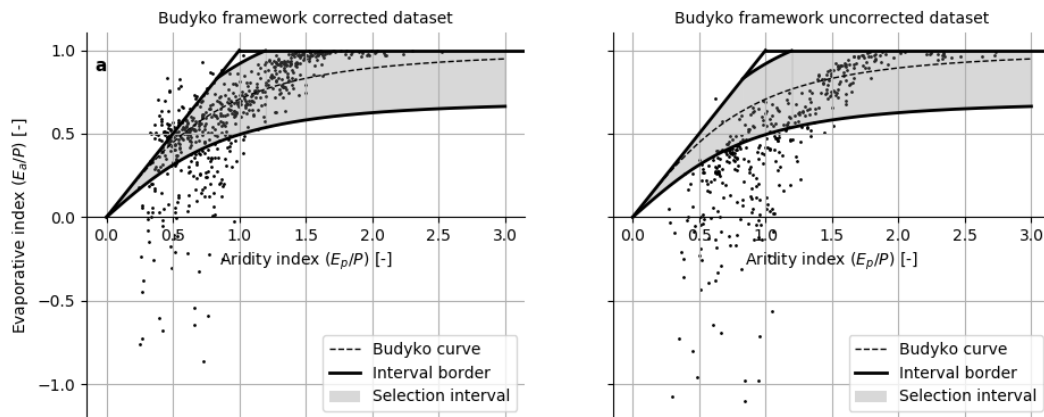


Figure 2.3: (a) The corrected dataset presented in the Budyko framework and (b) the dataset presented in the Budyko framework before correction. The dataset after correction shows a better fit. Catchments within the interval of (a) are used in this study.

### 2.2.4. Elevation data

Like mentioned earlier, calibration of the snow module parameters requires distribution of catchments in different elevation zones. These elevation zones are derived from HydroSHEDS (Lehner et al., 2008), which provides void-filled digital elevation data with 3 arc-seconds resolution up to 60 degrees latitude. Elevation data from catchments that are (partly) located more northerly are derived by the 30 arc-seconds resolution GTOPO30 DEM dataset (USGS, 1997). Apart from their function in defining elevation zones, the elevation data are also used to define several different landscape variables that may influence  $S_r$ .

### 2.2.5. Land cover data

Land cover data have two functions in this study. They are used to define land cover dependent parameters during the computation of  $S_r$  (see Section 2.3.2 and Section 2.3.4) and they are applied to define several landscape parameters that may describe  $S_r$ . The land cover data used in this study are obtained from ESA CCI (ESA, 2017), which provides yearly global land coverage with a 300 m resolution from 1992 to 2015. In this study, parameters that are derived from land cover maps are determined using a different land cover map for every year. Any required land cover information before 1992 has been obtained from the 1992 dataset. All types of land cover defined in this the ESA CCI dataset are redistributed over 5 classes, like shown in Appendix A. The 5 land cover classes used in this study are:

- Bare cover
- Grassland cover
- Cropland cover
- Shrubland & Herbaceous cover
- Forest cover

### 2.2.6. Catchment selection

Like already stated in Section 2.2.1, not all catchments from CANOPEX can be used in this study due to several restrictions regarding  $S_r$  computation. Firstly, in order to compute catchment average  $S_r$ , at least 20 years of daily precipitation and potential evaporation records are required. Furthermore, because the long term average water balance is used to estimate transpiration (see Section 2.3.4), at least 10 years of discharge data (albeit modified) without missing values are required to have a description of long term average discharge. Besides, the application of a snow module (Section 2.3.1) in the procedure of  $S_r$  computation requires calibration with MODIS Snow Cover data. These data are only available from 2000 onwards and with a 5 year period for calibration and testing, catchment records are required until at least 2006. Additionally, catchments before 1985 are not considered to avoid too large variation in climate and land-use within catchments. As such, only catchments with sufficient data between 1985 and 2012 that meet predefined conditions are used in this study.

Furthermore, catchments are also selected based on their data reliability. The position of the CANOPEX catchments in this framework is shown in Figure 2.3a, where a simple parametric formulation defined by Fu (1981) is used to approximate the Budyko curve (Zhang et al., 2004). As stated earlier (Section 2.2.2), catchments generally plot around this Budyko curve. This theory has been used as a proxy for data reliability in this study. Only the catchments that are located within a 30% range around the Budyko curve and that fall inside the physical limits of the framework are therefore used.

## 2.3. Approach for root zone storage capacity computation

This section provides a description of the method that is used to compute  $S_r$  in the selected Canadian catchments. The method is based on the theory that vegetation evolutionarily optimises its root system based on climatic conditions with a certain return period, in order to avoid water shortage as well as over-investment in below-ground carbon expenses (Guswa, 2008, Kleidon, 2004). This has led to a way of describing  $S_r$  with merely climate variables (Gao et al., 2014), which has been adjusted by i.e. De Boer-Euser et al. (2016) and Nijzink et al. (2016). Their approach of computing  $S_r$  based on the yearly maximum water deficit for transpiration with a vegetation-specific return period will also be used in this study and is explained in this section.

In the conventional approaches, direct daily precipitation and transpiration estimates are used to determine the daily water shortage for transpiration, also called the daily storage deficit. However, in catchments where snow dynamics plays an important role, infiltration of water is delayed by the accumulation of solid precipitation to the snow pack and liquid infiltration into the soil will happen during the melt phase. Direct daily precipitation inputs are therefore not representative to determine daily storage deficits. Instead, the daily liquid input in this study is described as a combination of snow melt and direct liquid precipitation. To estimate the snow melt input, a snow module is used, which is described in Section 2.3.1. Subsequently, the other fluxes that are used to determine storage deficits, being effective precipitation and transpiration, are described in respectively Section 2.3.2 and 2.3.3. Lastly, the procedure of computing root zone storage capacities from storage deficits is described in Section 2.3.4. A schematic overview of the entire procedure used to determine the root zone storage capacity is provided in Figure 2.4. Note that the entire approach has been applied using a temporal resolution of 1 day.

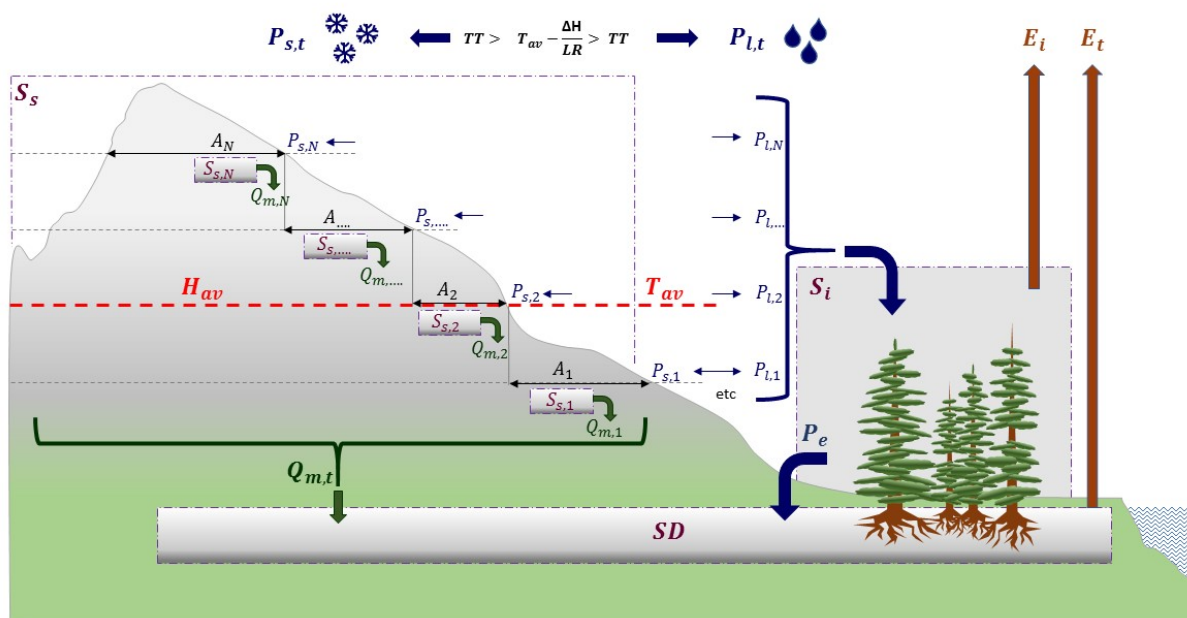


Figure 2.4: A schematic overview of the procedure applied to determine root zone storage capacities. Precipitation is distributed into solid or liquid precipitation per elevation zone. Solid precipitation is stored in the snow storage reservoir of an elevation zone and released whenever a melt threshold is exceeded. The total liquid precipitation is passed through an interception reservoir, which releases effective precipitation. The storage deficits are then defined using fluxes of snow melt, effective precipitation and transpiration. Root zone storage capacities are obtained from these storage deficits.

### 2.3.1. Snow module

As stated before and as can be derived from Figure 2.4, the daily liquid input from snow melt plays an important role in the determination of storage deficits, which are used to determine  $S_r$ . However, the lack of snow water equivalent observations and the large heterogeneity in elevation in the study catchments complicate the use of point observations for snow melt estimation. Therefore, snow behaviour is simulated using a semi-distributed version of the HBV snow routine (Bergstroem, 1975) in this study. In this subsection the structure of the snow module is explained and the calibration procedure that is required to define snow parameters is described. Note that sublimation is neglected in this study, as it is likely that the effect of sublimation during winter time is small because potential evaporation rates are small.

#### Module setup

As shown in Figure 2.4, the snow module used in this study consists of several snow storage reservoirs that are filled during a snow event and emptied due to snow melt. For simplicity, the procedure within one snow storage reservoir is explained first. Both the solid precipitation input and the melt output from a reservoir are temperature dependent. Firstly, precipitation will only be in solid state whenever temperatures are below a certain threshold. Generally, this threshold is best described using a temperature dependent transition phase between liquid and solid precipitation (Bergstroem, 1975), however for simplicity a sharp temperature limit is defined in this study. Secondly, snow melt from the snow storage reservoir will only occur when temperatures are below a certain threshold and will likely increase in magnitude whenever temperatures increase.

To be able to describe these fluxes, two parameters are used in this version of the HBV snow routine. Firstly a temperature threshold (TT) describes whether precipitation is solid or liquid (equation 2.3) and whenever melt can occur. Secondly, the degree day factor (MF) relates the rate of melt to a certain temperature above TT (equation 2.4). Obviously, snow melt will not occur when the snow storage reservoirs are empty ( $S_s = 0$ ).

$$P_s = \begin{cases} P, & \text{if } T_a(t) > TT \\ 0, & \text{if } T_a(t) < TT \end{cases} \quad (2.3)$$

$$Q_m = \begin{cases} MF(T_a - TT), & \text{if } T_a(t) > TT \\ 0, & \text{if } T_a(t) < TT \end{cases} \quad (2.4)$$

where:

- $P_s$  = Solid precipitation
- $P$  = Total precipitation
- $Q_m$  = Snow melt
- $MF$  = Degree day factor
- $TT$  = Threshold temperature
- $T_a$  = Air temperature

MF and TT are the only two parameters used in this model to avoid over-parametrisation. Whenever these two parameters are known, precipitation and temperature data are sufficient to provide an estimate of the snow melt and the solid precipitation input. However, since temperature largely varies with elevation, catchment average values of  $T_a$  are not representative for all elevations in catchments with large elevation difference, which will also complicate  $P_s$  and  $Q_m$  estimation. Therefore, a distribution of the catchment in different elevation zones is required for determining  $P_s$  and  $Q_m$ .

Catchments are distributed using data from the digital elevation models described in Section 2.2.4. A new zone is assigned for every 250 meters and every elevation zone has its own snow storage reservoir (see Figure 2.4). Equations 2.3 and 2.4 are applied for every elevation zone. The average temperature of an elevation zone has been estimated using a simple lapse rate formulation as described in Equation 2.5.

$$T_a = T_{av} - \frac{\Delta H}{LR} \quad (2.5)$$

where:

- $T_a$  = Air temperature in elevation zone
- $T_{av}$  = Average catchment temperature
- $\Delta H$  = Elevation difference between elevation zone and mean elevation
- $LR$  = Lapse rate

Lapse rates differ with latitude and are location dependent. However there is insufficient information on the regional lapse rates that apply in the study catchments. Therefore, an average value of 6.4 °C/km is used for LR (e.g. Muralikrishna and Manickam, 2017). It is important to note that the catchment mean temperature has been linked to the catchment average elevation in this study (see Figure 2.4). This can be done because the temperature data are derived from a gridded product where temperatures between gauges are interpolated based on elevation, which means the average temperature in the catchment is representative for the average elevation in the catchment.

Equations 2.3, 2.4 and 2.5 are applied to all snow reservoirs in every elevation zone (with MF and TT being equal in every elevation zone). This leads to a description of  $Q_m$  and  $P_s$  per elevation zone. The total catchment average daily melt output is then derived by taking the sum of the melt output from every elevation zone, after this has been scaled by multiplication with the relative area of every elevation zone, as shown in equation 2.6.

$$Q_{m,t} = \sum_{i=1}^N \frac{A_i}{A_t} Q_{m,i} \quad (2.6)$$

where:

- $Q_{m,t}$  = Total catchment melt
- $Q_{m,i}$  = Elevation zone melt
- $A_i$  = Elevation zone area
- $A_t$  = Total catchment area
- $N$  = Total number of elevation zones

As such, whenever catchment average parameters TT and MF are known, equations 2.3, 2.4, 2.5 and 2.6 can be used to estimate the daily liquid input by snow melt, which is one of the important fluxes to determine storage deficits.

### Parameter calibration

The two catchment average model parameters MF and TT require calibration. This is done by comparing the presence of snow in the MODIS snow cover dataset (Section 2.2.3) with the presence of snow in the snow storage reservoir of the snow module per elevation zone as shown in Figure 2.5. Every pixel of the MODIS data can consist of snow, no snow or NaN values related to cloud cover. An elevation zone is defined as snow-covered when the majority of the MODIS pixels in the zone show snow coverage. Similarly, when the majority of the pixels in an elevation zone consists of NaN values, the elevation zone is defined as NaN for this day.

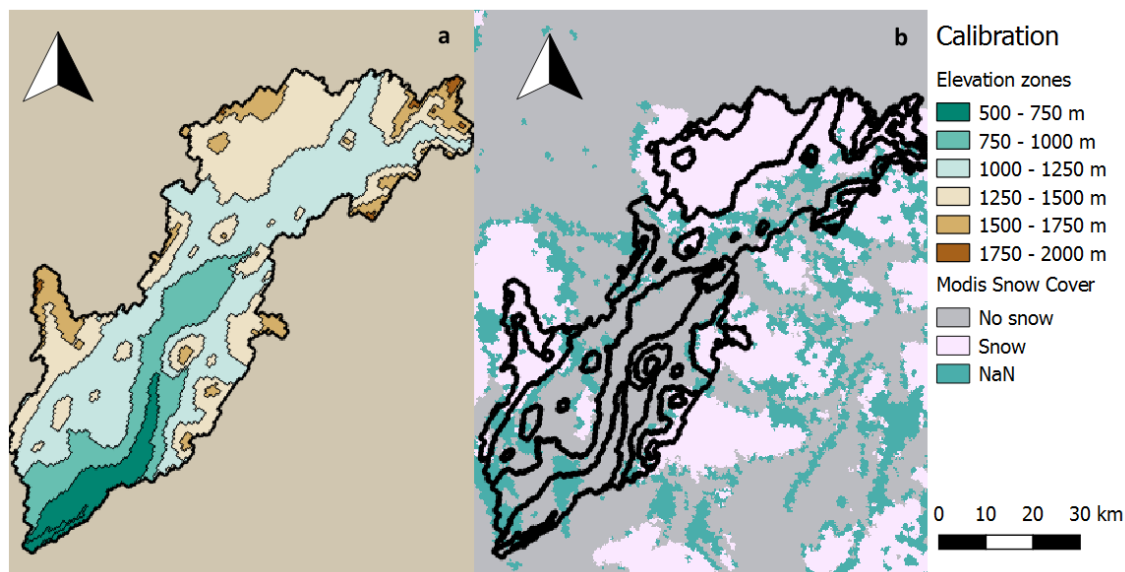


Figure 2.5: Comparison of the presence of snow between (a) elevation zones and (b) MODIS snow cover data in catchment 22. Clear distinction in snow cover between different elevation zones can be identified.

During calibration, 2000 randomly chosen parameter sets with varying combinations of MF and TT are applied to the snow module. The parameter performance is judged based on a comparison of the total number of matching days between the MODIS data and the snow reservoir content in each elevation zone for the period between 2002 and 2004. On days where the majority of the pixels in an elevation zone consisted of NaN values, comparison was not applied. The five parameter sets with the best performance were subsequently tested over the year 2005, after which a value for TT and MF was chosen for every catchment based on the combined performance of the calibration and testing phase. An overview of TT and MF per catchment is given in Appendix B, along with the calibration and validation performance of the final parameter combination for every catchment.

The advantage of parameter calibration is that any mistakes in the temperature estimations of the elevation zones (e.g. due to use of an average lapse rate or due to wrong catchment average temperature descriptions), are likely buffered by the model parameters.

### 2.3.2. Effective precipitation

The precipitation that does not fall in solid state, will enter the system directly in liquid state. This may differ per elevation zone. The total amount of precipitation falling in a catchment is derived in the same way as the total amount of snow melt (Equation 2.6), by taking the sum of every elevation zone after this has been scaled by multiplication with the relative area of every elevation zone. The liquid precipitation is generally first intercepted by vegetation before it can infiltrate or run off. The procedure of interception evaporation is simulated by the interception reservoir ( $S_i$ ), with a water balance as described in equation 2.7. Note that this interception reservoir is applied on the catchment scale, with the catchment total precipitation input and not for every different elevation zone. Soil evaporation is included in the interception flux.

$$\frac{dS_i}{dt} = P_{l,t} - E_i - P_e \quad (2.7)$$

where:

- $S_i$  = Interception storage
- $P_{l,t}$  = Total liquid precipitation
- $E_i$  = Interception evaporation
- $P_e$  = Effective precipitation

Moisture in the interception reservoir will evaporate following potential evaporation rates for the time moisture is available and the maximum interception capacity ( $I_{max}$ ) is not reached, as described in equation 2.8. All water that exceeds  $I_{max}$  is available for infiltration or runoff and is defined as the effective precipitation ( $P_e$ ), which is described in equation 2.9.  $P_e$  is the second flux that is required to determine storage deficits.

$$E_i = \begin{cases} E_p, & \text{if } E_p dt < S_i \\ \frac{S_i}{dt}, & \text{if } E_p dt \geq S_i \end{cases} \quad (2.8)$$

$$P_e = \begin{cases} 0, & \text{if } S_i \leq I_{max} \\ \frac{S_i - I_{max}}{dt}, & \text{if } S_i > I_{max} \end{cases} \quad (2.9)$$

where:

- $I_{max}$  = Maximum interception capacity
- $E_p$  = Potential evaporation

$I_{max}$  is a measure for the total amount of water that can be intercepted by leaves and is therefore dependent on the distribution of land use in a catchment. Evidently, catchments with a larger leaf cover have a high maximum interception capacity compared to catchments with lower leaf cover. To account for this effect, the land classes defined in Section 2.2.5 are distributed into 4 interception classes, being bare cover, grassland (for both grassland and cropland), shrubland and forest. Their corresponding  $I_{max}$  values as assumed in this study are respectively 0, 1, 2 and 3 mm. The actual value of  $I_{max}$  assigned to a catchment is then described by an addition of these land cover representative  $I_{max}$  values scaled by the appearance percentage of the corresponding land cover type in a catchment. Note that since land cover may change annually, so may the maximum interception capacity.

### 2.3.3. Transpiration

Apart from the liquid input, storage deficit computation also requires a description of the transpiration output in a catchment, as this describes the water flux from the root zone into the atmosphere. Currently, no approaches of measuring daily transpiration on the catchment scale exist. The long term average transpiration can however be estimated from the long term catchment water balance, assuming negligible storage change, deep percolation and groundwater recharge, as shown in equation 2.10.

$$\overline{E_t} = \overline{P_{liq}} - \overline{Q} \quad (2.10)$$

where:

$E_t$  = Transpiration

$P_{liq}$  = Combined liquid input by snow melt and effective precipitation

$Q$  = Discharge

Note that the long term average values in this study are only taken from years without missing discharge data (see Section 2.2.1). Daily transpiration rates can now be estimated by scaling the long term average transpiration with the ratio between the remaining daily potential evaporation after interception has occurred and long term average potential evaporation subtracted with the long term average interception (Nijzink et al., 2016), like shown in Equation 2.11. Using this method, the seasonal signal of transpiration is described without violating long term average transpiration.

$$E_t(t) = \overline{E_t} \frac{E_p - E_i}{\overline{E_p} - \overline{E_i}} \quad (2.11)$$

### 2.3.4. Storage Deficits

The main principle used in the approach of this study is the assumption that vegetation evolutionarily optimises its root system based on a yearly maximum storage deficit with a certain return period. Storage deficits are defined as the outgoing flux of transpiration that is not immediately covered by incoming liquid input. Or in other words, the transpiration that occurs for which storage of water in the root zone is required. During dry periods with large transpiration output and relatively few liquid input, the cumulative daily storage deficit will increase towards a yearly maximum direct moisture shortage, after which a period of large liquid input and few transpiration will lead to a decrease in storage deficits again. This procedure is described with equation 2.12 and the yearly signal of cumulative storage deficits is shown in Figure 2.6. Note that storage deficits do not become negative and that the moisture deficit is assumed to be 0 at the start of time series.

$$SD(t) = \int_{t_0}^{t_1} (E_t - P_e) dt \quad (2.12)$$

where:

$SD(t)$  = Cumulative storage deficit at time t

The yearly moisture shortage ( $SD_y$ ) that needs to be bridged by the use of water from the root zone is determined by subtracting the maximum storage deficit in a representative year by the minimum storage deficit that occurs in the period before in that same year, as described in Equation 2.13. Note that the years are split at the start of the month with averagely the lowest storage deficit. The exact splitting month therefore differs per catchment.

$$SD_y = \max(SD(t_2)) - \min(SD(t_1)), \text{ with } t_2 > t_1 \quad (2.13)$$

According to Gao et al. (2014), vegetation root zone storage capacities are optimised based on a drought return period of 20 years. Wang-Erlandsson et al. (2016) subsequently showed that these return periods likely depend on the type of vegetation and its survival strategy. Grasses for example are likely to go dormant during dry periods and are therefore expected to design root systems based on a very low return period of approximately 2 years (Wang-Erlandsson et al., 2016). Trees on the other hand are a lot more likely to invest in root growth and are therefore usually modelled using a return period of 20 years. In this study, shrubland and herbaceous cover is assumed to have a return period somewhere in between (5 years). Besides bare land

Table 2.2: Land cover classes used in this study and their corresponding return periods.

Land cover	Return period [years]
Bare area	Undefined
Grassland & Cropland	2
Shrubland & Herbaceous cover	5
Forest cover	20

cover likely has no root growth at all, which is why the return period of this land cover class is undefined. The land cover classes used in this study and their corresponding return periods are summarised in Table 2.2.

Because land cover may change through the years, the return period may differ per year. For every year, the actual catchment return period is described by an addition of the land cover specific return period values scaled by the appearance percentage of the corresponding land cover in a catchment. Since no roots grow in bare area, this type of land cover will not contribute the addition of return periods, but does contribute to the total catchment area and therefore to the scaling of the other types of land cover. The actual drought return period in a catchment is then the average value of these yearly return periods.

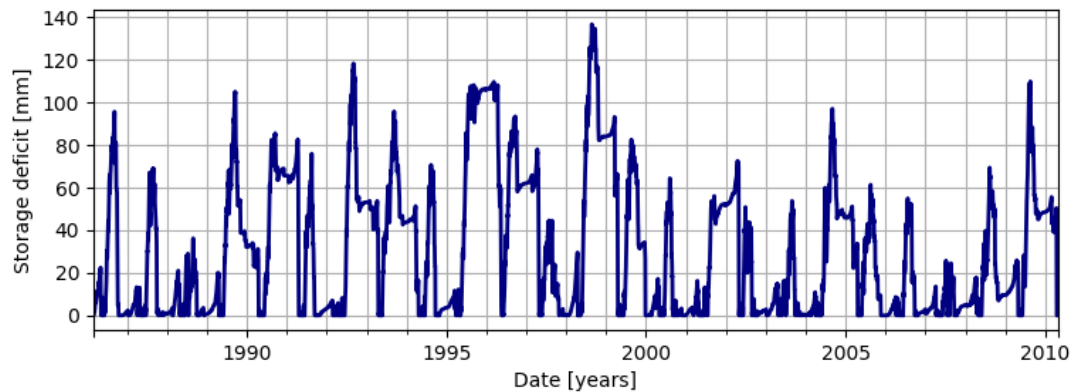


Figure 2.6: Graphical representation of the cumulative storage deficits for catchment 22.

Finally, a Gumbel extreme value distribution (Gumbel et al., 1941), was used to link  $S_r$  with storage deficits that have a land cover specific return period. This was done by fitting the extreme value distribution through the yearly storage deficits as defined by Equation 2.13 and subsequently linking  $S_r$  to the storage deficit in this distribution with corresponding catchment specific return period.

### 2.3.5. Catchment selection

In most cases, storage deficits return to zero after a few years, as presented in Figure 2.6. However, there are some outlying catchments in which this does not happen. For these catchments it is likely that the total transpiration is overestimated, mostly due to unrealistically low representation of discharge. The few catchments for which this happened were not considered in the analysis and therefore manually removed from the study catchment set. The final dataset consists of 230 catchments, like shown in Figure 2.1.

## 2.4. Descriptor variables

After computation of  $S_r$ , a set of catchment characteristics must be computed to test whether they can be considered descriptor variables of  $S_r$ . The parameters that are examined in this study can be subdivided into climate, landscape and discharge variables, or are a combination of these three. The variables that are frequently considered in this study and require some additional explanation are described in this section. An overview of all parameters that are analysed is presented in Appendix C.

### 2.4.1. Climate variables

A description of the climate variables that have been frequently considered in this study and require some additional explanation is provided in this subsection.

**Aridity index**

The aridity index (AI) is a parameter that is often used in hydrology. It describes the dryness of a catchment. As shown in equation 2.14, it relates the long term average evaporation and precipitation. AI is an important parameter in the Budyko framework, as shown in Section 2.2.2. A high aridity index indicates an arid area with relatively few liquid input compared to the atmospheric water demand. Vice versa, a low aridity index means that the water input is dominant over potential evaporation.

$$AI = \frac{\overline{E_p}}{\overline{P}} \quad (2.14)$$

**Seasonality index**

The seasonality index (SI) generally describes the yearly spread of precipitation. However, because this study considers snow dynamics, the seasonality of liquid input (liquid precipitation and snow melt) is used. A description for SI is given with Equation 2.15 (Gao et al., 2014). SI can vary between 0 and  $\frac{11}{6}$ . A high seasonality index means most precipitation is falling in a relatively small time period (e.g. a few months), whereas a low seasonality index indicates precipitation falls relatively well distributed throughout the year.

$$SI = \frac{1}{\overline{P_a}} \sum_{m=1}^{m=12} \left| \overline{P_m} - \frac{\overline{P_a}}{12} \right| \quad (2.15)$$

where:

$\overline{P_a}$  = Average annual liquid Input

$\overline{P_m}$  = Average monthly liquid input of month m

**Phase lag liquid and energy input**

Another important climate parameter that may have a significant effect on  $S_r$  is the phase lag ( $\phi$ ) between liquid input and the energy input in a catchment. Expectedly, transpiration rates largely follow potential evaporation rates and it is likely that the largest liquid output happens whenever the atmospheric energy input is highest. Therefore, the average phase lag between the maximum monthly Liquid Input and Potential Evaporation is considered in this study ( $\phi_{liq,Ep}$ ). Additionally, the phase lag between maximum monthly snow melt and Potential Evaporation ( $\phi_{melt,Ep}$ ) is considered, because snow dynamics plays an important role in many of the study catchments.

**Seasonality timing index**

The combined effect between Seasonality and Timing is also examined in this study. This effect can be tested using the seasonality timing index (ST) as described in Berghuijs et al. (2014) and Woods (2009), where it is assumed that climatic variability can be modelled using simple sine curves. The amplitude and phase of these curves are measures for the seasonality and timing of the seasonal variability. This way, the precipitation and evaporative signals of all study catchments can be approximated by fitting the formulations given in respectively equation 2.16 and 2.17, where the evaporative signal is described by temperature variations.

$$P(t) = \overline{P} [1 + \delta_p \sin(2\pi(t - s_p)) / \tau_p] \quad (2.16)$$

$$T(t) = \overline{T} + \Delta_T [\sin(2\pi(t - s_T)) / \tau_T] \quad (2.17)$$

where:

$t$  = Time (days)

$P(t)$  = Liquid input as a function of t (mm/d)

$T(t)$  = Temperature as a function of t (mm/d)

$\overline{P}$  = Yearly average precipitation (mm)

$\overline{T}$  = Yearly mean temperature (°C)

$\tau$  = Seasonal cycle duration (365 days)

Furthermore,  $\delta_p$  and  $\Delta_T$  are parameters describing the seasonal cycle and  $s_p$  and  $s_T$  are parameters describing phase shift. Application of a least squares optimisation leads to a best fit of these equation parameters for the precipitation and temperature time series in all study catchments. These parameters are subsequently passed to Equation 2.18.

$$ST = \delta_p \operatorname{sgn}(\Delta_T) \cos(2\pi(s_p - s_T)/\tau) \quad (2.18)$$

The dimensionless variable  $ST$  describes the combined effect of liquid input seasonality and the timing difference between liquid input and potential evaporation signals. The index ranges between -1 and 1, where a negative value represents a seasonal, out of phase signal and a positive value shows a seasonal, in phase signal. An  $ST$  value around zero shows that the seasonality of a study catchment is low.

### Interstorm duration

Another climate variable that is used in this study is the mean interstorm duration (ID). This variable describes the average time period between liquid input events (defined with a threshold of 1 mm in this study). Snow dynamics may complicate providing a good description of the Mean interstorm duration, because no liquid will enter the root zone in winter time leading to unrealistically large values of ID. Therefore, in this study, the mean interstorm duration is only computed in non-winter months.

### Snow parameters

The influence of snow on the root zone storage capacity is an important investigation topic in this study. Therefore, different snow parameters have been analysed in this study, ranging from average yearly maximum snow water equivalent to the total number of snow days in a catchment (both determined from the snow module). However, the parameter that is used most in this study and is generally considered representative for the influence of snow in a catchment, is the relative amount of precipitation falling as snow ( $P_{s,rel}$ ). This parameter is determined with equation 2.19.

$$P_{s,rel} = \frac{P_s}{P_{tot}} \quad (2.19)$$

where:

$$\begin{aligned} P_s &= \text{Solid precipitation input} \\ P_{tot} &= \text{Total liquid input} \end{aligned}$$

The solid precipitation input is obtained from the snow module. An overview of the other snow parameters that have been considered in this study can be found with the other climate parameters in Appendix C.1.

## 2.4.2. Landscape variables

The landscape variables that are used in this study either define topographical variation or land cover differences. The parameters that are used most frequently and require explanation are discussed in this subsection. Other landscape parameters can be found in Appendix C.2.

### Land cover

The types of land cover that have been considered in this study are bare soil, grassland, cropland, shrubland or herbaceous cover and forest. Their influence on  $S_r$  is checked by determining the percentage catchment coverage of each land cover type. The dataset used to define this coverage is given in Section 2.2.5. In this study, the land cover dataset from 2002 is used to represent cover percentage over the entire study period, being the middle year of the land cover dataset extraction period.

### Topographical descriptors

A few of the topographical parameters that are considered in this study are the percentages northerly, southerly, westerly and easterly aspect, catchment average and maximum slope and ruggedness and mean elevation of a catchment. However, the parameter that is used most in this study and is generally considered representative for the influence of topography in a catchment, is the elevation difference in a catchment ( $\Delta H$ ). Note that all topographical variables that are used in this study are derived from the Digital Elevation Models described in Section 2.2.4.

### 2.4.3. Discharge variables

Lastly, a variety of discharge signatures was tested to see whether these could be used to describe  $S_r$ . An overview of all parameters is provided in Appendix C.3. Only the parameters that are discussed in the results section of this study are explained in this subsection.

#### Phase lag discharge and potential evaporation

The phase lag between discharge and potential evaporation ( $\phi_{Et,Q}$ ) describes the amount of time that expectedly exists between the two largest fluxes of water from a catchment. It is defined as the average number of months between the discharge peak and the potential evaporation peak in a catchment.

### 2.4.4. Runoff coefficient or evaporative index

The runoff coefficient (RC) is a parameter that can not be subdivided in one of the parameter classes. It describes how the liquid input in a catchment is distributed between evaporation and discharge, as presented by equation 2.20. This distribution of water may depend on a lot of different parameters, amongst others landscape variables such as vegetation or land cover (e.g. Donohue et al., 2007, Zhang et al., 2001), topographical influences (e.g. Shao et al., 2012) and climatic variables (e.g. Chen et al., 2007). A high runoff coefficient indicates most of the water in a catchment runs off, whereas a low RC means more water is evaporated in a catchment. The runoff coefficient is directly related to the evaporative index ( $RC = 1 - EI$ ) and is therefore an important parameter in the Budyko framework. Like the evaporative index, the runoff coefficient in the Budyko framework is bound by the energy limit and the water limit as explained in Section 2.2.2. In this study, both RC and EI are used interchangeably.

$$RC = \frac{\overline{Q}}{\overline{P}} \quad (2.20)$$

where:

$$\begin{aligned} \overline{Q} &= \text{Long term average discharge (mm/d)} \\ \overline{P} &= \text{Long term average liquid input (mm/d)} \end{aligned}$$

## 2.5. Assessment strategies

To achieve the main goal of this research, the relationship between  $S_r$  and all the climate, landscape and discharge variables has to be identified. The techniques that have been applied to do this are explained in this section. Besides, the approach used to identify the influence of snow on the root zone storage capacity and the approach to determine the regional difference of several descriptor variables are discussed.

### 2.5.1. Individual relationships

All parameters considered in this study are individually compared with  $S_r$  to identify strong individual relationships. This has been done by making scatter plots in which the root zone storage capacity of a catchment is plotted against the potential descriptor variable for all catchments. If a relationship between the catchment parameter and  $S_r$  exists, a certain plotting pattern is expected. Furthermore, the correlation between all study parameters and  $S_r$  is analysed using Pearson's correlation coefficient, where the statistical significance of the results is provided with the p-value.

### 2.5.2. Combined relationships

It is expected that  $S_r$  can not purely be explained by individual catchment parameters only, but rather by a combination of descriptor variables. This has been tested in several ways. Firstly, different combinations of potential descriptor variables are analysed using multi-dimensional plots, in which colour variation is used to increase dimensionality.

Furthermore, several multiple linear regression techniques are used to identify the combined effect of several key parameters on  $S_r$ . To start with, parameters that show too much multicollinearity are excluded from the analysis. After this, two sequential feature selection techniques are applied. Although often used to find an optimal subset of variables, in this study the sequential feature selection techniques are used to identify which variables have the largest influence on the performance of a multiple linear regression model for  $S_r$ .

A sequential forward selection (SFS) is an algorithm that adds features of a dataset to a certain evaluation model and presents the model performance for every iteration. During every iteration, the parameter that improves model performance the most is added to the model and the model performance is presented graphically (e.g. Marcano-Cedeno et al., 2010). The other sequential feature selection method applied in this study is the sequential backward elimination (SBE). In this algorithm, all parameters are part of the model and the least significant parameter to model performance is removed from the model during every iteration.

Using the most important parameters that are identified in the preceding analyses, subsequently a multiple linear regression model is applied and used to predict  $S_r$  in Canada using cross-validation, this way checking whether these parameters are indeed controlling the root zone storage capacity in Canada and what the predictive capability of these controls is. Besides, the multiple linear regression model derived for Canada is used to estimate  $S_r$  in Finland, using data from de Boer-Euser et al. (2019), to check whether the descriptor variables of  $S_r$  in Canada can also be used to predict root zone storage capacities in other boreal regions.

The two performance metrics that are used to analyse multiple linear regressions are the coefficient of determination ( $R^2$ ) (e.g. Maddala, 1986, Menard, 2000) and  $R^2$ -adjusted (e.g. Diez et al., 2012), like defined in respectively Equation 2.21 and 2.22.

$$R^2 = 1 - \frac{\sum_i (y_i - \hat{y})^2}{\sum_i (y_i - \bar{y})^2} \quad (2.21)$$

$$R_{adj}^2 = 1 - \frac{\sum_i (y_i - \hat{y})^2}{\sum_i (y_i - \bar{y})^2} * \frac{n-1}{n-k-1} \quad (2.22)$$

where:

- $y_i$  = Observed value of dependent variable
- $\hat{y}$  = Predicted value of dependent variable
- $\bar{y}$  = Mean value of dependent variable
- $n$  = Number of cases used to fit the model
- $k$  = Number of predictor variables in the model

In a regression, the coefficient of determination is equal to the square of the Pearson correlation coefficient. However, when such a regression is used in a prediction which is subsequently compared to data that are not used in the model-fitting procedure,  $R^2$  can become negative. This will happen when the fitted regression model performs worse than the mean of the data (when the numerator is larger than the denominator in Equation 2.21). Furthermore,  $R^2$ -adjusted penalises the performance of the regression model whenever it is using too many variables.

### 2.5.3. Snow influence

As stated before, the study catchments experience snow dynamics during winter time. The influence of such snow dynamics on the root zone storage capacity is tested by comparison of two different  $S_r$  computations, derived with ( $M_s$ ) and without snow module ( $M_n$ ). The difference in  $S_r$  (Equation 2.23) and the relative difference in  $S_r$  (Equation 2.24) will give information about the importance of snow on the root zone storage capacity and can be compared to other snow related variables.

$$\Delta S_r = S_{r,n} - S_{r,s} \quad (2.23)$$

$$\frac{\Delta S_r}{S_r} = \frac{S_{r,n} - S_{r,s}}{S_{r,s}} \quad (2.24)$$

where:

- $S_{r,s}$  = Root zone storage capacity computed with snow module
- $S_{r,n}$  = Root zone storage capacity computed without snow module

It has to be noted that in both model runs, interception is not taken into account. This is because the difference in total interception between  $M_s$  and  $M_n$  (caused by the fact that no interception occurs during the snow period in the model run with snow module), causes a difference in total estimated transpiration to occur from the catchment long term water balance (equation 2.25).

$$\overline{E}_t = (\overline{P} - \overline{E}_i) - \overline{Q} \quad (2.25)$$

As such, the total transpiration would be larger for  $M_s$ , which has an effect on computed storage deficits and as such computed  $S_r$ . Because the only parameter of interest in this comparison is the influence of snow, the maximum interception capacity is set to 0 in both model runs, so no transpiration differences between the two model runs occur.

As stated before, the difference in  $S_r$  is compared to different earlier defined snow parameters, to better identify the influence of snow on the root zone storage capacity. However, because snow is expected to play a role in the seasonality and timing of the liquid input into the root zone, it is likely that parameters such as the difference in seasonality, timing and ST will change between the different model runs. The difference in  $S_r$  between  $M_s$  and  $M_n$  is therefore also compared with the difference of these seasonality and timing parameters between the two model runs.

#### 2.5.4. Regional variability of descriptor variables

To test whether different variables may have a distinct effect on the root zone storage capacity in catchments with different climatic and geographical functionality, catchments are clustered based on similar functioning. Besides, to test whether such difference in functionality is caused by the geospatial spread of catchments, the distribution of the functional clusters in Canada is mapped. Clusters of similar functioning are obtained by application of a principal component analysis (PCA) in combination with a k-means clustering approach, both of which are explained in this section.

A PCA is an example of a dimensionality reduction procedure that increases the readability of a dataset without losing much information (Smith, 2002). In a PCA, the dataset is first standardised after which a set of orthogonal vectors is used to describe the variance in a dataset with multiple dimensions. The eigenvector through the origin that explains most of the variance (has the largest eigenvalue) is called principal component 1 (PC1). This eigenvector is a linear combination of all dimensions in the dataset. An orthogonal eigenvector to the PC1 vector that explains the second most variance is then called PC2. This is repeated until there are equally as many vectors as dimensions in the dataset. In the PCA-plot the first two principal components are used as axes. The original data can then be mapped in the principal component plot using the linear combination of all dimensions as described by the two eigenvectors of the principal components. Because not all principal components can be used in this PCA-plot, some of the information of the dataset is lost, but it gives a good overview of the largest spread of the data. This way, data points that plot close to each other in a PCA plot show largely similar behaviour for most of the variables that are considered.

The main variables of a dataset can also be plotted in a principal component analysis. The importance of a variable on a principal component can be obtained from the eigenvector. This way, from the first two eigenvectors, every variable can be plotted as a vector on the PCA-plot. The direction and magnitude of a variable then tell something about its influence on the principal components of the plot. Variables that plot in the same direction are therefore largely correlated, while variables that plot in different directions are negatively correlated. In the same way, whenever a variable vector plots in the same direction as several data points, this variable exerts a large influence on these data points. Likewise, an opposite pointing vector shows a negative relationship between the data points and the variable. Lastly, whenever variables and data points are orthogonal to each other, they are not largely related.

Because a PCA-plot can show data points that have similar behaviour and shows the main variables that influence these data points, the principal component analysis can be used to identify data clusters of similar functioning. Clustering is performed by application of k-means clustering (MacQueen et al., 1967). In this procedure, k clusters are identified in an iterative process of finding centroids of the clusters. Starting with a group of randomly selected centroids, every iteration optimises the position of the centroids by moving them closer to the nearest data group. Once the centroids are indeed in the centre of every cluster they are stabilised and no change will occur in further iterations. This way, k clusters are identified. Note that the number of clusters is an arbitrary choice in this clustering procedure. In this study, the number of clusters has been

derived by trial and error. Application of k-means clustering in the principal component analysis leads to identification of groups that are defined by the same variables and therefore show similar functioning. In this study, the PCA clustering leads to catchment clusters of similar functioning, which are plotted on a map to see whether their geographical spread influences their behaviour. Using a comparison of the root zone storage capacity within each cluster, the influence of certain variables on  $S_r$  in different functional clusters is analysed.

Lastly, the entire approach of this study has been coded in Python. An overview of the most relevant scripts that have been used is provided in Appendix D.

# 3

## Results

In this chapter, the results are presented and discussed. Firstly, the root zone storage capacities that have been obtained using the water balance approach are described in Section 3.1. Subsequently, the individual relationships between climate, landscape and discharge variables and  $S_r$  are presented in Section 3.2, after which the combined effect of several descriptor variables on  $S_r$  and their predictive capability is discussed in Section 3.3. In Section 3.4, the influence of snow on the root zone storage capacity is analysed, after which the catchments are clustered based on similar functioning in Section 3.5 to identify how  $S_r$  behaves differently in different types of catchments and how this is influenced by their geographical location in Canada.

### 3.1. Root zone storage capacity magnitudes

Figure 3.1 presents the distribution of root zone storage capacities in 230 Canadian catchments, computed using the water balance approach as described in Section 2.3. The precise magnitudes of  $S_r$  per catchment can be found in Appendix E.

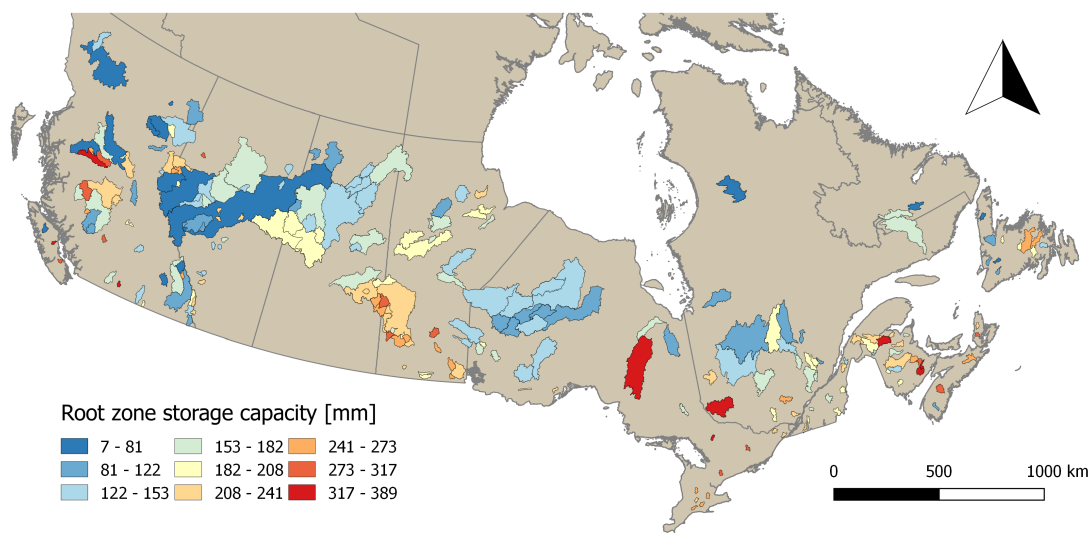


Figure 3.1: Distribution of root zone storage capacities in the study catchments. High magnitudes occur in the south east and centre of Canada. Low magnitudes are found in the north western regions.

$S_r$  is normally distributed over the Canadian catchments with a mean magnitude of 183 mm and a standard deviation of 70 mm. The minimum and maximum magnitudes found in this study are respectively 7 mm and 389 mm. The range of storage capacities in Canada coincides with results found in earlier climate-derived  $S_r$  studies (e.g de Boer-Euser et al., 2019, Gao et al., 2014). The geospatial spread as shown in Figure 3.1 shows some distinct clusters in different regions, suggesting that the descriptor variables of the root zone storage

capacity may vary in different regions. This is further investigated in Section 3.5. In general it seems that larger values for  $S_r$  occur in the south-east of Canada, while lower values are found in the north west of the country.

## 3.2. Individual effects of descriptor variables

To understand why the root zone storage capacities spread out over Canada like shown in Figure 3.1, it is important to identify its main descriptor variables. This is attempted by comparing different climate, landscape and discharge parameters and their corresponding root zone storage capacity between all catchments in several scatter plots and by testing their linear correlation using the Pearson correlation coefficient. Only a selection of parameters is presented in this section. The parameters that are displayed either show a relatively high correlation with  $S_r$  or are expected to show a good correlation based on earlier studies. An overview of all scatterplots is given in Appendix F.

### 3.2.1. Climate variables

Figure 3.2 shows the relationship between a selection of climate parameters and  $S_r$ . The Pearson correlation coefficient ( $r$ ) is shown in the title as a measure of the linear regression performance, together with the p-value that defines the statistical relevance of the relationship. Colours indicate the fraction of solid precipitation in a catchment ( $P_{s,rel}$ ).

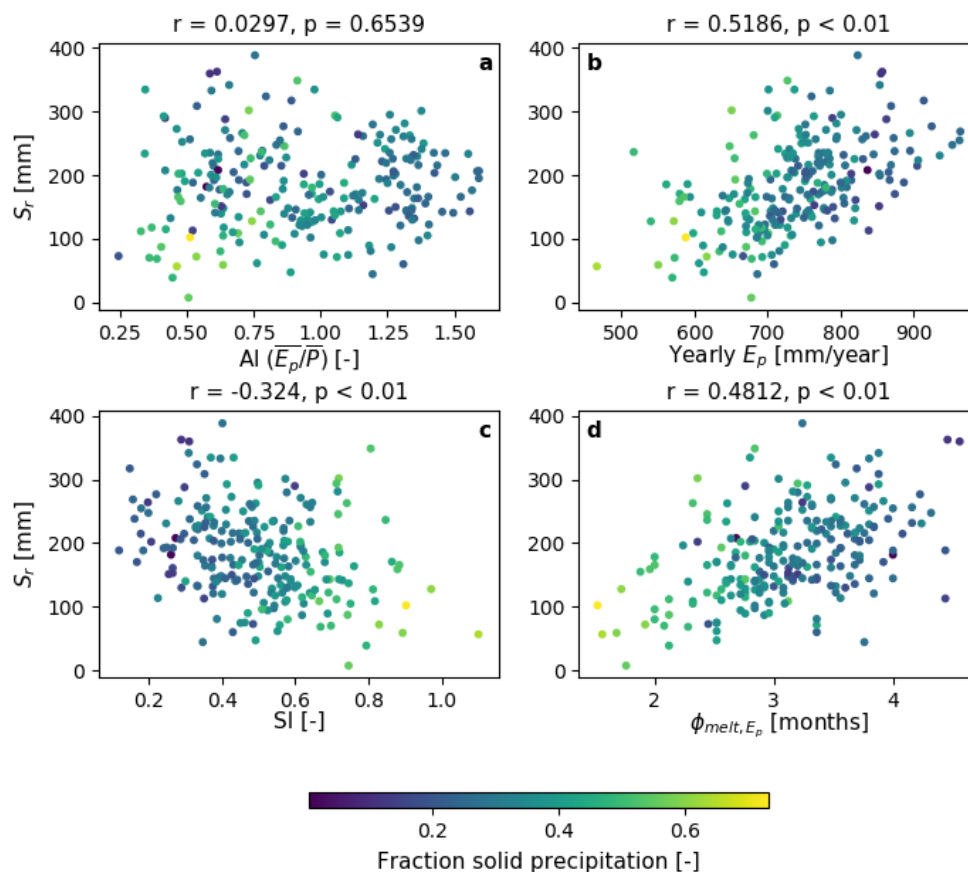


Figure 3.2: Relationships between  $S_r$  and climate indices (a) aridity index, (b) yearly potential evaporation, (c) seasonality index and (d) phase lag between maximum melt input and potential evaporation output. Colours indicate percentage solid precipitation. Titles show Pearson's  $r$  and statistical  $p$ -values.

### Aridity index

The aridity index (AI) that is presented in Figure 3.2a individually has no significant relationship with  $S_r$  in Canadian catchments ( $r = 0.03$ ,  $p = 0.65$ ). Although different studies (e.g. Gentine et al., 2012, Yang et al., 2016) have shown that variation in AI may affect the magnitude of  $S_r$ , these studies considered different climatic regions with other atmospheric demands and precipitation inputs compared to Canada. Apparently in Canadian climates,  $S_r$  is fairly well distributed for different catchment aridities, which is consistent with root depth observations in boreal temperate regions done by (Schenk and Jackson, 2002). However, this does not mean that AI does not effect  $S_r$  at all. In fact, catchment aridity has shown to be an important descriptor in combination with other variables, as presented in Section 3.3 and further.

### Annual potential evaporation

A parameter that shows a significantly better relationship with  $S_r$  ( $r = 0.5186$ ) is the yearly average potential evaporation ( $E_p$ ), as shown in Figure 3.2b. The root zone storage capacity increases with rising annual average potential evaporation. A large  $E_p$  means there is a high atmospheric water demand. As such,  $E_p$  gives an upper bound for the total amount of yearly transpiration that can possibly occur. This means that higher  $E_p$  increases the potential of a larger outgoing evaporative water flux from a catchment which, depending on several other conditions also increases the requirement a larger storage capacity. However, it should be noted that the amount of water that enters the system (yearly precipitation) and the way in which this water is allocated to transpiration due to different catchment characteristics also play a significant role in determining total transpiration flux, which is further explained in Section 3.3.

### Seasonality index

The relationship between the seasonality index of the liquid input (SI) and the root zone storage capacity is shown in Figure 3.2c. SI shows a slight negative correlation with  $S_r$  ( $r = -0.324$ ). This is a rather unexpected result compared to conventional studies (e.g. Gao et al., 2014), where a clearer, positive relationship between seasonality and root zone storage capacity generally occurs. The main difference between these earlier studies and this study is the influence of snow. Presumably, therefore, the occurrence of snow in Canadian catchments and its influence on the timing of liquid input causes the correlation between  $S_r$  and SI to be negative as opposed to conventional studies. Further elaboration on how snow dynamics influences timing and how this may affect the effect of SI on  $S_r$  is provided in Section 3.3.2 and Section 3.4.

It should be noted that snow dynamics generally increases the seasonality of liquid input in most Canadian catchments, which is confirmed by the higher values for liquid input SI compared to SI based on precipitation (shown in Figure E2 number 26 in Appendix F). In regions with snow dynamics, liquid can only enter the system during the time of year in which temperatures are above a certain threshold. Therefore, the total period in which liquid can enter the system in catchments with a long winter period is limited, leading to an increase of seasonality. Besides, all precipitation that falls spread out during the winter period enters the system as snow melt, which has a very seasonal character. Thus, like shown in Figure 3.2c, the seasonality index increases for increasing fractions of solid precipitation ( $P_{s,rel}$ ).

### Phase difference snow melt and potential evaporation

The last climate variable that is presented in 3.2d is the phase difference between the peak input of snow melt and the peak input of atmospheric energy demand ( $\phi_{melt,Ep}$ ), which shows a relatively large individual correlation with  $S_r$  ( $r = 0.4812$ ). Snow melt potentially has a large share in the liquid input into the system. As such, whenever the peaks of the snow input and energy input are further away from each other, this leads to fewer direct overlap between the liquid input due to snow melt and output due to transpiration, which generally follows atmospheric energy demand patterns. In such case, the yearly water deficit is larger and more water needs to be stored to account for the evaporative demand. Therefore, decreasing  $\phi_{melt,Ep}$  leads to an increase in  $S_r$ .

It is important to note that the influence of snow melt on the root zone storage capacity decreases whenever the liquid input is dominated by liquid precipitation rather than snow melt (i.e. when  $P_{s,rel}$  is low). This means that for catchments with low  $P_{s,rel}$ , the liquid input of snow melt will be relatively low and the influence of  $\phi_{melt,Ep}$  on  $S_r$  is expected to be smaller. In these cases, the peak of the liquid input is not equal to the peak of the melt input, which becomes clear by comparing Figure 3.2d with Figure F.1 number 12 in Appendix F, where the phase lag between the peak input of total liquid input and the peak energy input is compared with  $S_r$ .  $\phi_{melt,Ep}$  is thus not representative for all catchments due to their large variation in  $P_{s,rel}$  and is therefore not considered a fair descriptor variable of  $S_r$ . It is interesting, however, that catchments with small

$P_{s,rel}$  still correlate well in Figure 3.2d, although not being largely melt dependent. In general, catchments with early snow melt also have an early onset of evaporation as both variables are temperature dependent. Therefore, catchments with large  $\phi_{melt,Ep}$  are likely to have a higher yearly  $E_p$ , which increases the chances of having a higher root zone storage capacity. This explains the ongoing relationship between  $\phi_{melt,Ep}$  and  $S_r$  in 3.2b for catchments with low  $P_{s,rel}$ .

### 3.2.2. Runoff coefficient

Figure 3.3a shows the relationship between the runoff coefficient (RC) and  $S_r$  ( $r = -0.35$ ). RC defines how the long term average water input in a catchment is distributed between runoff (Q) and actual evaporation ( $E_a$ ). The magnitude of the runoff coefficient depends on both landscape and climate characteristics, like stated in Section 2.4.4. A relatively low RC indicates that a catchment allocates most of the water towards actual evaporation. As a result, the outgoing transpiration flux is large and it is likely that large storages are required, which explains the negative correlation between RC and  $S_r$ . It is important to note that the relationship between  $S_r$  and RC is also dependent on atmospheric conditions, e.g. the amount of water that can actually be distributed over the catchment. Therefore, it's expected that the variance visible in Figure 3.3a can be explained by other indices that describe these atmospheric conditions. Further elaboration on this combined effect of RC and atmospheric conditions can be found in section 3.3.

### 3.2.3. Landscape variables

Figure 3.3b-f shows a collection of landscape parameters that are expected to influence  $S_r$ . Again, the Pearson correlation coefficient and the statistical p-value are shown in the title of the Figures. Fractional grassland cover is not considered in this section, because this type of land cover is underexposed in the study catchments.

#### Land cover

Many different studies have shown that the total amount of transpiration in a catchment depends on the type of land cover that is present in the catchment. Following their results, it is expected that catchments with a large forest cover require a larger storage compared to catchments with few forest cover (e.g. Zhang et al., 2001). Figure 3.3b shows how  $S_r$  varies for different catchment fractional forest cover ( $P_f$ ). No clear correlation between the total percentage of forest in a catchment and  $S_r$  is shown, which deviates from earlier stated expectations. The lack of correlation between  $P_f$  and  $S_r$  could have several causes. Firstly, the total forest fraction is high in most catchments considered in this study, leading to few variation in land cover. Comparison of the influence of forest cover on the root zone storage capacity is therefore complicated and differences in  $S_r$  are likely caused by variation in other controls (e.g. climate controls). Secondly, water uptake for transpiration may vary largely per tree type. Differences in tree types were not considered in this study, potentially contributing to the large spread in  $S_r$  for high forest cover. Lastly, forest cover density, a variable that was not considered in this study either, may also be a complicating factor in relating  $S_r$  with  $P_f$ . The density of forests can have large influence on the total catchment average transpiration and therefore on  $S_r$ . Variety in forest density could therefore cause spread in  $S_r$  for high forest cover percentages.

Although there are several possible explanations for the scatter shown for large fractional forest cover, another striking observation is that  $S_r$  does not show a decreasing trend for smaller forest cover percentages. A possible explanation for this is that catchments with small forest cover fraction and large  $S_r$  are generally covered with a large fraction of cropland ( $P_c$ ) in the study catchments (Figure 3.3c). According to computations of  $S_r$  in this study, crops require a relatively high root zone storage capacity. This is not conform expectations, considering forest covered catchments are expected to transpire more than agricultural catchments in rain-fed conditions. A potential reason for these unexpected results is irrigation. Whenever rain water is stored and later used for irrigation this water will end up in the evaporative flux, whereas it would normally end up in the discharge flux. Using this water for irrigation causes the liquid to enter the system during an entire different period then accounted for in this study. This could potentially lead to overestimated storage deficits in this study and therefore larger root zone storage capacities. However, land cover maps suggest that most agricultural catchments are rain fed and not irrigated, so whether the high  $S_r$  for crop cover is really related to irrigation is questionable. Another possible explanation is that crops may design their root zone storage capacity based on short term dynamics, as they are generally harvested within a few years. This may complicate application of the approach used in this study in agricultural areas and lead to unexpected results (see also Section 4.3.5).

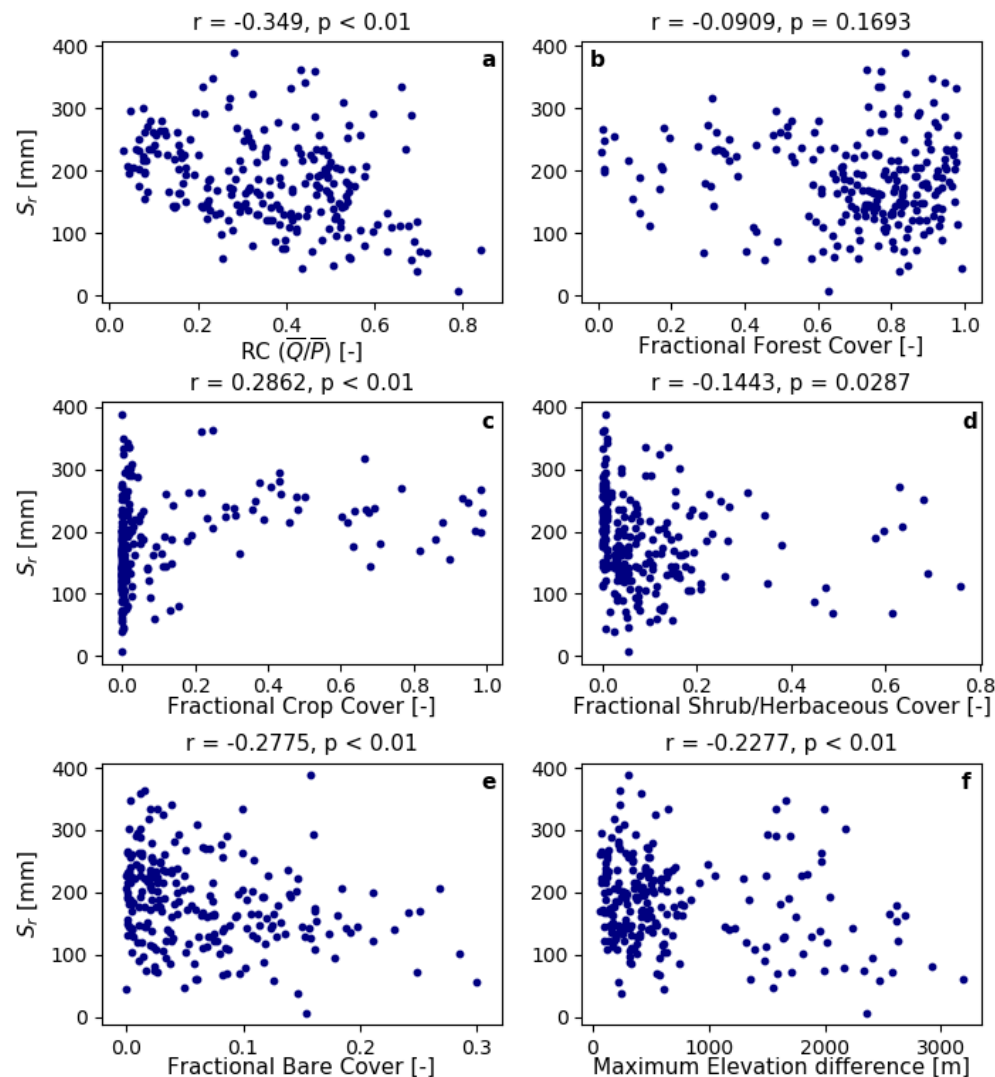


Figure 3.3: Relationships between  $S_r$  and landscape indices (a) runoff coefficient, (b) fractional forest cover, (c) fractional crop cover, (d) fractional shrub/herbaceous cover, (e) fractional bare cover and (f) maximum elevation difference. Titles show Pearson's  $r$  and statistical  $p$ -values.

The other land cover types that are considered in this study (a combination of shrublands and herbaceous cover ( $P_s$ ) and bare soil ( $P_b$ )) do show a slight decrease in  $S_r$  for increasing land cover percentage, although also showing considerable variance (Figure 3.3d and 3.3e). Particularly the increase of bare land cover percentage in a catchment shows a significant influence on  $S_r$  ( $r = -0.28$ ), which can be rationalised by the fact that no water can be stored in soil without vegetation and as such a lower  $S_r$  is evident. The large scatter for percentages close to zero is probably related to other descriptors (since  $P_b$  has no influence here). It should be noted that the decrease in  $S_r$  for larger percentages of bare land cover may be partly related the undefined return periods that are applied in these catchments.

In this study, all different land cover types that are present in Canada have been merged into 4 categories for simplicity. It is possible that variance in land use types within a chosen category complicates interpretation

of its relationship with  $S_r$ , which may explain why landscape parameters do not behave as expected and show weak correlations with  $S_r$ . It is therefore interesting to consider larger variety in land cover categories in future studies on  $S_r$  descriptor variables.

### Topographical influence

Lastly, the influence of topographical indicators on  $S_r$  is tested by using the maximum elevation difference ( $\Delta H$ ) in a catchment as a proxy for its ruggedness, slope and total elevation, which are also considered individually in Appendix E2. Figure 3.3f shows the relationship between  $\Delta H$  and  $S_r$  ( $r = -0.23$ ) and indicates that  $S_r$  is generally slightly lower for larger elevation difference in catchments. A potential reason for this is that catchments with large elevation differences generally have shallower soils at higher elevation and therefore limited room for water storage. Besides, sloped areas may increase the runoff capacity of preferential pathways that are particularly present in forested slopes, leading to larger runoff and fewer storage of water. Lastly, catchments with large elevation difference are likely to have large snow dynamics. This means that the effects of snow melt (see section 3.4), may also reduce root zone storage capacities in regions with large elevation difference.

### 3.2.4. Discharge variables

Lastly, the relationship between a discharge variable and the root zone storage capacity is shown in Figure 3.4. Again, the Pearson correlation coefficient and the statistical p-value are shown in the title of the Figure.

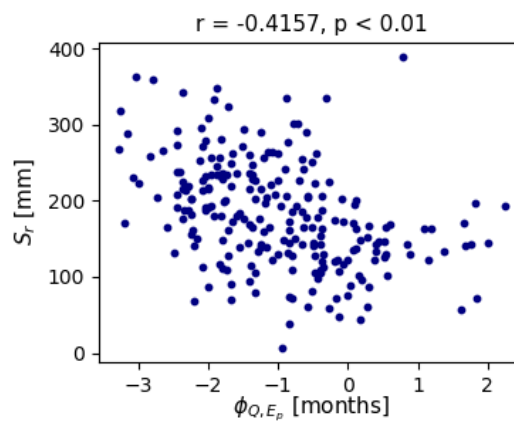


Figure 3.4: Relationships between  $S_r$  and the phase lag between discharge and potential evaporation. The title shows Pearson's  $r$  and statistical  $p$ -value.

### Phase difference potential evaporation and discharge

The discharge parameter that shows highest correlation ( $r = -0.42$ ) with  $S_r$  is the phase difference between the peaks in  $E_p$  and  $Q$  ( $\phi_{Q, E_p}$ ), as presented in Figure 3.4a. The figure shows that whenever the phase lag between both peaks decreases,  $S_r$  becomes smaller. It is likely that the timing of the discharge peak is related to the timing of the liquid input peak. A small  $\phi_{Q, E_p}$  would then indicate large overlap between maximum liquid input and output from the root zone, reducing the need for large storages.

Other discharge variables were also considered in this study, but they generally showed poor correlation with the root zone storage capacity. Besides, due to their relationship with many climate variables, discharge variables are difficult to directly relate to  $S_r$ .

To conclude this section, analysis of scatter plots and linear regression has shown that yearly  $E_p$ , RC and SI have the most relevant individual relationship with  $S_r$ , whereas land cover variables generally show poorer correlations. Particularly the relationship between SI and  $S_r$  is different from conventional studies. Discharge variables have shown to be related to climate variables and are difficult to directly relate to  $S_r$ . The relatively large variance for all individual relationships between catchment variables and  $S_r$  suggests that the root zone storage capacity is better explained by a combination of descriptor variables, which will be investigated in the following section.

### 3.3. Combined effects of descriptor variables

The analysis of the individual relationship between  $S_r$  and several variables has shown that although some parameters show decent correlation with  $S_r$ , there is still considerable variance in all of these relationships. This likely indicates that the root zone storage capacity is rather controlled by a combination of parameters instead. Therefore, this section describes how a combination of several parameters may influence root zone storage capacities in Canada.

#### 3.3.1. Budyko framework

Firstly, the spread of  $S_r$  on the Budyko framework as shown in Figure 3.5 is considered. As stated before, this framework is a graphical description of the expected separation of water between runoff and actual evaporation for a given atmospheric situation. The aridity index describes how arid a climate is by relating the long term average atmospheric water demand ( $E_p$ ) to the long term average liquid input ( $P$ ). The evaporative index on the other hand describes distribution of the long term average liquid input into discharge and actual evaporation (note that the evaporative index equals  $1 - RC$ ). The curve represents the expected separation of  $P$  for a given climate and has been tested with catchments from all over the world (e.g. Budyko et al., 1974, Gentile et al., 2012, Ye et al., 2015). More of the total water is generally expected to evaporate in dry catchments with a relatively high atmospheric demand and low liquid input (water limited). Vice versa, a wet catchment with low potential evaporation can not evaporate a lot due to limited atmospheric demand (energy limited), which leads to a predominant separation of the total liquid input towards streamflow. Although most catchments plot approximately along the Budyko curve, variations from the curve are possible and predominantly caused by catchment characteristics such as soil structure, vegetation type and topographic controls (Greve et al., 2015), as well as climate parameters. However, a clear description of the combined effect of these parameters on deviations from the Budyko framework still lacks in hydrology.

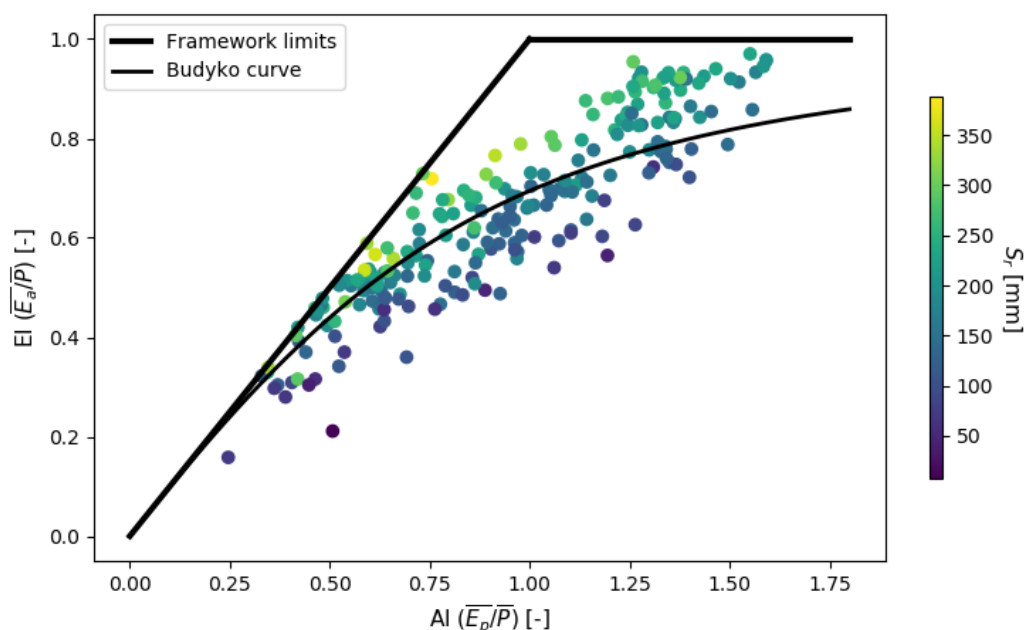


Figure 3.5: Variation of  $S_r$  in the Budyko framework. A strong relationship of AI and EI on  $S_r$  can be observed. Colours indicate the magnitude of  $S_r$ .

Figure 3.5 shows how the Canadian catchments locate on the Budyko framework. Note that outlying catchments were removed based on their distance towards the framework, which explains why all catchments in Figure 3.5 plot relatively close to the Budyko curve. The colours in 3.5 indicate  $S_r$  magnitude. The distribution of the root zone storage capacity in the Budyko framework shows large dependency on the combined effect of the evaporative index and the aridity index.

Like mentioned before, the aridity index is a descriptor of the long term atmospheric conditions in a catchment and therefore describes the boundaries of water and evaporative energy availability in a catchment. With these given atmospheric conditions, the evaporative index indicates how the total amount of water is distributed between runoff and actual evaporation due to a combination of landscape and climate characteristics. A larger EI relates to a larger flux of actual evaporation, for which generally a larger root zone storage capacity is required, which explains the vertical distribution of  $S_r$  in Figure 3.5 for a given AI.

Variation in AI can theoretically be caused by a change in potential evaporation but in Canada is generally dominated by change in precipitation as shown by the correlations between AI and its determining parameters in Figure 3.6. This means that an increase in aridity index in the study catchments leads to a decrease in total amount of water that can be distributed. Such a shift in AI for an equal ratio between  $E_t$  and P (or equal EI) leads to a lower amount of actual evaporation and thus generally lower required  $S_r$ . As such, it seems that long term average properties that describe landscape and climate (EI and AI) work together as good indicators of  $S_r$  in the study catchments in the way they describe its total actual evaporation.

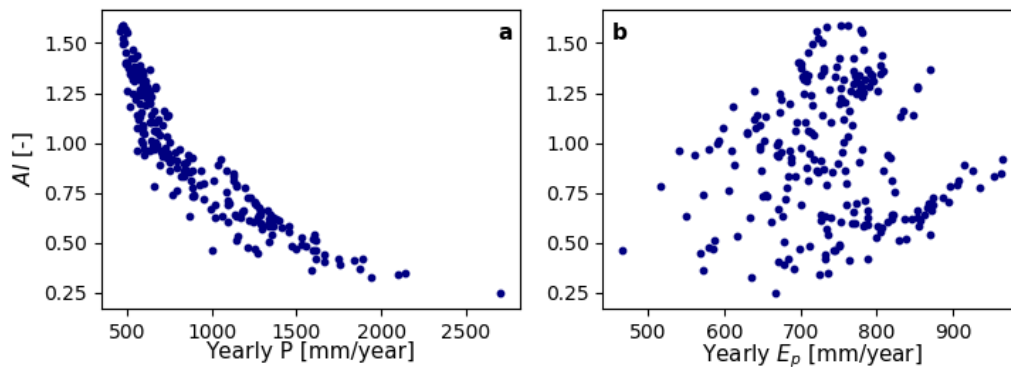


Figure 3.6: Correlation between AI and (a) yearly average precipitation and (b) yearly average potential evaporation. The figures indicate that change in AI is largely dominated by yearly average precipitation.

It is striking that relative components such as AI and EI give an indication of the absolute magnitude of  $S_r$ . In theory, AI and EI can plot on the same location in the Budyko framework with a complete different magnitude of precipitation, which will in turn lead to a different absolute magnitude of actual evaporation and as such another  $S_r$ . However, in Canada, precipitation highly dominates variation in AI (compared to potential evaporation), which means that the total amount of P is approximately equal for a certain AI value (see Figure 3.6a). Therefore, the relative indices AI and EI give a good indication of an absolute value of  $S_r$  in Canada. In regions where the P and  $E_p$  are both largely variable, relative components AI and RC may not indicate absolute  $S_r$  magnitude as good as in the Canadian study catchments.

The representation of  $S_r$  in the Budyko framework helps understand the global distribution of  $S_r$  for different catchment aridities as shown in e.g. Yang et al. (2016). Generally, the largest root zone storage capacities are found for average AI between approximately 0.7 and 1.5. This is also the range where the curve is not particularly close to the framework limits (water and energy limit), allowing for more variation between the curve and the limits, as shown in Figure 3.5. For a changing AI in positive or negative direction, the catchments will generally plot closer to either the water limit or the energy limit, meaning that either  $E_p$  (for the case  $AI < 1$ ) or P (for  $AI > 1$ ) are ceiling actual evaporation rates. For AI close to 1, P and  $E_p$  are fairly close to each other, allowing for larger actual evaporation rates and thus increasing the need for larger root zone storage capacities. This is consistent with results found in e.g. Guswa (2008).

In order to help visualisation of the combined correlation between AI, EI and other control parameters with  $S_r$ , the combined effect of AI and EI on  $S_r$  is encapsulated in a one dimensional indicator in this study, being the relative evaporative index (REI). This new parameter describes the vertical position of a catchment compared to the Budyko curve. Since the Budyko framework relates AI with EI, the relative position of a point compared to the curve indicates how water is distributed for given climatic conditions. As such the REI component is a measure for the position of a catchment on the Budyko framework, which is an important

indicator of  $S_r$  like explained previously. In Figure 3.7a, the relationship between REI and  $S_r$  is presented. The large correlation ( $r = 0.7181$ ) emphasises again the combined effect AI and EI have on the root zone storage capacity.

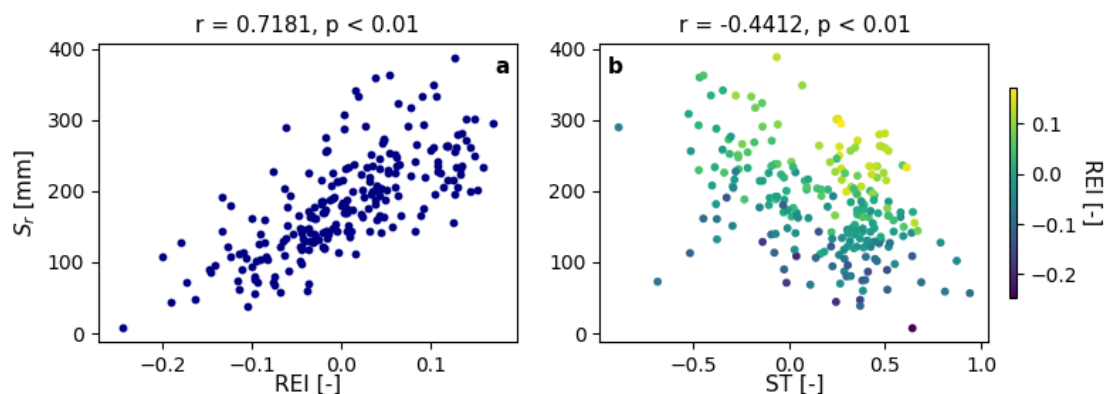


Figure 3.7: Relationship between  $S_r$  and (a) the relative evaporative index and (b) the seasonality timing index, where colours indicate REI. The titles show Pearson's  $r$  and statistical  $p$ -values.

Concluding, this section has shown that root zone storage capacities in Canada have a very strong relationship with the combined effect of long term average catchment parameters AI and EI, in the way they indicate how much of the total water is allocated to transpiration. This makes the Budyko framework an excellent indication tool of  $S_r$  behaviour in Canada. The combined effect of AI and RC in this study has been encapsulated in a one dimensional indicator (REI) to facilitate visualisation in combination with other indicators.

### 3.3.2. Seasonality and timing effects

Earlier results have shown that the seasonality and timing of the liquid input relate with the influence of snow in the Canadian catchments (Section 3.2.1). Whenever the relative amount of precipitation largely consists of snow, seasonality on average becomes larger and the timing difference between the peaks of liquid and energy input decreases. Snow may therefore play a role in how a combination of seasonality and timing effects have influence on the root zone storage capacity. In a country like Canada, where the influence of snow dynamics largely differs between catchments and where large variation in seasonality and timing exists, it is therefore interesting to see how the combined effect of seasonality and timing affects  $S_r$ .

Figure 3.7b shows the relationship between a combined index for seasonality and timing (ST) and the root zone storage capacity, where colours indicate the value of REI. A large negative value for ST relates to a seasonal liquid input that is out of phase with the atmospheric energy demand. Vice versa, a large positive value for ST means the liquid input is seasonal, but in phase with the expected liquid output. Whenever ST locates around 0, the liquid input signal is unseasonal. The Figure shows that seasonal, out of phase behaviour generally leads to high root zone storage capacities, whereas seasonal, in phase behaviour leads to much lower root zone storage capacities, with average values for non-seasonal situations. As such it seems that seasonality in phase with the atmospheric energy demand may indeed reduce root zone storage capacities, whereas out of phase seasonality induces large  $S_r$ . Clearly, seasonality and timing have a combined influence on the magnitude of the root zone storage capacity. The cooperative effect of these two climate variables is related to the total amount water that enters the root zone during the transpiration period. The more direct input of liquid during the transpiration phase, the fewer storage of water is required. Figure 3.8 shows with a simplified schematisation of seasonal and timing components that different combinations of seasonality and timing have another impact on the overlap of liquid input and output during the transpiration phase. In general, whenever the signal of liquid input is unseasonal, timing does not have a large influence on the total overlap of liquid input and output in the transpiration phase. For a seasonal signal however, timing clearly has a large effect on the total overlap of liquid input and transpiration output. Besides, in phase seasonal liquid input will generally provide a larger overlap than non seasonal input, which explains the trend shown in Figure 3.7b.

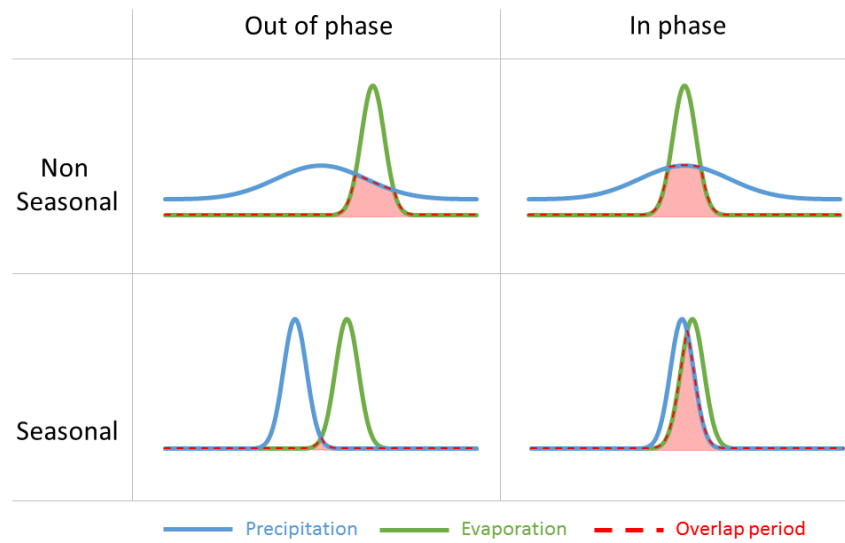


Figure 3.8: How the combined effect of seasonality and timing may influence the period of overlap between liquid input due to precipitation or snow melt and the liquid output due to evaporation.

Generally, the larger the influence of snow in a catchment, the more seasonal the liquid input will be. Besides, the extent of the winter period determines the period of the year during which liquid can enter the root zone and this way snow dynamics influences timing as well. There is large variety in snow influence in the considered study catchments, which explains why such a large variety in the  $S_r$  parameter exists. This indicates that the combined effect of seasonality and timing may vary greatly between different Canadian catchments. Therefore, in the study catchments and expectedly also in other northern regions, use of a combined index for seasonality and timing presents the behaviour of  $S_r$  regarding seasonal dynamics better than solely a seasonality or timing descriptor. This is also shown by the fact that  $ST$  has a larger Pearson correlation coefficient compared to e.g.  $SI$  or  $\phi_{liq, E_p}$ . Note that  $\phi_{melt, E_p}$  has a higher Pearson correlation coefficient, but this parameter is not representative for the liquid input in catchments that are not melt dominated and is therefore not entirely trustworthy as descriptor variable for  $S_r$ .

Figure 3.7b also shows that the variance in the relationship between  $ST$  and  $S_r$  can largely be explained by the earlier identified REI parameter. A large REI indicates more water transpires in a catchment, whereas a small REI shows the opposite. Logically, larger root zones occur whenever the transpiration in a catchment is higher, which is the main source for the variance in the relationship between  $S_r$  and  $ST$ . For a given REI,  $ST$  has a very clear negative correlation with  $S_r$ . As such it seems that  $S_r$  magnitude can be largely explained by how long term average components AI and EI allocate the water for transpiration in a catchment and by how this water is distributed seasonally relative to the atmospheric energy demand.

Concluding, it seems that particularly in regions with large variety in snow dynamics, a combined index of seasonality and timing explains the  $S_r$  magnitude better compared to individual seasonality or timing indicators, due to the different possibilities in which seasonality and timing can cooperate. Furthermore, the combined effect of how AI and EI describe allocation of water for transpiration and how  $ST$  describes seasonal distribution of this water and therefore the overlap between liquid input and atmospheric demand largely describe  $S_r$  magnitude in the study catchments. Note that the individual relationships that were found earlier in Section 3.2 are encapsulated in the descriptor variables found in this section.

### 3.3.3. Multiple linear regression

The combined influence of EI, AI and  $ST$  has shown that a description of the root zone storage capacity requires multiple dimensions. In this subsection, the cooperate effect of the earlier mentioned variables on  $S_r$  is therefore tested using a multiple linear regression and two feature selection techniques. Besides, us-

ing these techniques, it is tested whether any other controls potentially affect the root zone storage capacity. Furthermore, the predictive capability of a multiple linear description of  $S_r$  using parameters that show the largest correlation is tested using both cross-validation in Canada and validation in a distinct boreal area.

Before testing the control parameters in a multiple linear regression analysis it is important to remove the predictor variables that show too much collinearity. This has been done using a correlation matrix and by manual selection. Additionally, parameters describing the timing of purely precipitation instead of liquid input were excluded from the parameter set. Furthermore, REI, SI and timing indices were left out as they are presented by respectively AI and RC and ST. An overview of the full parameter set that has been used in the multiple linear regression analysis is provided in Appendix G.

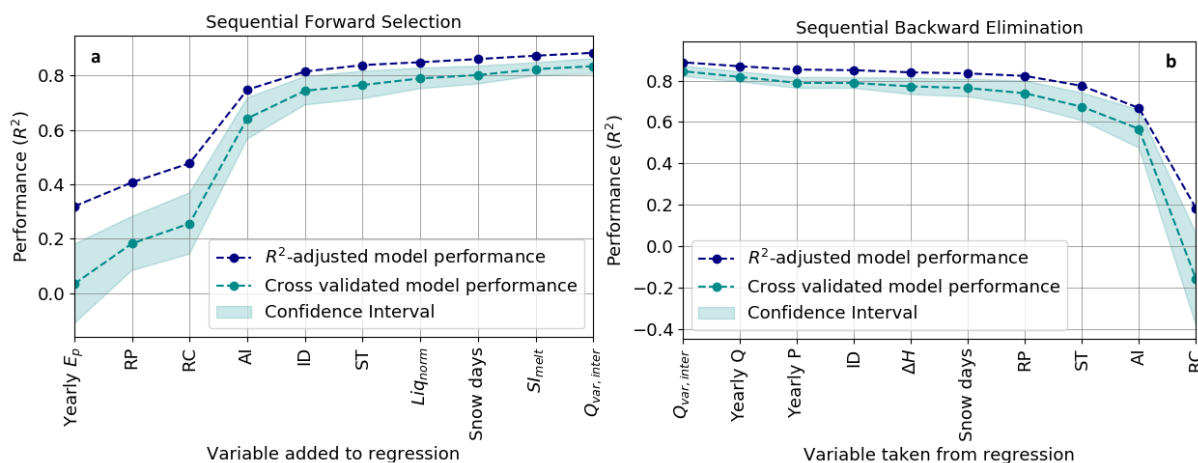


Figure 3.9: The results of (a) sequential forward selection and (b) sequential backwards elimination based on a linear regression model. Variables that are not defined in the text are  $Liq_{norm}$  and  $S_{melt}$ , which respectively are the ratio between the 90 percentile liquid input and the mean liquid input and the seasonality index of snow melt. Note that  $R^2$  can become negative for the cross-validated model performance, whenever prediction by the regression model is worse than the mean of the cross-validation sets. A more detailed description of the coefficient of determination ( $R^2$ ) is provided in Section 2.5.2.

### Sequential Feature Selection

Figure 3.9 shows the results of respectively a sequential forward selection (SFS) and a sequential backward elimination (SBE) procedure. The horizontal axis shows variables that were added to the linear regression in SFS or subtracted in SBE for every iteration. The vertical axis shows the performance of the linear regression model in  $R^2$  after respectively an addition or a subtraction of the parameter on the horizontal axis. Note that  $R^2$  is based on the combined performance of a 10-fold cross validation and on  $R^2$ -adjusted which are both measures that compensate for over-fitting of the model. The cross-validated  $R^2$  can become negative when the performance of the regression in the cross-validation sets is worse than the mean (as explained in more detail in Equation 2.21 of Section 2.5.2). Only addition and subtraction of the first 10 parameters is shown in the figures, because the linear model did not improve significantly for the rest of the parameter set. Please note that RC used as parameter in the multiple linear regression analyses of this section describes the same as EI ( $RC = 1 - EI$ ).

Both SFS and SBE confirm that the combined effect of RC (or EI) and AI significantly describes  $S_r$  magnitude. Once AI is added in SFS or subtracted in SBE, with RC still in the multiple regression set, the model performance changes significantly. This is consistent with the results found earlier in this study. Furthermore, particularly SBE shows the significance of ST, by showing a considerable decrease in  $R^2$  performance when left out of the linear regression model. Surprisingly, the model performance in SFS increases by a much smaller rate when ST is added to the model, which is not expected considering earlier results. This offset is probably caused by the correlation between ST and yearly  $E_p$  as shown in Figure 3.10. Due to the fact that  $E_p$  has the strongest individual correlation with response variable  $S_r$  (see Section 3.2.1), it is added to the linear regression model in the first iteration of SFS. However, since ST and  $E_p$  have a certain correlation, the influence ST has on  $S_r$  is already partly explained by the  $E_p$  variable. Therefore, an addition of ST to the linear

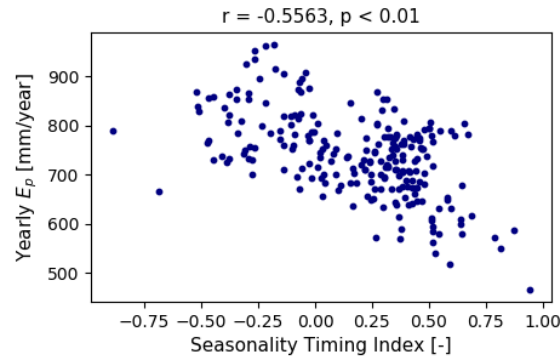


Figure 3.10: Relationship between yearly potential evaporation and seasonality timing index.

model will lead to less improvement of the model performance ( $R^2$ ) whenever  $E_p$  is already in the model, compared to when this is not the case (e.g. in the SBS).

The correlation between ST and  $E_p$  as presented in Figure 3.10 is presumably caused by the snow-dynamics in Canada. Both  $E_p$  and the timing of liquid input are related to temperature. The rise of temperature after the winter period will lead to an onset of evaporation as well as the possibility of liquid to enter the system (which is not happening during winter due to the accumulation of snow). Late onset of potential evaporation generally leads to smaller annual  $E_p$ , while a late entrance of liquid into the system leads to more in phase behaviour of the input and output of liquid and as such a larger ST value.

A variable that has not shown a dominant relationship with the root zone storage capacity by itself but does show a significant increase in performance for both the forward and backward feature selection is the Inter-storm Duration of the non-winter months (ID). Particularly for the forward feature selection the addition of this variable led to a major performance improvement. The coefficient of ID in the linear regression model is positive, which means that it is positively correlated with the root zone storage capacity, which is consistent with previous studies (Gao et al., 2014). A large Inter-storm Duration corresponds to a high number of dry days and few days of precipitation. It is possible that the addition of ID to the regression model accounts for daily variation within the seasonal signal as presented by ST, or that it is an extra description of seasonality that may not be entirely captured by the seasonality timing index. However, the exact reason for model improvement with addition of this parameter is difficult to understand from solely the sequential feature selection analysis.

Other parameters that showed to be relatively important in both feature selection methods are the drought return period catchments optimise their root system to (RP), the inter-annual variability of discharge ( $Q_{var,inter}$ ) and the number of days with snow cover. The effect of the return period may be directly related to the method, where higher drought return periods are linked with larger  $S_r$  by fitting a Gumbel distribution over yearly maxima.  $Q_{var,inter}$  is largely dependent on precipitation, but as root zone storages describe partitioning of water between evaporation and discharge it is possible that the inter-annual variability of discharge is influenced by the root zone storage capacity. Lastly, the number of days with snow cover describes snow dynamics and additionally indicates seasonal behaviour and the period of possible liquid input. A more thorough analysis of the influence of snow dynamics on  $S_r$  is provided in Section 3.4. It should be noted that since multiple linear regressions are difficult to visualise, it is hard to interpret why addition or subtraction of a certain parameter in the feature selection methods leads to model improvement and therefore the influence of the earlier mentioned parameters on  $S_r$  can only be presumed. Besides, the effects of these parameters on model performance are quite small and may therefore rather be a mathematical artefact of the feature selection procedure rather than actually explaining a physical contribution to  $S_r$ .

Lastly, it should be noted that the best combination of parameters has most likely not been found during the forward and backward sequential feature selection. Ideally, the best parameter set would be selected by comparing all possible combinations of variable sets, however this requires too much computational time for the large parameter set used in this study. Additionally, the feature selection results are dependent on the choice of parameters in the first place. Addition of one variable in both SFS and SBE may lead to an entirely different, potentially better subset description. Some parameters that could lead to such change in the SFS

or SBE subset description may not have been considered at all in this analysis (e.g. soil characteristics), or may have been excluded from the feature selection in order to reduce collinearity. This is another reason why it is difficult to interpret the results of the sequential feature selections. Furthermore, it is important to note that all the descriptions considered in this section are based on a linear combination of variables. In practice, the effect of certain parameters on  $S_r$  may be non-linear. Whether this is the case and how this would give a different representation of the controls on  $S_r$  is not considered in this study.

#### Predictive capability of main descriptor variables

The good performance of cross-validated  $R^2$  in the  $S_r$  description using SFS and SBE has led to the theory that  $S_r$  can be predicted using a multiple linear regression with its most descriptive variables. This has been tested by applying 10-fold cross-validation to several multiple linear regression models with different parameter combinations. During such cross-validation, the total dataset is distributed in 10 subsets, which are all individually predicted with a linear regression of the 9 other sets, leading to a predicted  $S_r$  value ( $S_{r,p}$ ) for every catchment. These predicted  $S_r$  values can subsequently be compared to the modelled  $S_r$  value ( $S_{r,m}$ ) from this study.

Many different parameter combinations with variables that showed good performance in the SFS and SBE were tested. The best linear regression model consisted of the parameters AI, RC and ST ( $R^2$ -predicted of 0.72), which is consistent with earlier results. A comparison of  $S_{r,p}$  and  $S_{r,m}$  for this parameter set is shown in Figure 3.11a. Addition of several other parameters that were found in the sequential feature selection methods to this linear regression model did not lead to significant improvement of the prediction.

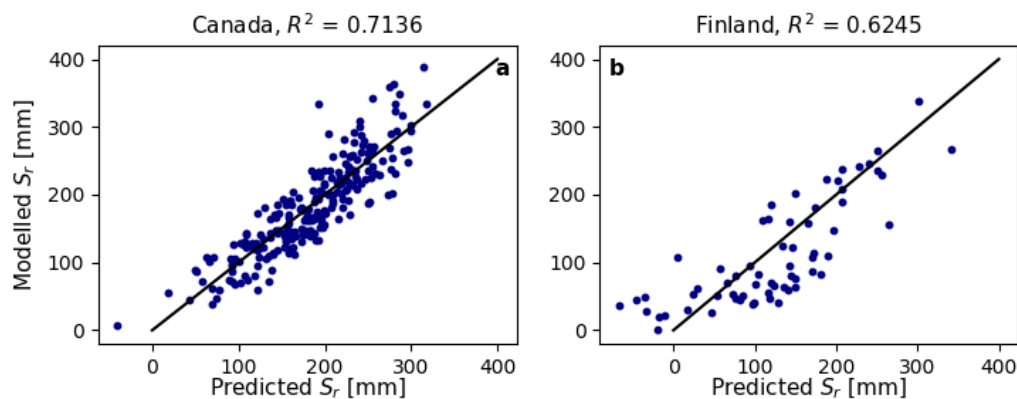


Figure 3.11: Relationship between modelled  $S_r$  and predicted  $S_r$  using a linear regression model with parameters AI, RC and ST in (a) Canada and (b) Finland.  $R^2$ -predicted is provided in the title as a measure for the performance of the prediction.

Figure 3.11 shows that the multiple linear regression model based on parameters AI, RC and ST is an unbiased estimator of  $S_r$ . The mean difference between modelled and computed  $S_r$  is approximately 0 mm, whereas the standard deviation is 32.8 mm. As such, a linear regression model with variables AI, RC and ST is capable of predicting  $S_r$  in Canada with a standard deviation of approximately 32.8 mm.

Note that AI and RC are actually derived from long term average precipitation, potential evaporation and discharge data. It is therefore striking that a multiple linear regression model with variables  $P$ ,  $E_p$ ,  $Q$  and ST performed significantly worse ( $R^2$ -predicted = 0.53) than the earlier discussed model with variables AI, RC and ST. Presumably, this is related to the fact that the precipitation input is not linear (see Figure 3.6) and therefore not well captured by a linear regression model. AI gives a more linearised description of the liquid input (because  $AI = E_p/P$ ), which could lead to a better representation of the set with relative parameter AI and RC rather than the set containing  $P$ ,  $E_p$  and  $Q$ .

Using different approaches, this study has shown that Canadian root zone storage capacities are well described and predicted using long term average catchment variables (AI and RC) and a long term average representation of seasonality and timing (ST). Apparently the daily time scale applied in the approach to derive  $S_r$  used in this study is not necessarily required in order to obtain climate derived root zone storage capacity estimates. In fact, weekly or monthly data of  $P$ ,  $E_p$  and  $Q$  are frequent enough to provide a description

of long term average AI and RC and to provide an estimate of ST. This increases the potential of estimating  $S_r$  in Canadian regions with a lower data sampling frequency and this way extending the overall database of climate derived  $S_r$ . Besides, such estimation of  $S_r$  using long term average parameters increases the potential of simplified application of  $S_r$  in climate models and hydrological models in Canada, or can help in constraining the  $S_r$  parameter in calibration of hydrological models.

In this study, several parameters have proven to be significant descriptors and predictors of  $S_r$ . However, since this study was only applied for Canadian catchments, the results may be biased to Canada-specific circumstances. To test this, and to see whether the predictability of the results in this study go beyond the borders of Canada, the linear regression model resulting from this study is also applied to predict  $S_r$  in Finland. Finland is also a boreal region with considerable snow dynamics and is therefore expected to show similar behaviour to Canada. Besides, data were readily available in Finland from a study performed by de Boer-Euser et al. (2019), thus computation of  $S_r$  is not necessary for these catchments. However, the disadvantage of using this dataset is that it is computed using a slightly different modelling approach. Firstly, the Finnish dataset consists of root zone storage capacities based on a return period of 20 years, whereas in this study return periods were considered variable over catchment land cover. Besides the snow-modelling approach in Finland was based on snow water equivalent measurements, whereas a snow module is used in this study. Another difference between the two modelling approaches is the estimate of the interception threshold. Nevertheless, the multiple linear regression model fitted on the Canadian dataset using the parameters AI, RC and ST seems to perform relatively well when applied to the Finnish dataset as shown in Figure 3.11b, with predicted  $R^2$  of 0.62. On average, the predictive model slightly overestimates  $S_r$ , with a mean difference between modelled and predicted  $S_r$  of 11 mm. The standard deviation of the difference between  $S_{r,m}$  and  $S_{r,p}$  is 52 mm.

Figure 3.11b shows better prediction performance of  $S_r$  for higher magnitudes. This may be related to the fact that low root zone storage capacities do not occur extensively in the Canadian dataset. Besides, the Finnish climate differs from the Canadian climate, with substantially lower potential evaporation rates and a more uniform distribution of precipitation, which could result in different dynamics between AI and RC compared to Canada. Furthermore it is possible that there are other variables that determine root zone storage capacities in Finland, which are not considered to be significant in Canada. For this reason, it is not advised to apply the results from this study on other regions without testing whether the main descriptor variables of  $S_r$  are the same and whether no other variables play a role in determining  $S_r$  magnitude. In general, the case-specificity of this study, and with it many other root zone storage capacity studies, complicates acquisition of the main descriptor variables of  $S_r$  on the global scale. Therefore it is recommended to test and compare root zone storage capacity descriptors in a combined study using catchments from different regions in the world.

In conclusion, using two sequential feature selection methods, earlier found descriptors of  $S_r$ , being AI, RC (EI) and ST were again found to be important indicators. Several attempts to find any other parameters of influence did not lead to significant new results. A multiple linear regression model of the key parameters subsequently showed that  $S_r$  can be predicted without bias in the Canadian catchments, potentially providing a way of estimating  $S_r$  in Canadian regions with a lower data sampling frequency and increasing applicability of  $S_r$  in climate and hydrological models. Application of the same regression model in Finland led to a fairly good prediction of  $S_r$  but also showed that the model parameters may cooperate differently in other regions or that other parameters may have influence on root zone storage capacities in regions outside Canada. To obtain a global overview of parameters that influence  $S_r$  it is therefore recommended to investigate and compare root zone storage capacity descriptors in a combined study of different areas in the world.

### 3.4. Influence of snow on root zone storage capacity

As mentioned several times before, snow dynamics is expected to have an effect on the root zone storage capacity, potentially by its influence on seasonality and timing of liquid input. The precise influence of snow on the root zone storage capacity has however not been tested yet. Since snow dynamics is not equally important in all Canadian catchments and there are multiple different other processes that influence  $S_r$ , a comparison between several snow parameters and the root zone storage capacity will not provide a clear representation of merely the influence of snow on  $S_r$ . Instead, the effect of snow on  $S_r$  in Canadian catchments has been tested by a sensitivity analysis between root zone storage capacities that are computed with snow module ( $M_s$ ) and without a snow module ( $M_n$ ). Figure 3.12 shows two histograms with the relative and total difference in root zone storage capacity between these two different computations of  $S_r$ .

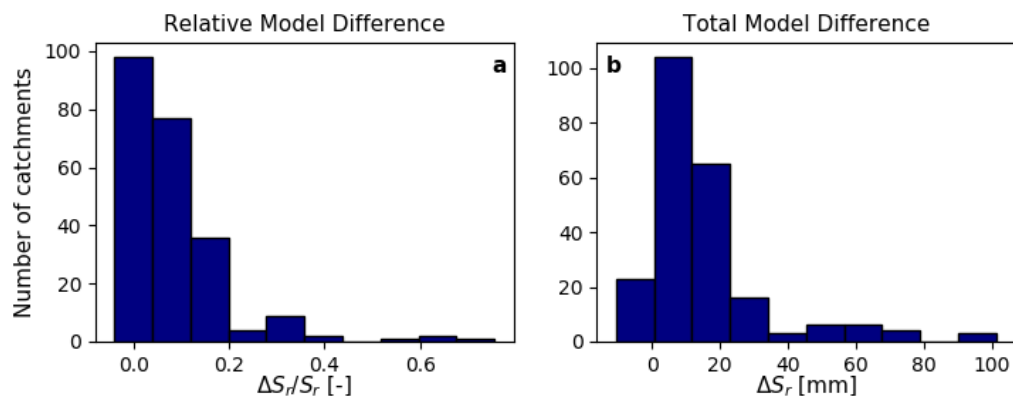


Figure 3.12: Histogram of the change in  $S_r$  between a model run with and without snow module where (a) shows the relative difference and (b) shows the total difference. An increase in  $\Delta S_r$  indicates a larger root zone storage capacity occurs in  $M_n$ .

As shown in Figure 3.12, the root zone storage capacity increases or remains approximately equal for generally all catchments whenever the snow module is not used. There are 6 catchments that have a minor decrease in  $S_r$  for  $M_n$ . However, manual inspection of these catchments showed that the storage deficits of both model runs were almost equal, so the slight increase may have been an artefact of e.g. Gumbel fitting. In general, the increasing behaviour of  $S_r$  without snow module indicates that snow dynamics either decreases the magnitude of  $S_r$ , or has no particular influence at all. The differences between catchments are large, which is likely related to the large difference in snow importance between the study catchments. In this study, the importance of snow in a catchment is described by the percentage of solid precipitation ( $P_{s,rel}$ ). Figure 3.13a therefore relates the relative difference in  $S_r$  between the two model runs and  $P_{s,rel}$ . Furthermore, the relationship between several other snow related parameters (which have large correlation with  $P_{s,rel}$ ) and the relative difference in  $S_r$  is given in Appendix H.

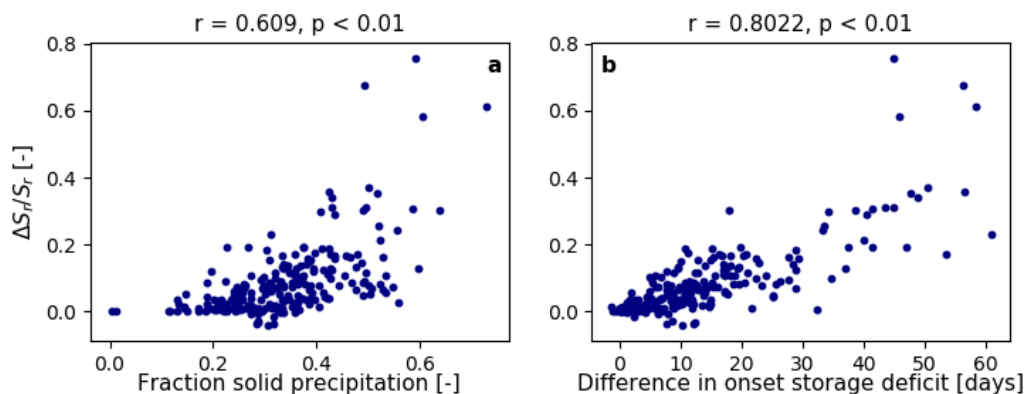


Figure 3.13: The relationship between the relative difference in  $S_r$  computed by the two different models and (a) the percentage of solid precipitation and (b) the difference in onset of storage deficit between the two models. The titles show Pearson's  $r$  and statistical  $p$ -values.

Figure 3.13a indeed shows that whenever snow is more important in a catchment, its influence on  $S_r$  (shown by the increase in the relative difference between the two model runs) is larger. In general, removal of the snow module leads to a total different timing input of winter precipitation. In this case, precipitation falling during winter, when evaporation rates are low, enters the root zone immediately when falling and therefore the overlap of liquid input and output decreases, leading to higher root zone storages. However, the magnitude of this decrease is highly dependent on the amount of solid precipitation that is stored in  $M_s$ . For example, whenever a large percentage of the total precipitation falls in solid state, the buffering effect of the snow pack has large influence on the magnitude of  $S_r$ , because the melt input then has significant overlap with outgoing transpiration for a long time and thus for increasing transpiration magnitudes. However, when the solid precipitation fraction is low, the buffering effect of a snowpack is limited, leading to small additional

liquid input and mainly in the period when evaporation rates are still small. This would lead to fewer change between  $M_s$  and  $M_n$ . For the study catchments, it appears that a relative snow fraction of approximately 0.4 is generally required before snow influence has a significant effect on  $S_r$  magnitude. In further research it is interesting to see whether this percentage solid precipitation also applies in other boreal areas.

The theory of fewer overlap between liquid fluxes towards and from the root zone when snow is not considered is also represented in the computed storage deficits. In fact, snow melt provides extra liquid during the start of the evaporation period, which means that the deficit of water likely occurs later. A delayed onset of storage deficit leads to lower cumulative storage deficit magnitudes, which is what causes the different representation of  $S_r$  between the two models. This relationship between the change in  $S_r$  and the difference in onset between the two models is shown in Figure 3.13b, which indeed shows a strong correlation ( $r = 0.80$ ).

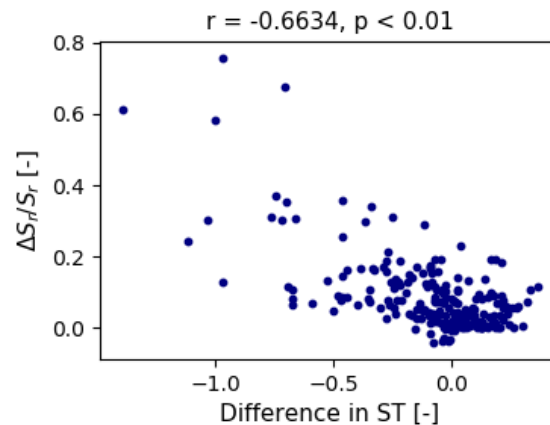


Figure 3.14: The relationship between the relative difference in  $S_r$  computed by the two different models and the difference in the seasonality timing index between the two models. A negative ST difference indicates a decrease in the ST component for  $M_n$ .

Since snow dynamics delays the liquid input into the root zone, it is likely that its effect on  $S_r$  is partly described by the seasonality timing index used in this study. Figure 3.14 shows the difference in ST between the two model runs compared to the difference in  $S_r$  between the two model runs. Clearly ( $r = -0.66$ ) a change towards fewer overlap between the liquid input signal and the atmospheric energy demand due to removal of the snow module (negative change in ST) leads to a large increase in root zone storage capacity. As such, the snow influence on  $S_r$  in this study is expectedly encapsulated in the seasonality timing index. The variance in Figure 3.14 may be related to the non-linearity of ST. A change of -0.5 could for example indicate an ST change from non-seasonal to seasonal out of phase, or a change from seasonal in phase situation to a non-seasonal signal. Both of these changes may lead to a different change in  $S_r$  between the model runs. Besides, ST is a measure of the total liquid input and not just snow melt. The way in which winter precipitation is distributed in  $M_n$  can therefore have influence on the change in ST, which may be a potential cause of the variance in Figure 3.14 too.

Note that  $M_n$  as used in this study only represents a theoretical situation and does not accurately portray reality. In fact, whenever snow dynamics does not occur, temperatures are expected to be higher, which would also lead to a different representation of e.g. potential evaporation and would likely increase outgoing transpiration. This has however not been taken into account in this model comparison, which purely compares the effect of snow on  $S_r$  based on its influence on the seasonal signal of liquid input.

Furthermore, additional climate components may influence the model comparison. For example, when there is additional precipitation input during melt phase, the influence of snow on storage deficits is smaller. Besides, differences in atmospheric water demand can also influence the relative difference of  $S_r$  between the two model runs. These climatic effects can potentially explain some of the variance in e.g. Figures 3.13 and 3.14. Due to such additional effects it is complicated to study purely the effect of snow on the root zone storage capacity, but it is expected that the results from this study provide a good estimation.

In conclusion, snow dynamics will generally lead to lower  $S_r$ , depending on the relative importance of snow in a catchment. In catchments with large snow dynamics, a delayed liquid input increases overlap between the ingoing and outgoing fluxes in the root zone storage capacity. In the model this leads to a later onset of storage deficits. It is likely that the snow influence is partly portrayed by the ST component in this study.

### 3.5. Regional variability of descriptor variables

In this section, an overview is provided of how the main descriptor variables of  $S_r$  vary for different functional clusters and how these clusters are spatially distributed throughout Canada. This way, the spread of  $S_r$  between different types of catchments is analysed and the geospatial variation of these catchments of similar functionality is presented to see whether any differences are caused by the geographical location of the catchments. Using this approach, it can be tested whether different variables exert influence on  $S_r$  in different types of catchments.

Clustering of catchments was done using a principal component analysis (PCA), as shown in Figure 3.15a. The variables that are used in the PCA all showed to have some relationship with  $S_r$  in earlier parts of this study, during the regression analyses or as snow parameter. Note that the combined effect of the aridity index and the runoff coefficient (or evaporative index) is presented by the REI parameter as defined in Section 3.3.1. Furthermore, several variables are added to the PCA to explain the spatial spread of several clusters. The variance explained by principal components 1 and 2 is respectively 31.1% and 26.5%. The vectors in the principal component analysis represent how a certain variable is described by principal components 1 and 2. The length of a vector describes how significant the influence of the parameter is in describing the variance of the dataset. In the principal component analysis, catchments with approximately the same functional behaviour are plotted close to each other. If the location of a catchment corresponds with the direction of a vector, this indicates a strong positive influence of this variable on the catchment. Likewise, a strong negative influence of a variable on a catchment is presented if the vector plots in opposite direction. Limited influence of a variable is described by vectors that plot perpendicular to the plotting location of a catchment.

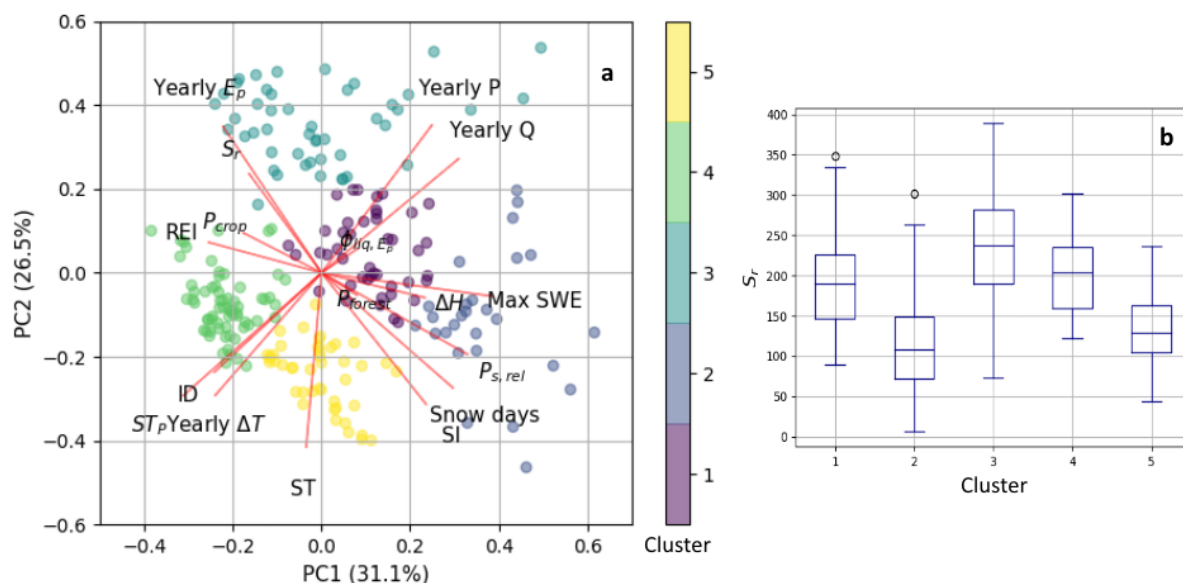


Figure 3.15: (a) 5 catchment clusters of similar functioning shown in a principal component analysis. (b) Boxplot showing the distribution of  $S_r$  within each cluster.

As catchments that plot around the same location in the PCA have shared descriptor variables, a k-means clustering approach in the PCA can be used to identify catchment clusters of similar functioning, which led to 5 different catchment classes in this study, all described by a different combination of variables. The variation of root zone storage capacities within a class is presented in the box plot in Figure 3.15b. Note that in general,  $S_r$  varies between the classes, but is approximately the same for classes 1 and 4. The geographical spread of

the 5 clusters is shown in Figure 3.16, which shows that the functional clusters defined in the PCA are largely gathered around the same geographical locations in Canada. The main influence of the most important descriptor variables for every class and the approximate magnitude of their root zone storage capacity is added to the legend of Figure 3.16.

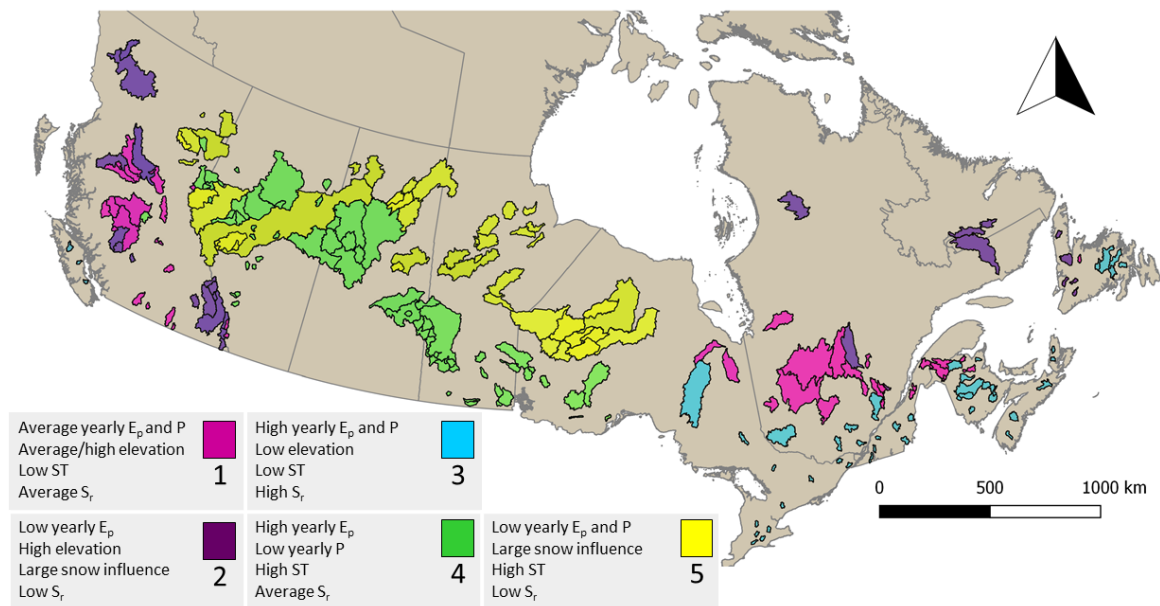


Figure 3.16: Geospatial distribution of functional catchment clusters in Canada.

The spatial spread of the clusters in Figure 3.16 shows that cluster 4 and cluster 5 share approximately the same geographical location. These catchments are located in the centre of Canada and therefore have a slightly different climate than the other catchments. Not only is there generally fewer precipitation in these areas, but the temperature difference between summer and winter time is also larger, predominantly caused by lower winter temperatures. The result is that the time period in which liquid can enter the root zone is smaller compared to the other clusters, likely leading to more in phase behaviour between the atmospheric demand and the liquid input in these catchments. Besides, particularly for cluster 4, the bulk of precipitation is falling in the summer period. As such, the seasonality timing index is large in cluster 4 and 5, whereas this value is generally smaller or negative in the other clusters (see Figure 3.15a). The low total precipitation input in these clusters additionally causes the catchments to have limited water available for transpiration relative to the other clusters. The seasonality timing components and total precipitation input are the main variables that cause difference in functional behaviour between cluster 4 and cluster 3 as well as cluster 5 and cluster 1 and are expectedly the reason for differences in  $S_r$  between these clusters.

Although sharing the same geographical location, cluster 4 and 5 do have differences. One of them is the influence of snow ( $P_{s,rel}$  or snow days in Figure 3.15) in the catchments, potentially caused by variation in elevation and latitude (cluster 4 generally has lower elevation difference and is located more southwards). The result is that the effect of seasonality and timing is particularly larger for cluster 5 compared to cluster 4. Besides, elevation and latitude also affect total yearly potential evaporation values, which are generally higher for cluster 4 compared to cluster 5 (which likely causes the large REI values for cluster 4). These differences generally cause a higher root zone to occur in cluster 4 relative to cluster 5.

Clusters 1 and 2 also share approximately the same geographical location, covering the western mountainous region and some catchments in the east. Cluster 1 plots in the centre of the PCA, with average elevation difference. Cluster 2 has more extreme influence of altitude and additionally shows larger influence of snow components. An additional effect of large elevation is that these catchments generally allocate more water to runoff (shown by e.g. the low REI). Potential reasons of why elevation difference can cause more runoff to occur are given in Section 3.2.3. The more average elevation of cluster 1 causes slightly higher potential

evaporation rates to occur in these catchments and additionally a relatively higher REI. Therefore, the root zone storage capacities in cluster 1 are averagely higher than in cluster 2.

Cluster 3 consists of the catchments that generally have the largest root zone storage capacity. These catchments both have high yearly potential evaporation and precipitation values due to their geographical location (in the south-east, near the coast, with low altitude), allowing for large amounts of total transpiration, which is also represented by the high REI for most of its catchments. Additionally, the precipitation generally falls out of phase with the atmospheric water demand considering the catchments plot in opposite direction of the seasonality timing index as shown in Figure 3.15a. These effects cause that generally a large root zone storage capacity is required for cluster 3. Note that there is a relatively large spread in  $S_r$  for this cluster, which is potentially caused by the somewhat more limited potential evaporation of several catchments in this cluster (which could be the catchments that are located at slightly higher latitudes, e.g. on the islands in the east and west of Canada). Lastly, note that the cropland percentage has large correlation with the yearly potential evaporation, because the agricultural fields are located entirely south in both clusters 3 and 4. The high  $S_r$  values for cropland as found in Section 3.2.3 could therefore be related to the high potential evaporation rates that are found in these areas.

As stated before, cluster 1 and 4 have approximately the same distribution of root zone storage capacity. However, the functional clusters of these two catchments vary. The main differences between the two clusters are the elevation difference and seasonal influences. Cluster 1 has more out of phase seasonal behaviour than cluster 4, which would indicate a larger required root zone storage capacity in this catchment cluster. However, the larger topographical difference in cluster 1 may lead to relatively more runoff and slightly fewer potential evaporation and consequently relatively fewer transpiration compared to cluster 4, which would suggest a larger  $S_r$  is required in cluster 4. As such, there are different descriptor variables in clusters 1 and 4 that balance out each others behaviour and lead to approximately the same root zone storage capacity.

In earlier sections, AI, RC and ST were identified as important descriptor variables of  $S_r$  magnitude. In this section it has been shown that there are other variables that exert influence on the root zone storage capacity in different functional and geospatial clusters. It should be noted that the influence of these different parameters is indirectly described in the variables RC, AI and ST, in the way they describe either climatic processes or water distribution in a catchment due to landscape effects.

To conclude, catchments were clustered based on similar functioning, after which their spatial spread was presented. In many cases, the functional behaviour of a cluster could be explained by the geographical location of the cluster. There is clear distinction between relevant descriptor variables of  $S_r$  in different functional and spatial clusters, which means that  $S_r$  is indeed described by different variables in contrasting regions in Canada. In general, however, these variables all exert influence on AI, RC or ST and the way they describe  $S_r$ .



# 4

## Discussion

The results that are presented in this study come with several uncertainties of different nature. This chapter therefore discusses the main uncertainties and limitations that are caused by the choice of study area, data and approach in respectively Section 4.1, 4.2 and 4.3. Lastly, some comments on wider application of the results from this study in other regions are provided in Section 4.4.

### 4.1. Study area

This study considers 230 catchments that are spread out over Canada, with different climate, land cover and elevation. Catchment selection based on several different criteria has led to a major reduction of used catchments compared to the original dataset of 698 catchments. Particularly in the north-east of Canada and in the mountain range in the west, a lot of catchments were not considered in this study, presumably largely caused by troubled discharge measurements. As such it is uncertain whether the results are representative for Canada in its entirety or whether application is limited to the study catchments.

Besides, the removed catchments are likely to have a large snow influence as they are located in relatively northern or mountainous areas. Therefore, although there are still enough catchments with snow dynamics in this study to comment on the relationship between snow dynamics and the root zone storage capacity, many of the existing Canadian catchments with large snow dynamics were not considered in this study. If future approaches on determining the root zone storage capacity or improvements of the CANOPEX datasets allow inclusion of these study catchments in investigation of  $S_r$ , it is recommended to test the results of this study with these additional catchments.

Additional comments must be made on the size of several catchments used in this study. In general, the catchments provided by CANOPEX are relatively large compared to the majority of the catchments used in other hydrological studies. The main disadvantage is that the study catchments are therefore prone to heterogeneity of e.g. land cover and climatological aspects, potentially troubling visualisation of the relationship between these parameters and  $S_r$ . Furthermore, particularly the hydrological response may vary largely between catchments with various sizes (de Wit, 2001, Pilgrim et al., 1982). However, the effect of catchment size on the results in this study is expected to be limited, because the most important descriptor variables mainly consist of long-term average catchment characteristics such as EI and AI, which are not necessarily influenced by heterogeneity or timing effects. Besides, the larger catchments are predominantly found in the central plains of Canada, where spatial variation of annual precipitation is limited. Additionally, timing differences within a catchment are decreased due to snow dynamics, because a large part of the winter precipitation enters simultaneously throughout the entire catchment in the melt phase. As such, the results found in this study are expected not to be troubled too much by the large catchment sizes. Note that catchments considered in this study are not smaller than 300 km<sup>2</sup> and that the results found in this study may therefore not be applicable to smaller catchments. Additional research on this matter is required.

## 4.2. Data

The meteorological dataset that is used in this study is retrieved from a gridded data product, in which an interpolation technique was used to model precipitation in areas between gauges (Section 2.2.2). The total number of gauges per area is therefore an important proxy for the reliability of the dataset. The spatial distribution of rain gauges in Canada is a lot denser in the south of Canada compared to the north (Hutchinson et al., 2009), which is why the precipitation and temperature data (and as such potential evaporation data) are expected to be more reliable for southern catchments.

An additional problem of the precipitation dataset is its proneness to undercatch, particularly in areas with much solid precipitation. It is important to note that the results in this study have been computed with a catchment average correction of the precipitation catch efficiency, using a formula that is generally used for local application (using local gauge data instead of catchment average data). In some cases, this application may have led to a wrong representation of precipitation, which could lead to a false representation of  $S_r$ . However, generally speaking the applied correction moved catchments closer to the Budyko curve in the Budyko framework (see Figure 2.3), which means that it is likely that the undercatch correction led to an increase of data reliability.

Furthermore, the hydrometric dataset that is used in this study is expected to be a source of uncertainty. Particularly catchments with a large number of data voids for discharge observations may have largely contributed to data uncertainty. Firstly, the linear reservoir based interpolation technique that has been applied to some catchments as described in Section 2.2.1 may not have been an accurate representation of the winter discharge in all catchments, because in some cases additional precipitation input during these periods without data may have led to fast, unregistered flows. This could potentially lead to an underestimation of catchment discharge and therefore an overestimation of transpiration and  $S_r$ . However, considering the large winter period in Canada during which no additional precipitation will contribute to discharge, this error is expected to be small for most catchments. Secondly, the approach to skip years with too many data voids for discharge (Section 2.2.1) and base the long term average discharge on the remaining years with data, may have led to a wrong representation of the catchment average discharge over the entire time period. If the actual discharge in these skipped years deviates a lot from the mean computed discharge in the remaining years, this could lead to a wrong representation of long term average discharge in this study, which could influence transpiration estimates and thus  $S_r$  computation.

In general, data uncertainties caused by wrong representation of either precipitation, discharge or potential evaporation are expected to be filtered out by the different catchment selection procedures (see Section 2.2.6 and Section 2.3.5). However, leaving out catchments has the risk of obtaining biased results towards catchments that fall within the selection criteria (e.g. only catchments within 30% of the Budyko framework were used). To test whether the results of this study are also applicable for unconsidered catchments, these are tested by comparing their predicted  $S_r$  using the linear regression model found in Section 3.3.3 with their modelled  $S_r$  from water-balance the approach used in this study. The results of this comparison are shown in Figure 4.1.

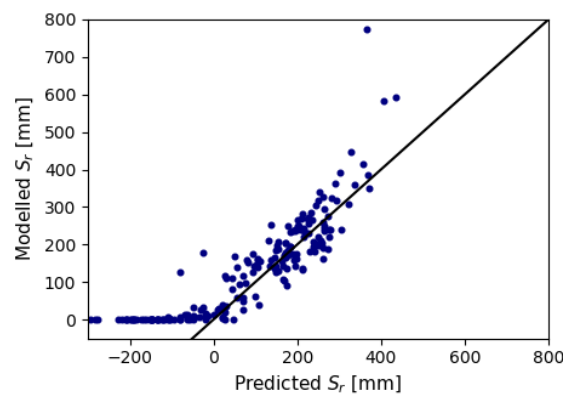


Figure 4.1: Comparison between modelled  $S_r$  and predicted  $S_r$  for catchments that were not considered in this study for falling outside several selection criteria.

Figure 4.1 indicates that the catchments that were not used in this study show approximately the same relationship between modelled and predicted  $S_r$  as the study catchments. It therefore seems that the results of this study are not biased towards the selected catchments. Note that some of the catchments have a negative predicted root zone storage capacity for a modelled  $S_r$  of zero. This is caused by the fact that  $S_r$  is limited to zero in the water balance method and in reality, but not in the linear regression model. As such, in extreme situations (e.g. very low RC), the regression model can predict negative  $S_r$ , which is what causes the offset in Figure 4.1. Potentially, the regression model can therefore be improved by setting a the minimum value for  $S_r$  to zero. Lastly, note that the data of catchments that are not used in this study is still expected to be less reliable, which means that the root zones computed using the water balance approach may deviate from reality in these cases.

The MODIS Snow Cover dataset used in this study (Section 2.2.3) contains many data voids due to cloud cover. The cloud cover in Canada is generally large, which troubles identification of snow presence on many days. Parameter calibration was applied to 3 years of data in order to have enough valid data points and additionally a test of 1 year was applied to check on the best performing parameters. However, some catchments with very frequent cloud cover were calibrated with fewer valid days than others (see Appendix B), which may have led to a larger uncertainty in the calibration parameters. How this is manifested in the computed root zone storage capacity is difficult to predict, but depends on the influence of snow cover in a catchment. On average, however, the impact of cloud cover in the MODIS data is expected to be small in this study.

For future studies that consider snow, there are several possible ways to avoid too much cloud cover in data. One opportunity is to use the 8-day MODIS Snow Cover product, which reports maximum snow cover extent during an eight-day period (Hall and Riggs, 2016a). Although expectedly resulting in a lot less data voids, the disadvantage of this approach is that it will lead to a large reduction of the temporal resolution of the data. Another possibility is to combine data from the Terra and Aqua satellite, which are two satellites both mapping snow cover with a 3 hour time lag (Xie et al., 2009). Since clouds are likely to have a different position in these three hours, there is a higher chance of measuring daily snow cover with fewer data voids in this combined product. The large amount of data that is required to apply this approach in Canada is the main reason why it was not applied in this study.

The land cover dataset used in this study is provided by ESA CCI (see Section 2.2.5). It is important to note that several parameters in this study (e.g. RP and  $I_{max}$ ) depend largely on land cover, which makes that the results are partly dependent on the accuracy of land cover maps. Due to the use of different, renewed land cover maps for every study year, the influence of anomalies in the land cover dataset on  $S_r$  is expected to be small.

It should also be noted that the estimates of land cover percentages that are used as landscape variables in this study are based on the land cover dataset of 2002. In hindsight, it may have been better to use yearly varying land cover for these variables, because land cover can be variable over the study period due to e.g. climatic or human influence. However, Figure 4.2 shows that the standard deviation of the land cover percentages over the study period is small, which indicates that the inter-annual land cover change in the study catchments is relatively small. Besides, inter-annual climate variability in Canada is not large either (see Section 4.4). As such the 2002 dataset for land cover is expected to be largely representative for the entire study period.

The elevation data (section 2.2.4) used in this study are primarily used to identify elevation zones that are required in the snow model of this study and are additionally used to identify topographical variables. The vertical accuracy of the source dataset for HydroSHEDS is 16 m (e.g. Rabus et al., 2003), which seems accurate enough for a distribution of catchments in elevation zones of 250 m and for representative catchment average topographical indices. As such, the elevation datasets in general are not expected to be a large source of uncertainty in this study.

### 4.3. Approach

The approach that has been used in this study requires some assumptions and choices. Therefore, the potential insecurities resulting from the method applied in this study and their expected effect on the results is discussed in this section.

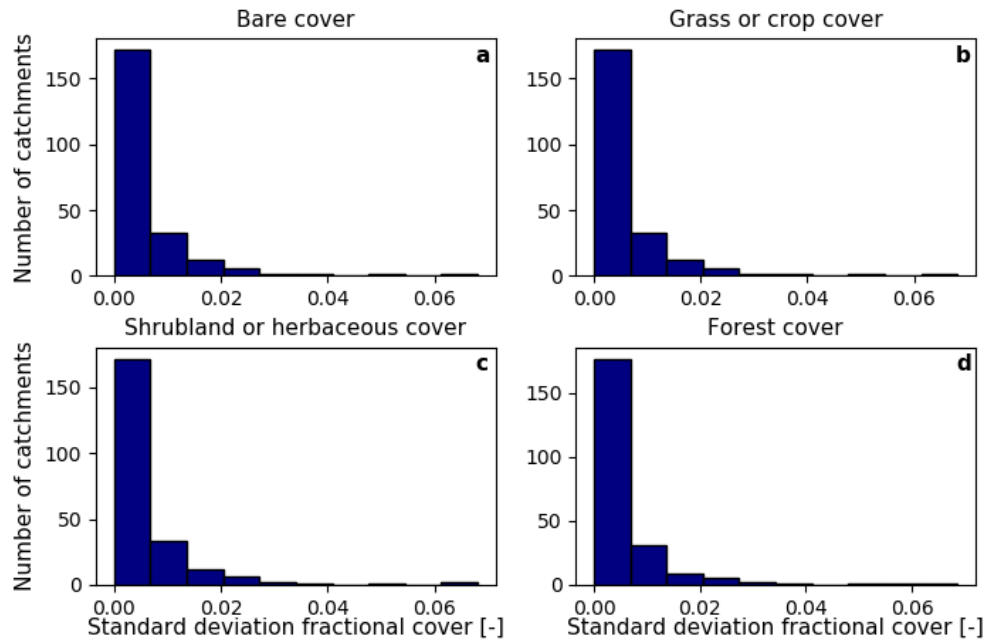


Figure 4.2: Standard deviation of coverage percentage to show land cover change over time for (a) bare cover, (b) grass or crop cover, (c) shrubland or herbaceous cover (d) forest cover. The results indicate that there is little land cover change throughout the study period.

### 4.3.1. Uncertainties in transpiration estimate

Transpiration is one of the two fluxes determining storage deficits in this study. The estimate of transpiration is therefore an important determinant in root zone storage capacity computation. In the applied method, transpiration is estimated from the long term average water balance and successively scaled with daily potential evaporation rates. Potential inter-annual variability of transpiration is therefore not included in the model approach, while water limitation or abundance may cause different transpiration signals to occur in varying years. The computed storage deficits in this study may therefore deviate from reality, potentially leading to a different representation of root zone storage capacities.

Besides, the validity of the transpiration estimate depends on vegetation type and survival strategy. Trees are likely to increase their root biomass to survive dry periods (Brunner et al., 2015), whereas grasses and other low vegetation generally go dormant in dry periods when their root zones are depleted (Wang-Erlandsson et al., 2016). As such, forests are likely to transpire all-year round, whereas grasses do not show any transpiration signal for some periods during relatively dry years. The assumptions used to derive an estimate for transpiration therefore do not hold for low vegetation. In future studies on the root zone storage capacity, it might be better to identify the transpiration period of grasslands and other low vegetation based on Normalised Difference Vegetation Index data (NDVI), to have a better idea on the timing of transpiration output and produce better results of storage deficits in grasslands. Note that forest is the main vegetation type in this study, which means that the transpiration estimate is valid for the majority of the study catchments.

Lastly, inaccuracies in computed potential evaporation rates may provide inaccurate representation of transpiration in this study. Potential evaporation is exclusively determined with temperature and top of atmosphere radiation data. In reality wind, relative humidity and other factors may also play a role.

### 4.3.2. Static root zone

In this study, the root zone storage capacity is treated as a static component, whereas it is expected that the actual value of  $S_r$  differs over time due to inter-annual climatic variation or landscape changes (Gao et al., 2014). Nijzink et al. (2016) for example showed that  $S_r$  indeed changes after deforestation. However, as presented in Figure 4.2, changes of landscape variables in the study catchments are generally small, meaning that based on these landscape variables,  $S_r$  is not expected to show large variability throughout the study period. Similarly, climatic variation is not limited in the study catchments over the considered time periods and is therefore also not expected to lead to large variability in  $S_r$ .

### 4.3.3. Alternative water sources for vegetation

It is important to note that the method used in this study is based on the assumption that all of the water used for transpiration is retrieved from the root zone storage capacity and there are no additional sources of water for vegetation. In regions with high water tables, trees can extract liquid from ground water, leading to larger transpiration fluxes than derived in this study. This is particularly true for catchments with large percentage of wetlands, which are located south of the Hudson Bay and in the central plains of Canada (Government of Canada, 2016). Application of the approach in these areas therefore requires more caution. Similarly, crop irrigation could act as additional water source in agricultural areas. However, according to the ESA-CCI land-cover maps agricultural croplands used in this study are primarily rainfed and not irrigated.

### 4.3.4. Direct infiltration estimate

The method used in this study implicitly assumes that effective precipitation or snow melt immediately infiltrates into the root zone. Theoretically, other processes such as infiltration-excess overland flow (IOF), saturation-excess overland (SOF) flow or preferential subsurface flow (PSF) can also occur. In temperate regions, the infiltration capacity of the soil is generally too high for IOF to occur, which is why this type of overland flow is not expected in Canada (Holden, 2005). However, several parts of Canada experience soil freezing, which may largely reduce infiltration capacities. Particularly in regions of permafrost this could lead to overland flow (although this is implicitly accounted for by the estimate of transpiration from the long term water balance). The influence of snow on  $S_r$  as described in this section is therefore only valid if the snow melt can indeed infiltrate into the soil, thus when the effect soil frost is limited. If snow melt starts before soil thawing, part of the snow melt can not infiltrate in the root zone while it does reduce the storage capacity in the model used in this study, causing an underestimation of the storage deficit and potentially also of  $S_r$ . However, since most catchments are located relatively south in Canada and the regions of large soil frost are located in the north of Canada (Vincent et al., 2017), this effect is expected to be limited for most catchments. Secondly, SOF could potentially occur during very wet periods in areas with high groundwater tables. In times of deficit, which is the main period of interest of this study, SOF is therefore not expected to happen, which means the infiltration assumption is generally valid in this study. For PSF to occur, location specific soil moisture thresholds must expectedly be exceeded (Huggett, 2007). Therefore, during periods of deficit, PSF is not expected to have large effect either. As such, the assumption that all available water immediately infiltrates in the root zones seems to be reasonably valid in most study catchments.

### 4.3.5. Choice of return period

The method used in this study is based on the theory that vegetation designs its root system based on a droughts with a certain return period. Using this approach, the root zone storage capacity is rather dependent on the return period in a catchment. Therefore it is important that return periods are correctly linked to vegetation type. In this study it is assumed that lower vegetation such as grasses and crops design roots for a smaller drought return period and vegetation consisting of more biomass invests into overcoming droughts with a larger return period, based on findings in earlier studies such as Wang-Erlandsson et al. (2016) and Gao et al. (2014). However, the exact magnitudes of return period used in this study are rather rough estimates, which may have influence on the eventual magnitude of  $S_r$ . To test the impact of return period choice on the end result, a comparison between the studied  $S_r$  and  $S_r$  computed using different return periods is performed in Figure 4.3a.

Figure 4.3a shows how root zone storages computed using a different return period set deviate from  $S_r$  used in this study. The return periods sets (high and low) that are used in this sensitivity analysis are presented in Table 4.1. The results suggest that the magnitude of  $S_r$  indeed depends on the choice of return period, because  $S_r$  computed for different RP sets deviates from  $S_r$  computed with main set. However, the relative change between catchments seems to be rather identical, as they follow approximately the same line. Therefore it appears that although the absolute magnitude of  $S_r$  changes for all catchments, their mutual relationship does not depend on return period choice. In this study, the relative behaviour of  $S_r$  between catchments is more important than the actual magnitude of  $S_r$ , which means that the main results are not likely to change if a different return period is used.

Interestingly, Figure 4.3 shows that some catchments deviate a little from the general linear trend. These catchments all have a low percentage of forest cover. It therefore seems that whenever there is a lot of difference in land cover between catchments, the choice of return period is more important than whenever this

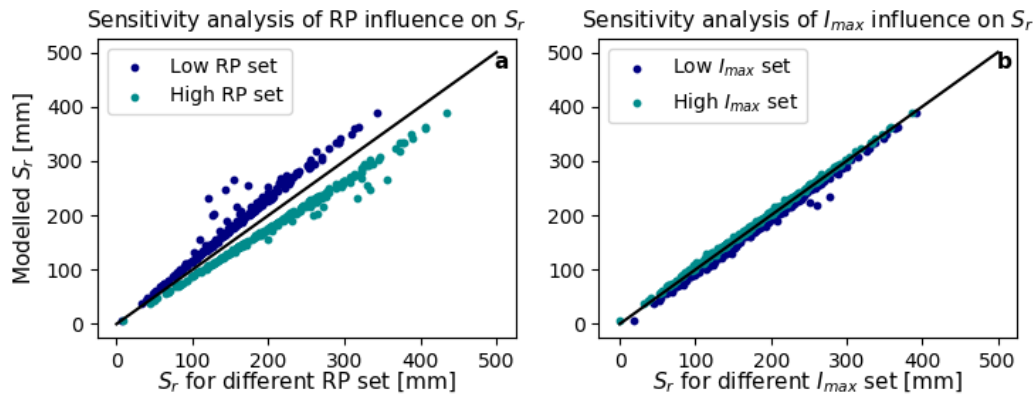


Figure 4.3: Sensitivity analysis on the influence of choosing a parameter set for (a) Return Period and (b) Maximum Interception Capacity. Deviation from the diagonal line indicates a larger difference between  $S_r$  for the set used in this study and the comparison set. Parameter sets for the model set are RP[undefined,2,5,20] and  $I_{max}$ [0,1,2,3]. High parameter sets are RP[undefined,5,10,40] and  $I_{max}$ [0,2,3,4]. Low parameter sets are RP[undefined,2,5,20] and  $I_{max}$ [0,0,1,2]. All for respectively bare cover, grass or crop cover, shrubland or herbaceous cover and forest cover.

Table 4.1: Overview of the different return periods and maximum interception capacities used in the sensitivity analysis of their influence on  $S_r$ .

	Low RP [years]	High RP [years]	Low $I_{max}$ [mm]	High $I_{max}$ [mm]
<b>Bare cover</b>	Undefined	Undefined	0	0
<b>Grass or crop cover</b>	1	5	0	2
<b>Shrub or herbaceous cover</b>	2	10	1	3
<b>Forest cover</b>	10	40	2	4

is not the case (the latter is particularly true in Canada). Therefore, in case that the absolute magnitude of  $S_r$  is important, or whenever there is large difference in land cover between catchments, the influence of RP choice on the  $S_r$  must always be considered. In fact it is recommended to further investigate the relationship between vegetation type and drought return period, in order to reduce the uncertainty caused by choice of return period.

Lastly, it is questionable whether the return period approach in general is applicable to all kinds of catchments. The study approach is based on the fact that vegetation designs its root zone storage capacity by long-term evolutionary optimisation. However, crops are generally harvested within a few years, which means they can not optimise their root zone storage capacity on long term conditions. Presumably, the root zone of agricultural crops may therefore be dependent on short term dynamics. This could be one of the reasons of the unexpectedly high root zone storage capacity magnitude for catchments with high cropland percentage in this study (see Section 3.2.3). Furthermore, the fact that grasses generally go dormant when in water stress may indicate that the survival strategy used by this vegetation type is not to invest in root growth, making use of the evolutionary optimisation approach based on drought return periods debatable for this vegetation type. In general, it is therefore recommended to further investigate whether the theory used to determine  $S_r$  in this study is applicable to both agricultural cropland and grasslands, or whether other, more short term effects may play a significant role here. However, considering most of the catchments used in this study have a relatively high forest cover and few short vegetation, application of the return period method in this study will generally lead to acceptable results.

#### 4.3.6. Choice of maximum interception capacity

Like the return period, the maximum interception capacity is another estimated quantity that plays an important role in this study.  $I_{max}$  is assumed to decrease with canopy size of different types of vegetation. This by itself is not unlikely, but the absolute magnitude of the interception capacity for each type of vegetation has also been assumed, which may affect the results. Therefore, the influence of interception capacity choice on  $S_r$  is evaluated by computing  $S_r$  for two extremal cases and comparing them with the root zone storage capacities used in this study. The results are shown in Figure 4.3b. The Figure shows that the interception

capacity has little influence on the magnitude of  $S_r$ , which means that the choice of  $I_{max}$  does not appear to have significant influence on the results in this study.

#### 4.3.7. Snow module assumptions

The snow module applied in this study is based on several assumptions. Firstly, sublimation has not been considered. Since potential evaporation rates are very low during Canadian winter time, it is expected that sublimation rates are also low mid-winter. However, whenever temperatures start increasing, the snow procedure could actually be affected by sublimation. The impact of sublimation on storage deficits is difficult to predict. On the one hand it may decrease total snow melt which could e.g. cause an earlier onset of storage deficits (due to the fact that there is fewer liquid flux into the system). On the other hand energy used for sublimation can not be used for transpiration, which leads to a reduction of the total transpiration and as such also a decrease in daily transpiration rates, which would decrease storage deficits. In this study, the total time period over which sublimation plays a significant role is assumed to be small.

Secondly, no interception reservoir is used in the snow module, indicating that no interception evaporation of solid precipitation occurs. In theory, snow is stored in the snow reservoir and will remain there until snow melt starts. Whether snow is stored on the ground or in the tree canopy is unimportant, making use of a separate interception reservoir unnecessary. Only during the melt phase, whenever snow melt occurs, part of the snow gathered on the leaves may be stored in the tree canopy for interception evaporation, but this amount is assumed to be small compared to the rest of the snow pack (considering most of the snow has generally fallen of the leaves before snow melt starts).

Lastly, the mean catchment elevation in this study has been linked with the mean catchment temperature, like described in Section 2.3.1. Any insecurities in the representation of snow dynamics caused by this assumption are expected to be largely filtered out by calibration of the snow module (and thus represented in the calibration parameters).

#### 4.3.8. Other methods that describe correlation

The individual correlations in this study have all been determined using Pearson's correlation coefficient. This correlation coefficient describes the statistical (linear) dependence between two variables. The Pearson correlation coefficient generally gives an adequate description of the correlation whenever the variables have a normal distribution.

However, there can be numerous combinations of variables in which the Pearson correlation coefficient may not describe the dependence of two variables adequately. Whenever one or both of the variables have a more skewed relationship (which occurs for example for several descriptor variables in Figure 3.3) and therefore show a non-linear relationship (e.g. Figure 3.13), ranked methods will give a better description of the correlation between two variables. Ranked methods such as Spearman's or Kendall's correlation coefficients describe the concept of monotonic dependence rather than linear dependence (Jonkman et al., 2015). In other words, correlation is computed using the ranks of the variables, rather than their absolute values. For consistency, this study has only used Pearson's correlation coefficient, but it must be taken into account that some variables may provide a higher correlation when one of these two ranked methods is applied.

A more formal and precise way of describing the ranked correlation between two variables is by using copulas. Copulas describe the dependence of two marginal distributions in a joint distribution, using a distribution corresponding to the ranks of the original variables (Jonkman et al., 2015). One of the main advantages of copulas is that they offer a more flexible way to model probabilistic dependence. In other words, they can specify the correlation of different parts of the marginal distributions and thus identify difference in correlation between different parts of the distributions. This is particularly useful in situations where the extremes of a distribution are of interest, which is the case for e.g. some of the landscape variables in this study. In further research, it may therefore be interesting to analyse the relationship between the root zone storage capacity and several descriptor variables using copulas.

#### 4.3.9. Model bias

In this study it is very important to note that the climate variables and RC are not independent from the method. As a matter of fact, climate parameters such as precipitation and temperature are a direct model input. Besides, the long term average water balance is used to compute long term average transpiration output, making the found distribution of  $S_r$  on the Budyko framework (Section 3.3.1) somewhat trivial. On the other hand, the method uses a daily time step, whereas catchment parameters like AI and RC are computed based on long term averages. The implication that  $S_r$  can be estimated using data obtained with lower sampling

frequency in Canada is therefore still significant. Besides, the result that  $S_r$  can be estimated using long term average variables may contribute to more straightforward and less computationally expensive implementation of water-balance derived root zone storage capacities in hydrological and climate models, or can help in constraining the  $S_r$  parameter in calibration of hydrological models in Canada.

#### 4.4. Wider application

The main descriptor variables of  $S_r$  that follow from this study are AI, RC and ST. The aridity index and runoff coefficient are both relative variables that are described by long term average components of precipitation, discharge and potential evaporation. Due to the relative character of AI and RC, it is possible that catchments have the same location on the Budyko framework with an entirely different description of P, Q and  $E_p$ . Since the root zone storage capacity depends on how much water is allocated for transpiration, this value is expectedly related to the absolute input of P, Q and  $E_p$ . In Canada, the distribution of precipitation and evaporation causes the relative components AI and RC to describe this absolute effect rather accurately, but this may not necessarily work in other regions in the world. Therefore it is not recommended to apply the results of this study in other regions without further consideration. Besides, it may be interesting to investigate the possibility of describing root zone storage capacities based on a long term average description of P, Q and  $E_p$  and a rough description of their seasonal behaviour in further research. Furthermore, to limit the relative effect of variables AI and RC in the multiple linear regression of Section 3.3.3, it is interesting to further investigate the potential of using  $S_r/P$  instead of  $S_r$  in a multiple linear regression as well (since AI and RC respectively describe  $E_p/P$  and  $Q/P$ ). Particularly with the intention of applying such a multiple linear regression on the global scale it is important that catchments from different regions with varying climates are used to fit this regression, so that it is not location specific.

Furthermore, wider application of the results in this study may be complicated by effects of inter-annual variability within catchments. In theory, vegetation optimises its root system based on droughts that occur with a certain return period. This means that extreme years are important in derivation of the root zone storage capacity. Whenever inter-annual variability is large, it is likely that climate variables in extreme years deviate more from the long term average climate variables. In an estimation of  $S_r$  using long term average variables and a long term average seasonal signal, the effects of extreme years are likely to be lost. In Canada, inter-annual variability of rainfall is small (with a coefficient of variation ranging between 0.1 and 0.24), which is expectedly why such a simplified estimation of  $S_r$  works. However, whenever inter-annual variability is large, it is questionable whether estimation of  $S_r$  based on long term average variables with a seasonal description as proposed in this study is accurate. It would therefore be interesting to analyse the effect of inter-annual variation on  $S_r$  in regions with significant difference in inter-annual variability.

# 5

## Conclusion

The goal of this exploratory study was to quantify catchment average root zone storage capacities, identify its main descriptor variables and their regional variability and determine the influence of snow on root zone storage capacities in Canada.

Catchment average root zone storage capacities were computed using a water-balance approach and were found to be normally distributed over 230 catchments in Canada with a mean magnitude of 183 mm and a standard deviation of 70 mm. Individual correlation of climate, landscape and discharge variables with  $S_r$  showed the most relevant individual relationships between  $S_r$  and yearly potential evaporation, seasonality index and runoff coefficient with Pearson's  $r$  values of respectively 0.52, -0.32 and -0.35. However, variance in these individual relationships was considerable.

Analysis of the combined relationship of parameters with  $S_r$  has shown that the variance in root zone storage capacities between catchments in Canada is mainly described by a combination of long term average variables (aridity index and runoff coefficient) and by the coherence of seasonal and timing effects (seasonality timing index). The aridity index and runoff coefficient describe allocation of water for transpiration in a catchment, whereas the seasonality timing index explains seasonal distribution of this water and therefore the synchronisation of liquid input and atmospheric water demand. Earlier derived individual descriptors of  $S_r$  are encapsulated in these main descriptor variables. Application of a multiple linear regression model using the aridity index, runoff coefficient and seasonality timing index showed that the root zone storage capacity can be predicted without bias and a standard deviation of 32 mm for all Canadian catchments with an  $R^2$  of 0.72. Subsequent application in Finland resulted in an  $R^2$  of 0.62, showing that the main descriptor variables found in Canada likely play a role in this boreal region too, but that application of the study results outside Canada without further investigation is not recommended.

The influence of snow on the root zone storage capacity in Canada was identified by comparing  $S_r$  magnitudes computed with and without a snow module. This analysis showed that for large enough percentages of solid precipitation, snow effects lead to a decrease in  $S_r$  magnitude. This is caused by an increase of the overlap between liquid input and transpiration output in a catchment. Such effects are portrayed by the seasonality timing index.

An analysis of the distribution of  $S_r$  in catchment clusters of similar functioning showed that different variables have an effect on  $S_r$  in different functionally comparable regions in Canada. A large part of the functional behaviour of these clusters can be recognised and explained by the geographical location of their catchments. The influence of these regionally dependent variables on the root zone storage capacity is encapsulated in earlier defined main descriptor variables aridity index, runoff coefficient and seasonality timing index.



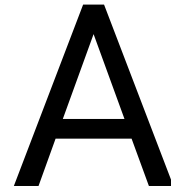
# References

- Arsenault, R., Bazile, R., Ouellet Dallaire, C., and Brissette, F. (2016). Canopex: A canadian hydrometeorological watershed database. *Hydrological Processes*, 30(15):2734–2736.
- Berghuijs, W. R., Sivapalan, M., Woods, R. A., and Savenije, H. H. G. (2014). Patterns of similarity of seasonal water balances: A window into streamflow variability over a range of time scales. *Water Resources Research*, 50(7):5638–5661.
- Bergstroem, S. (1975). The development of a snow routine for the hbv-2 model. *Hydrology Research*, 6(2):73.
- Beven, K. (2006). A manifesto for the equifinality thesis. *Journal of Hydrology*, 320(1-2):18–36.
- BeWilder (2014). A walk in the winter wonderland.
- Brunner, I., Herzog, C., Dawes, M. A., Arend, M., and Sperisen, C. (2015). How tree roots respond to drought. *Frontiers in Plant Science*, 6:547.
- Budyko, M., Budyko, M., and Miller, D. (1974). *Climate and Life*. International geophysics series. Academic Press.
- Chen, L., Liu, C., Li, Y., and Wang, G. (2007). Impacts of climatic factors on runoff coefficients in source regions of the huanghe river. *Chinese Geographical Science - CHIN GEOGR SCI*, 17:047–055.
- Collins, D. B. G. and Bras, R. L. (2007). Plant rooting strategies in water-limited ecosystems. *Water Resources Research*, 43(6).
- Crow, W. T., Berg, A. A., Cosh, M. H., Loew, A., Mohanty, B. P., Panciera, R., De Rosnay, P., Ryu, D., and Walker, J. P. (2012). UPSCALING SPARSE GROUND-BASED SOIL MOISTURE OBSERVATIONS FOR THE VALIDATION OF COARSE-RESOLUTION SATELLITE SOIL MOISTURE PRODUCTS. *Reviews of Geophysics*, 50:1–20.
- De Boer-Euser, T., McMillan, H. K., Hrachowitz, M., Winsemius, H. C., and Savenije, H. H. (2016). Influence of soil and climate on root zone storage capacity. *Water Resources Research*, 52(3):2009–2024.
- de Boer-Euser, T., Palalane, J., Savenije, H., and Juízo, D. (2019). How climate variations are reflected in root zone storage capacities. *Physics and Chemistry of the Earth*, (March 2018):0–1.
- de Wit, A. M. W. (2001). *Runoff controlling factors in various sized catchments in a semi-arid Mediterranean environment in Spain*. PhD thesis.
- Dee, D. P., Uppala, S. M., Simmons, A. J., Berrisford, P., Poli, P., Kobayashi, S., Andrae, U., Balmaseda, M. A., Balsamo, G., Bauer, P., Bechtold, P., Beljaars, A. C. M., van de Berg, L., Bidlot, J., Bormann, N., Delsol, C., Dragani, R., Fuentes, M., Geer, A. J., Haimberger, L., Healy, S. B., Hersbach, H., Hólm, E. V., Isaksen, L., Kållberg, P., Köhler, M., Matricardi, M., McNally, A. P., Monge-Sanz, B. M., Morcrette, J.-J., Park, B.-K., Peubey, C., de Rosnay, P., Tavolato, C., Thépaut, J.-N., and Vitart, F. (2011). The era-interim reanalysis: configuration and performance of the data assimilation system. *Quarterly Journal of the Royal Meteorological Society*, 137(656):553–597.
- Diez, D. M., Barr, C. D., and Cetinkaya-Rundel, M. (2012). *OpenIntro statistics*. OpenIntro.
- Donohue, R. J., Roderick, M. L., and McVicar, T. R. (2007). On the importance of including vegetation dynamics in Budyko's hydrological model. *Hydrology and Earth System Sciences*, 11(2):983–995.
- Donohue, R. J., Roderick, M. L., and McVicar, T. R. (2012). Roots, storms and soil pores: Incorporating key ecohydrological processes into Budyko's hydrological model. *Journal of Hydrology*, 436-437:35–50.

- Dozier, J. (1989). Spectral signature of alpine snow cover from the landsat thematic mapper. *Remote Sensing of Environment*, 28:9 – 22.
- ESA (2017). Land cover cci product user guide version 2.
- Fenicia, F., Kavetski, D., and Savenije, H. H. (2011). Elements of a flexible approach for conceptual hydrological modeling: 1. motivation and theoretical development. *Water Resources Research*, 47(11).
- Fenicia, F., Savenije, H. H. G., Matgen, P., and Pfister, L. (2006). Is the groundwater reservoir linear? Learning from data in hydrological modelling. *Hydrology and Earth System Sciences Discussions*, 10(1):139–150.
- Fu, B. (1981). On the calculation of the evaporation from land surface. *Sci. Atmos. Sin*, 5(1):23–31.
- Gao, H., Hrachowitz, M., Schymanski, S. J., Fenicia, F., Sriwongsitanon, N., and Savenije, H. H. (2014). Climate controls how ecosystems size the root zone storage capacity at catchment scale. *Geophysical Research Letters*, 41(22):7916–7923.
- Gentine, P., D’Odorico, P., Lintner, B. R., Sivandran, G., and Salvucci, G. (2012). Interdependence of climate, soil, and vegetation as constrained by the Budyko curve. *Geophysical Research Letters*, 39(19):2–7.
- Government of Canada (2016). Extent of canada’s wetlands. <https://www.canada.ca/en/environment-climate-change/services/environmental-indicators/extent-wetlands.html>.
- Government of Canada (2018). National water data archive: Hydat. <https://www.canada.ca/en/environment-climate-change/services/water-overview/quantity/monitoring/survey/data-products-services/national-archive-hydat.html>.
- Greve, P., Gudmundsson, L., Orlovsky, B., and Seneviratne, S. I. (2015). Introducing a probabilistic budyko framework. *Geophysical Research Letters*, 42(7):2261–2269.
- Gumbel, E. et al. (1941). The return period of flood flows. *The Annals of Mathematical Statistics*, 12(2):163–190.
- Guswa, A. J. (2008). The influence of climate on root depth: A carbon cost-benefit analysis. *Water Resources Research*, 44(2):1–11.
- Hall, D. K. and Riggs, G. A. (2007). Accuracy assessment of the modis snow products. *Hydrological Processes*, 21(12):1534–1547.
- Hall, D. K. and Riggs, G. A. (2016a). MODIS/Terra Snow Cover 8-Day L3 Global 500m SIN Grid, Version 6 .
- Hall, D. K. and Riggs, G. A. (2016b). MODIS/Terra Snow Cover Daily L3 Global 500m SIN Grid, Version 6 .
- Härer, S., Bernhardt, M., Siebers, M., and Schulz, K. (2018). On the need for a time- and location-dependent estimation of the ndsi threshold value for reducing existing uncertainties in snow cover maps at different scales. *The Cryosphere*, 12(5):1629–1642.
- Hargreaves, G. and Samani, Z. (1985). Reference crop evapotranspiration from temperature. *Applied Engineering in Agriculture*, 1.
- Holden, J. (2005). *An introduction to physical geography and the environment*. Pearson Education.
- Huggett, R. (2007). *Fundamentals of geomorphology*. Routledge.
- Hutchinson, M. F., McKenney, D. W., Lawrence, K., Pedlar, J. H., Hopkinson, R. F., Milewska, E., and Padopol, P. (2009). Development and testing of canada-wide interpolated spatial models of daily minimum–maximum temperature and precipitation for 1961–2003. *Journal of Applied Meteorology and Climatology*, 48(4):725–741.
- Jonkman, S., Steenbergen, R., Morales-Nápoles, O., Vrouwenvelder, A., and Vrijling, J. (2015). Probabilistic design: Risk and reliability analysis in civil engineering. *Lecture Notes CIE4130. Delft University of Technology*.

- Kleidon, A. (2004). Global datasets and rooting zone depth inferred from inverse methods. *Journal of Climate*, 17(13):2714–2722.
- Kleidon, A. and Heimann, M. (1998a). A method of determining rooting depth from a terrestrial biosphere model and its impacts on the global water and carbon cycle. *Global Change Biology*, 4(3):275–286.
- Kleidon, A. and Heimann, M. (1998b). Optimised rooting depth and its impacts on the simulated climate of an atmospheric general circulation model. *Geophysical Research Letters*, 25(3):345–348.
- Kleidon, A. and Heimann, M. (2000). Assessing the role of deep rooted vegetation in the climate system with model simulations: mechanism, comparison to observations and implications for Amazonian deforestation. *Climate Dynamics*, 16:183–199.
- Kochendorfer, J., Rasmussen, R., Wolff, M., Baker, B., Hall, M. E., Meyers, T., Landolt, S., Jachcik, A., Isaksen, K., Brækkan, R., and Leeper, R. (2017). The quantification and correction of wind-induced precipitation measurement errors. *Hydrology and Earth System Sciences*, 21(4):1973–1989.
- Lehner, B., Verdin, K., and Jarvis, A. (2008). New global hydrography derived from spaceborne elevation data. *Eos, Transactions American Geophysical Union*, 89(10):93–94.
- MacQueen, J. et al. (1967). Some methods for classification and analysis of multivariate observations. In *Proceedings of the fifth Berkeley symposium on mathematical statistics and probability*, volume 1, pages 281–297. Oakland, CA, USA.
- Maddala, G. S. (1986). *Limited-dependent and qualitative variables in econometrics*. Number 3. Cambridge university press.
- Maes, W. H., Gentine, P., Verhoest, N. E., and Miralles, D. G. (2019). Potential evaporation at eddy-covariance sites across the globe. *Hydrology and Earth System Sciences*, 23(2):925–948.
- Marcano-Cedeno, A., Quintanilla-Domínguez, J., Cortina-Januchs, M., and Andina, D. (2010). Feature selection using sequential forward selection and classification applying artificial metaplasticity neural network. In *IECON 2010-36th annual conference on IEEE industrial electronics society*, pages 2845–2850. IEEE.
- Menard, S. (2000). Coefficients of determination for multiple logistic regression analysis. *The American Statistician*, 54(1):17–24.
- Milly, P. C. (1994). Climate, soil water storage, and the average annual water balance. *Water Resources Research*, 30(7):2143–2156.
- Milly, P. C. D. and Dunne, K. A. (1994). Sensitivity of the global water cycle to the water-holding capacity of land. *Journal of Climate*, 7(4):506–526.
- Mines ParisTech (2014). Extraterrestrial irradiance (e0) and top of atmosphere (toa) radiation. <http://www.soda-pro.com/web-services/radiation/extraterrestrial-irradiance-and-toa>.
- Muralikrishna, I. and Manickam, V. (2017). *Environmental Management: Science and Engineering for Industry*.
- Nijzink, R., Hutton, C., Pechlivanidis, I., Capell, R., Arheimer, B., Freer, J., Han, D., Wagener, T., McGuire, K., Savenije, H., and Hrachowitz, M. (2016). The evolution of root-zone moisture capacities after deforestation: A step towards hydrological predictions under change? *Hydrology and Earth System Sciences*, 20(12):4775–4799.
- Pilgrim, D. H., Cordery, I., and Baron, B. C. (1982). Effects of catchment size on runoff relationships. *Journal of Hydrology*, 58(3):205 – 221.
- Porporato, A., Daly, E., and Rodriguez-Iturbe, I. (2004). Soil water balance and ecosystem response to climate change. *American Naturalist*, 164(5):625–632.
- Rabus, B., Eineder, M., Roth, A., and Bamler, R. (2003). The shuttle radar topography mission—a new class of digital elevation models acquired by spaceborne radar. *ISPRS Journal of Photogrammetry and Remote Sensing*, 57(4):241 – 262.

- Sankey, T., Donald, J., McVay, J., Ashley, M., O'Donnell, F., Lopez, S. M., and Springer, A. (2015). Multi-scale analysis of snow dynamics at the southern margin of the north american continental snow distribution. *Remote Sensing of Environment*, 169:307 – 319.
- Savenije, H. H. (2018). HESS Opinions: Linking Darcy's equation to the linear reservoir. *Hydrology and Earth System Sciences*, 22(3):1911–1916.
- Schenk, H. J. and Jackson, R. B. (2002). The global biogeography of roots. *Ecological monographs*, 72(3):311–328.
- Sevruk, B. (1982). *Methods of correction for systematic error in point precipitation measurement for operational use / by B. Sevruk*. Secretariat of the World Meteorological Organization Geneva, Switzerland.
- Shao, Q., Traylen, A., and Zhang, L. (2012). Nonparametric method for estimating the effects of climatic and catchment characteristics on mean annual evapotranspiration. *Water Resources Research*, 48(3).
- Smith, L. I. (2002). A tutorial on principal components analysis. Technical report.
- USGS (1997). Usgs 30 arc-second global elevation data, gtopo30.
- Vincent, W., Lemay, M., and Allard, M. (2017). Arctic permafrost landscapes in transition: Towards an integrated earth system approach. *Arctic Science*, 3.
- Wang-Erlandsson, L., Bastiaanssen, W. G., Gao, H., Jägermeyr, J., Senay, G. B., Van Dijk, A. I., Guerschman, J. P., Keys, P. W., Gordon, L. J., and Savenije, H. H. (2016). Global root zone storage capacity from satellite-based evaporation. *Hydrology and Earth System Sciences*, 20(4):1459–1481.
- Wang-Erlandsson, L., Van Der Ent, R. J., Gordon, L. J., and Savenije, H. H. (2014). Contrasting roles of interception and transpiration in the hydrological cycle - Part 1: Temporal characteristics over land. *Earth System Dynamics*, 5(2):441–469.
- Wolff, M., Isaksen, K., Petersen-Øverleir, A., Ødemark, K., Reitan, T., and Brækkan, R. (2015). Derivation of a new continuous adjustment function for correcting wind-induced loss of solid precipitation: results of a norwegian field study. *Hydrology and Earth System Sciences*, 19(2):951–967.
- Woods, R. A. (2009). Analytical model of seasonal climate impacts on snow hydrology: Continuous snow-packs. *Advances in Water Resources*, 32(10):1465 – 1481.
- Xie, H., Wang, X., and Liang, T. (2009). Development and assessment of combined terra and aqua snow cover products in colorado plateau, usa and northern xinjiang, china. *Journal of Applied Remote Sensing*, 3.
- Yang, D., Goodison, B. E., Metcalfe, J. R., Louie, P., Leavesley, G., Emerson, D., Hanson, C. L., Golubev, V. S., Elomaa, E., Gunther, T., Pangburn, T., Kang, E., and Milkovic, J. (1999). Quantification of precipitation measurement discontinuity induced by wind shields on national gauges. *Water Resources Research*, 35(2):491–508.
- Yang, Y., Donohue, R. J., and McVicar, T. R. (2016). Global estimation of effective plant rooting depth: Implications for hydrological modeling. *Water Resources Research*, 52(10):8260–8276.
- Ye, S., Li, H.-Y., Li, S., Leung, L. R., Demissie, Y., Ran, Q., and Blöschl, G. (2015). Vegetation regulation on streamflow intra-annual variability through adaption to climate variations. *Geophysical Research Letters*, 42(23):10,307–10,315.
- Zhang, L., Dawes, W. R., and Walker, G. R. (2001). Response of mean annual evapotranspiration to vegetation changes at catchment scale. *Water Resources Research*, 37(3):701–708.
- Zhang, L., Hickel, K., Dawes, W. R., Chiew, F. H. S., Western, A. W., and Briggs, P. R. (2004). A rational function approach for estimating mean annual evapotranspiration. *Water Resources Research*, 40(2).
- Zhao, J., Xu, Z., and Singh, V. P. (2016). Estimation of root zone storage capacity at the catchment scale using improved mass curve technique. *Journal of Hydrology*, 540:959 – 972.



## Land cover distribution in classes

Table A.1: Distribution of the ESA-CCI land cover classes into 5 classes of approximately equal behaviour regarding  $I_{max}$  and RP.

<b>Code</b>	<b>Label</b>	<b>Type</b>
0	No Data	
10	Cropland, rainfed	Cropland
20	Cropland, irrigated or post-flooding	Cropland
30	Mosaic cropland (\50%) / natural vegetation (tree, shrub, herbaceous cover) (50%)	Cropland
40	Mosaic natural vegetation (tree, shrub, herbaceous cover) (50%) / cropland (50%)	Shrubland
50	Tree cover, broadleaved, evergreen, closed to open (15%)	Forest
60	Tree cover, broadleaved, deciduous, closed to open (15%)	Forest
70	Tree cover, needleleaved, evergreen, closed to open (15%)	Forest
80	Tree cover, needleleaved, deciduous, closed to open (\15%)	Forest
90	Tree cover, mixed leaf type (broadleaved and needleleaved)	Forest
100	Mosaic tree and shrub (50%) / herbaceous cover (50%)	Shrubland
110	Mosaic herbaceous cover (\50%) / tree and shrub (50%)	Grassland
120	Shrubland	Shrubland
130	Grassland	Grassland
140	Lichens and mosses	Bare cover
150	Sparse vegetation (tree, shrub, herbaceous cover) (15%)	Grassland
160	Tree cover, flooded, fresh or brakish water	Forest
170	Tree cover, flooded, saline water	Forest
180	Shrub or herbaceous cover, flooded, fresh/saline/brakish water	Shrubland
190	Urban areas	Bare cover
200	Bare areas	Bare cover
210	Water bodies	Bare cover
220	Permanent snow and ice	Bare cover



# B

## Calibration and validation overview

Catchment	MF [ $\frac{mm}{d^{\circ}C}$ ]	TT [°C]	Performance calibration [-]	Performance validation [-]
1	1.192	-5.08	0.983	0.984
2	6.654	-2.338	0.991	0.997
5	7.637	1.745	0.988	0.986
6	2.584	-0.934	0.993	0.989
14	2.812	-0.002	0.991	0.99
16	2.539	-2.126	0.992	0.985
19	4.786	0.793	0.988	0.985
22	9.875	1.235	0.99	0.993
23	1.845	-3.226	0.998	0.989
26	7.46	-10.64	0.951	0.954
27	2.999	-3.388	0.994	0.985
28	2.338	-2.894	0.99	0.989
31	2.581	-3.28	0.944	0.934
32	6.57	-2.679	0.997	0.981
33	3.337	-2.296	0.982	0.982
36	9.991	-1.72	0.996	0.981
37	5.747	1.501	0.995	0.979
40	8.439	0.823	0.995	0.992
42	1.488	-4.812	0.966	0.981
43	1.912	-2.364	0.989	0.985
46	6.573	-2.409	0.997	0.981
48	5.425	0.027	0.991	0.985
49	0.561	-8.127	0.967	0.969
50	2.539	-0.449	0.995	0.984
51	9.212	-2.96	0.991	0.986
52	2.92	-1.715	0.991	0.985
53	1.622	-6.702	0.994	0.985
54	2.711	-1.318	0.989	0.992
55	7.923	-4.482	0.808	0.863
57	0.956	-4.995	0.957	0.973
58	3.255	-1.033	0.991	0.986
62	5.598	-2.028	0.995	0.996
63	1.967	-4.73	0.999	0.992
64	6.58	-1.374	0.994	0.986
65	2.511	-0.328	0.995	0.992
66	1.73	-3.169	0.986	0.985
68	8.783	1.27	0.996	0.997
69	5.282	-0.278	0.992	0.978

<b>Catchment</b>	<b>MF [<math>\frac{mm}{d^{\circ}C}</math>]</b>	<b>TT [°C]</b>	<b>{Performance calibration [-]}</b>	<b>Performance validation [-]</b>
70	5.184	2.323	0.988	0.99
71	1.638	-4.145	0.982	0.974
72	2.609	-1.157	0.992	0.988
73	4.27	-4.388	0.966	0.977
74	1.278	-3.054	0.949	0.974
75	2.95	-0.396	0.993	0.993
76	2.043	-3.487	0.948	0.95
77	0.942	-3.309	0.983	0.988
78	2.432	-4.466	0.975	0.988
79	4.971	1.724	0.995	0.996
80	4.135	0.235	0.976	0.969
82	7.256	-0.076	0.97	0.972
84	1.898	-2.109	0.994	0.981
85	1.854	-4.072	0.988	0.995
86	0.983	-6.738	0.971	0.973
88	7.261	-0.393	0.997	0.992
90	5.313	-0.796	0.997	0.994
93	1.784	-1.564	0.991	0.984
95	1.42	-0.613	0.993	0.991
96	5.441	-0.277	0.956	0.957
98	1.246	-5.661	0.97	0.985
99	8.972	1.868	0.992	0.964
100	3.438	-0.441	0.97	0.979
101	1.563	-3.118	0.982	0.986
102	3.895	0.166	0.99	0.982
104	1.503	-3.139	0.972	0.974
105	3.286	-1.262	0.994	0.987
106	5.452	0.724	0.988	0.966
107	2.416	-1.227	0.98	0.965
108	3.086	1.488	0.993	0.995
110	6.946	2.232	0.995	0.995
111	9.151	0.923	0.997	0.995
112	3.699	-8.971	0.95	0.948
113	2.498	-4.793	0.996	0.995
114	2.776	-2.148	0.993	0.98
115	3.987	3.015	0.993	0.995
116	1.497	-3.963	0.959	0.971
117	8.036	1.994	0.987	0.98
118	9.775	3.9	0.994	0.994
119	1.489	-4.046	0.989	0.997
120	0.16	-14.233	0.957	0.969
125	7.701	-0.351	1.0	0.997
126	1.278	-3.463	0.985	0.99
127	3.551	-1.77	0.984	0.974
129	2.55	-4.338	0.996	0.996
132	6.621	0.367	0.991	0.986
134	3.099	1.441	0.981	0.974
135	1.706	-3.299	0.994	0.992
137	0.779	-2.11	0.984	0.986
138	4.869	0.021	0.986	0.978
139	1.554	-2.887	0.982	0.99
140	8.385	0.672	0.992	0.992
142	2.133	-3.727	0.995	0.981
143	8.786	-0.849	0.994	0.99
144	2.901	-1.379	0.991	0.988

<b>Catchment</b>	<b>MF<math>[\frac{mm}{d^{\circ}C}]</math></b>	<b>TT [°C]</b>	<b>{Performance calibration [-]}</b>	<b>Performance validation [-]</b>
145	1.059	-7.028	0.96	0.969
150	2.129	-2.742	0.976	0.96
151	0.782	-4.034	0.961	0.977
153	3.832	0.701	0.994	0.996
155	2.031	-4.517	0.979	0.986
157	2.37	-4.06	0.991	0.992
158	5.683	-1.049	0.997	0.986
162	7.181	-0.812	0.996	0.976
163	6.713	-1.032	0.989	0.988
164	5.041	-1.688	0.993	0.992
167	6.287	-0.735	0.998	0.993
169	5.987	-0.202	0.984	0.977
170	2.953	0.041	0.994	0.992
171	6.379	0.228	0.984	0.968
173	4.277	-1.529	0.998	0.997
174	3.576	-2.042	0.992	0.987
175	2.154	-2.98	0.991	0.992
178	1.723	-2.682	0.987	0.988
179	3.293	-2.141	0.995	0.995
180	3.444	-1.495	0.995	0.988
181	2.351	-2.824	0.983	0.984
183	4.097	-1.814	0.996	1.0
186	4.555	-1.107	0.998	0.993
188	3.756	1.416	0.992	0.997
189	4.418	0.863	0.993	0.994
191	5.664	0.278	0.99	0.992
194	4.181	-1.949	0.975	0.977
195	3.702	-2.419	0.992	0.995
197	7.512	-0.867	0.99	0.993
198	8.572	0.599	0.99	0.992
199	1.723	-3.003	0.991	0.995
200	1.988	-0.51	0.992	0.994
202	3.635	-1.411	0.992	1.0
203	2.493	0.461	0.989	0.992
204	5.525	0.355	0.997	0.997
206	3.978	-2.887	0.979	0.97
207	4.784	0.592	0.994	0.997
208	8.302	-0.355	0.991	0.99
210	9.868	-1.043	0.994	0.989
211	4.771	0.047	0.995	0.996
212	0.859	-3.74	0.994	0.995
213	4.595	-3.555	0.966	0.976
214	1.712	-2.978	0.984	0.988
215	2.61	-4.896	0.989	0.99
216	2.241	-0.36	0.991	0.994
217	5.767	1.787	0.986	0.988
218	5.959	0.32	0.981	0.981
219	1.407	-3.943	0.983	0.993
221	3.441	-2.591	0.994	0.988
223	8.312	-0.841	0.995	0.992
226	0.405	-9.514	0.986	0.989
227	2.045	-3.379	0.985	0.997
228	4.93	1.466	0.994	0.994
229	4.213	-2.593	0.981	0.99
230	3.845	-2.328	0.996	0.997

<b>Catchment</b>	<b>MF [<math>\frac{mm}{d^{\circ}C}</math>]</b>	<b>TT [°C]</b>	<b>{Performance calibration [-]}</b>	<b>Performance validation [-]</b>
232	6.071	-0.698	0.995	0.99
233	4.229	-0.363	0.998	0.998
236	4.954	-2.506	0.991	0.996
237	1.547	-4.087	0.987	0.995
238	1.356	-6.772	0.985	0.992
241	0.859	-6.194	0.992	0.997
242	2.906	3.044	0.981	0.987
243	9.666	0.329	0.988	0.995
245	3.251	-3.085	0.999	0.993
246	5.228	-0.805	0.995	0.99
249	6.887	-0.866	0.997	0.997
251	2.568	-2.993	0.988	0.992
253	9.219	-0.393	0.994	0.996
254	2.959	2.613	0.985	0.985
255	2.395	-2.388	0.99	0.995
258	4.811	-0.49	0.994	0.992
259	9.547	-0.611	0.986	0.99
260	8.751	-1.937	0.986	0.985
262	9.633	0.778	0.995	0.99
263	3.745	1.094	0.988	0.984
267	4.266	-2.786	0.993	0.993
268	5.297	0.933	0.989	0.983
270	5.588	-0.031	0.999	0.997
271	7.097	-2.242	0.992	0.979
272	4.512	-3.349	0.991	0.995
274	3.494	-3.445	0.994	0.992
276	7.317	-1.517	0.991	0.997
277	8.185	-0.945	0.994	0.99
283	2.138	-4.861	0.986	0.995
285	2.958	-0.739	0.995	0.992
286	2.525	0.167	0.988	0.987
288	8.757	-2.243	0.985	0.995
290	8.26	1.166	0.998	0.997
291	6.313	-2.222	0.998	0.995
292	9.913	0.206	0.989	0.999
293	3.288	-3.551	0.983	0.995
294	2.553	-5.323	0.988	0.995
295	5.67	-1.093	0.994	0.967
296	3.097	-3.434	0.991	0.997
297	4.055	-3.036	0.979	0.992
298	2.185	-1.919	0.985	0.986
301	9.019	-0.36	0.989	0.978
303	9.834	-2.477	0.987	0.975
306	8.246	0.435	0.997	0.994
311	5.26	-0.445	0.998	0.991
319	8.696	0.793	0.994	0.995
320	9.498	-0.198	0.993	0.99
321	8.995	-0.942	0.993	0.997
324	9.903	-0.965	0.989	0.982
325	7.99	-0.726	0.994	0.993
326	4.154	-2.283	0.982	0.966
328	7.248	-1.547	0.995	0.989
331	3.895	-4.659	0.97	0.973
335	2.457	-6.541	0.984	0.981
338	9.946	-1.216	0.995	0.996

<b>Catchment</b>	<b>MF<math>[\frac{mm}{d^{\circ}C}]</math></b>	<b>TT [°C]</b>	<b>{Performance calibration [-]}</b>	<b>Performance validation [-]</b>
342	9.007	-0.234	0.995	0.996
343	8.301	-1.31	0.997	0.993
344	5.648	-2.297	0.963	0.934
345	6.823	-1.304	0.987	0.984
347	4.644	-3.728	0.958	0.957
348	7.437	-1.353	0.991	0.986
350	4.021	-2.199	0.982	0.982
352	7.463	-1.722	0.969	0.974
353	3.648	-3.183	0.983	0.98
354	2.027	-3.763	0.975	0.977
355	2.828	-3.74	0.984	0.968
356	9.786	-9.268	0.972	0.947
357	9.939	-19.941	0.923	0.932
362	8.77	-2.35	0.966	0.957
364	2.316	-4.953	0.984	0.982
365	2.24	-3.619	0.979	0.964
366	2.436	-4.325	0.983	0.978
367	2.211	-4.557	0.985	0.989
368	0.426	-9.39	0.973	0.963
369	0.592	-6.676	0.985	0.978
373	2.343	-3.76	0.981	0.974
374	0.861	-7.956	0.984	0.989
375	1.842	-3.158	0.979	0.986
377	7.577	-1.724	0.981	0.997
378	3.616	-2.832	0.981	0.99
379	3.512	-19.648	0.988	0.99
381	1.682	0.951	0.98	0.986
383	9.199	-0.803	0.996	0.99
384	1.945	-1.257	0.977	0.977
385	2.017	-1.993	0.987	0.991
386	1.058	-4.704	0.969	0.971
387	3.287	-0.211	0.977	0.972
388	2.876	-0.888	0.991	0.982
390	0.335	-9.494	0.967	0.982
392	1.481	-3.161	0.99	0.987
393	2.27	-3.077	0.983	0.989
394	1.774	-4.14	0.983	0.987
395	2.3	-0.054	0.993	0.985
396	3.571	0.194	0.987	0.974
397	4.066	-0.88	0.992	0.979
398	7.352	1.892	0.993	0.993
399	0.447	-9.799	0.96	0.971
402	2.032	-2.565	0.982	0.987
406	1.952	-0.353	0.994	0.995
408	2.128	-4.057	0.993	0.995
412	0.932	-3.419	0.988	0.989
416	4.132	-1.517	0.996	0.997
417	1.939	-1.887	0.991	0.995
418	2.362	-4.1	0.985	0.983
420	6.174	-2.072	0.993	0.996
422	3.223	-0.723	0.994	0.99
426	9.724	-0.85	0.991	0.987
428	2.644	-1.125	0.993	0.998
430	7.724	-1.883	0.984	0.994
432	2.196	-4.958	0.957	0.989

<b>Catchment</b>	<b>MF[<math>\frac{mm}{d^{\circ}C}</math>]</b>	<b>TT [°C]</b>	<b>{Performance calibration [-]}</b>	<b>Performance validation [-]</b>
435	2.235	-3.236	0.996	1.0
436	5.028	-1.157	0.991	0.995
438	6.398	-1.434	0.996	0.99
441	2.207	-3.056	0.984	0.984
446	9.731	-0.378	0.993	0.993
448	5.708	1.331	0.992	0.992
449	8.792	-0.577	0.99	0.974
452	7.211	-0.86	0.998	0.997
454	1.45	-1.323	0.984	0.985
455	1.636	-2.623	0.974	0.977
457	4.42	-4.451	0.989	0.99
458	3.86	-1.174	0.978	0.971
459	3.141	-2.963	0.979	0.981
460	1.991	-3.675	0.984	0.975
461	1.725	0.489	0.993	0.991
462	1.816	-3.453	0.986	0.988
463	5.007	-1.201	0.997	0.995
465	2.995	-3.19	0.991	0.993
466	3.236	-1.69	0.993	0.991
469	2.141	-1.408	0.984	0.981
470	4.107	-2.153	0.992	0.993
472	4.727	-2.339	0.976	0.993
473	5.678	0.073	0.988	0.983
474	3.064	-3.499	0.975	0.977
475	9.438	1.297	0.988	0.993
476	2.277	-1.513	0.993	0.989
477	1.531	-3.653	0.983	0.99
480	6.565	0.655	0.988	0.988
481	2.001	-0.457	0.991	0.995
482	0.955	-4.375	0.993	0.994
484	9.876	0.015	0.99	0.989
485	2.309	0.782	0.994	0.994
486	2.606	-2.471	0.996	0.995
490	2.524	-0.02	0.993	0.988
491	4.583	-4.232	0.99	0.989
492	3.328	-0.322	0.994	0.995
494	1.613	0.378	0.994	0.992
496	0.795	-2.647	0.991	0.994
497	1.904	-2.367	0.986	0.996
498	1.797	-1.821	0.979	0.97
500	1.54	-1.513	0.988	0.989
502	4.099	-0.794	0.993	0.993
504	1.708	-1.643	0.988	0.987
506	6.309	-1.43	0.992	0.991
507	2.163	-3.731	0.985	0.984
510	2.342	-0.078	0.994	0.995
511	0.836	-2.893	0.991	0.996
512	4.502	-0.898	0.991	0.989
514	2.278	-3.559	0.981	0.988
515	2.646	-1.949	0.994	0.994
516	0.766	-4.879	0.982	0.979
518	0.254	-6.638	0.991	0.994
521	9.919	-3.901	0.96	0.968
523	1.112	-7.038	0.956	0.95
525	1.668	-3.552	0.967	0.967

<b>Catchment</b>	<b>MF [<math>\frac{mm}{d^{\circ}C}</math>]</b>	<b>TT [°C]</b>	<b>{Performance calibration [-]}</b>	<b>Performance validation [-]</b>
527	4.145	-0.259	0.992	0.982
528	2.22	-3.4	0.989	0.989
529	1.221	-5.064	0.97	0.973
530	9.218	-0.343	1.0	0.999
531	4.38	-1.582	0.999	0.999
532	1.31	-3.617	0.958	0.966
533	6.185	-0.853	0.982	0.985
534	9.618	-7.532	0.971	0.99
535	1.402	-3.336	0.978	0.979
538	1.985	-0.779	0.985	0.972
539	4.113	3.139	0.994	0.99
540	0.741	-4.702	0.974	0.981
541	9.964	4.85	0.985	0.99
542	1.12	-3.326	0.971	0.975
543	8.565	1.053	0.993	0.975
544	8.666	1.625	0.994	0.962
545	6.801	1.691	0.992	0.996
546	3.249	-0.557	0.975	0.977
547	5.341	0.655	0.995	0.97
549	3.173	-14.045	0.962	0.942
550	5.505	-0.463	0.993	0.995
551	7.169	0.142	0.99	0.986
552	6.353	1.434	0.992	0.989
553	1.342	-4.021	0.987	0.984
554	3.395	-1.18	0.979	0.961
558	0.6	-8.6	0.957	0.978
560	2.367	-1.881	0.983	0.97
562	0.523	-4.406	0.984	0.99
563	3.458	2.106	0.993	0.996
564	4.751	-0.917	0.993	0.992
565	7.483	-0.444	0.992	0.989
567	5.354	-2.105	0.997	0.996
569	2.188	-4.908	0.979	0.979
570	3.543	-1.542	0.998	0.995
571	4.567	-0.178	0.992	0.984
572	7.365	-0.89	0.996	0.989
573	2.309	-3.258	0.979	0.974
574	1.673	-6.19	0.963	0.963
575	4.985	-2.473	0.995	1.0
576	6.465	2.707	0.993	0.993
577	3.803	-1.169	0.959	0.964
578	5.369	0.387	0.99	0.992
579	3.242	-2.947	0.959	0.972
580	1.669	-6.507	0.966	0.959
582	9.363	0.124	0.994	0.99
583	9.458	0.964	0.993	0.977
586	4.623	-0.136	0.993	0.989
587	9.646	0.492	0.995	0.992
588	2.937	-2.537	0.983	0.992
589	2.292	-3.79	0.995	0.997
591	5.591	-1.571	0.991	0.988
596	9.935	-0.227	0.995	0.988
600	2.72	-0.853	0.98	0.989
601	4.315	-2.815	0.994	0.997
602	3.327	-0.172	0.995	0.992

<b>Catchment</b>	<b>MF [<math>\frac{mm}{d^{\circ}C}</math>]</b>	<b>TT [°C]</b>	<b>{Performance calibration [-]}</b>	<b>Performance validation [-]</b>
603	9.65	0.405	0.988	0.99
604	5.733	-1.091	0.993	0.99
605	4.707	-1.755	0.971	0.976
606	4.459	-1.901	0.995	0.995
607	8.996	-0.062	0.988	0.99
608	3.611	-0.679	0.979	0.98
609	2.778	-3.879	0.992	0.995
610	9.7	1.333	0.982	0.986
611	1.872	-0.944	0.991	0.988
613	5.96	-3.0	0.993	0.995
614	6.286	1.867	0.999	0.999
615	7.08	-2.51	0.988	0.988
616	5.901	0.243	0.99	0.98
617	5.151	-2.124	0.994	0.985
619	3.124	-0.537	0.987	0.974
620	7.616	-0.377	0.989	0.993
621	9.738	0.095	0.992	0.993
622	4.014	-0.327	0.993	0.97
623	6.642	-1.709	0.997	0.984
624	9.765	0.611	0.908	0.915
625	5.311	-1.491	0.99	0.993
626	7.964	-1.993	0.99	0.993
627	7.171	-0.439	0.989	0.986
628	7.421	-11.199	0.97	0.953
630	9.925	0.455	0.979	0.971
631	9.26	0.543	0.995	0.995
634	2.222	-2.333	0.987	0.987
639	1.516	-13.493	0.981	0.984
641	8.894	-1.419	0.99	0.996
643	0.631	-9.547	0.963	0.984
644	1.077	-6.287	0.97	0.99
646	9.117	0.175	0.994	0.996
647	3.916	-2.026	0.994	0.986
648	2.312	-3.556	0.995	0.985
651	5.435	-1.823	0.991	0.983
652	9.56	0.192	0.997	0.999
653	5.656	-0.91	0.993	0.988
654	4.029	-2.423	0.989	0.977
655	9.198	-0.702	0.984	0.986
657	1.039	-4.343	0.988	0.975
658	5.252	-0.7	0.985	0.984
659	4.725	-4.295	0.975	0.973
662	9.342	-2.646	0.979	0.975
663	2.226	-3.465	0.978	0.976
664	6.712	-0.882	0.994	0.993
666	9.561	-18.727	0.962	0.972
667	9.968	-0.904	0.994	0.99
668	2.785	-2.153	0.997	0.994
669	0.88	-7.489	0.974	0.975
670	1.339	-4.851	0.995	1.0
671	1.423	-4.427	0.972	0.962
674	5.521	-2.659	0.978	0.984
675	2.387	-4.032	0.987	0.977
676	8.613	0.181	0.99	1.0
677	4.608	-4.983	0.986	0.982

<b>Catchment</b>	<b>MF</b> $[\frac{mm}{d^{\circ}C}]$	<b>TT</b> [°C]	<b>{Performance calibration [-]}</b>	<b>Performance validation [-]</b>
<b>678</b>	1.255	-4.156	0.996	0.992
<b>680</b>	2.991	-2.057	0.993	0.997
<b>681</b>	2.126	-3.993	0.974	0.97
<b>684</b>	9.388	-2.052	0.996	1.0
<b>685</b>	9.831	-1.808	0.997	0.997
<b>686</b>	1.978	-2.842	0.992	0.99
<b>687</b>	6.562	-1.881	0.993	0.995
<b>688</b>	3.507	-3.002	0.987	0.995
<b>690</b>	8.873	-0.716	0.999	1.0
<b>691</b>	8.594	-0.82	0.996	0.997
<b>692</b>	8.023	-0.546	0.998	0.997
<b>693</b>	9.873	0.658	0.994	0.999
<b>694</b>	8.751	-1.508	0.993	0.997
<b>695</b>	9.744	0.347	0.995	0.992
<b>697</b>	9.626	0.794	0.994	0.989
<b>698</b>	9.305	0.64	0.995	0.993

Table B.1: Overview of the values used for the calibration parameters and the calibration and validation performance per catchment. The performance of the calibration and validation is based on the percentage of matches between the MODIS snow cover dataset and the snow reservoir in all elevation zones in a catchment for all days on which the MODIS dataset does not provide NAN-data.



# C

## Overview of descriptor variables

This appendix provides an overview of all climate, landscape and discharge parameters that were considered in this study. The abbreviations used in this appendix will also be used in the plots presented in Appendix F.

### C.1. Climate variables

The climate variables considered in this study are summarised in this section. Whenever needed, a short parameter explanation is provided. No parameter description is given for variables that are explained in the main body of this study.

- Aridity Index (AI)
- Offset of potential evaporation ( $E_{p,off}$ )
  - Describes the end of the potential evaporation period
- Onset of potential evaporation ( $E_{p,on}$ )
  - Describes the start of the potential evaporation period
- Yearly average potential evaporation ( $E_p$ )
- Interstorm duration liquid input (ID)
- Interstorm duration precipitation ( $ID_p$ )
- Yearly average precipitation (P)
- 90-percentile liquid input ( $Liq_{perc}$ )
- Normalised 90-percentile liquid input ( $Liq_{norm}$ )
  - The 90-percentile liquid input has been normalised using the mean liquid input to identify how much high input deviates from mean input.
- 90-percentile precipitation ( $P_{perc}$ )
- Normalised 90-percentile precipitation ( $P_{norm}$ )
  - The 90-percentile precipitation has been normalised using the mean liquid input to identify how much high precipitation deviates from mean precipitation.
- Phase difference maximum liquid input and potential evaporation ( $\phi_{liq,E_p}$ )
- Phase difference maximum melt input and potential evaporation ( $\phi_{melt,E_p}$ )
- Phase difference precipitation and potential evaporation ( $\phi_{P,E_p}$ )

- Phase difference potential evaporation offset and snow onset ( $\phi_{off,on}$ )
- Phase difference potential evaporation onset and snow offset ( $\phi_{on,off}$ )
- Percentage of solid precipitation ( $P_{s,rel}$ )
- Duration melt period ( $Q_{m,days}$ )
- Runoff Coefficient (RC)
  - Combines climate and landscape influences
- Yearly average maximum snow water equivalent ( $S_{cov}$ )
- Total number of snow cover days ( $S_{days}$ )
- Day with maximum snow cover ( $S_{idx,max}$ )
- Snow-off day ( $S_{off}$ )
  - Describes the end of the snow cover period
- Snow-on day ( $S_{on}$ )
  - Describes the start of the snow cover period
- Seasonality index liquid input (SI)
- Seasonality index precipitation ( $SI_p$ )
- Seasonality index melt input ( $SI_{melt}$ )
- Seasonality timing index liquid input (ST)
- Seasonality timing index precipitation ( $ST_p$ )
- Average catchment temperature ( $T_{av}$ )
- Yearly temperature difference ( $T_{diff}$ )
- Maximum catchment temperature ( $T_{max}$ )
- Minimum catchment temperature ( $T_{min}$ )
- Interannual variability of liquid input ( $P_{inter}$ )
  - Coefficient of variation of yearly precipitation totals

## C.2. Landscape variables

The landscape variables considered in this study are summarised in this section. Whenever needed, a short parameter explanation is provided. No parameter description is given for variables that are explained in the main body of this study.

- Eastern facing slopes percentage (aspect) ( $As_{east}$ )
- Northern facing slopes percentage (aspect) ( $As_{north}$ )
- Southern facing slopes percentage (aspect) ( $As_{south}$ )
- Western facing slopes percentage (aspect) ( $As_{west}$ )
- Direction of majority of slopes ( $As_{maj}$ )
  - The direction is indicated in degrees, with 0 and 360° being north.
- Relative evaporative index (REI)

- Average catchment elevation ( $H_{av}$ )
- Elevation difference in a catchment ( $\Delta H$ )
- Maximum interception capacity ( $I_{max}$ )
- Percentage bare cover ( $P_b$ )
- Percentage cropland ( $P_c$ )
- Percentage grassland ( $P_g$ )
- Percentage shrubland or herbaceous cover ( $P_s$ )
- Percentage forest cover ( $P_f$ )
- Return period (RP)
- Average ruggedness ( $Rugg_{av}$ )
  - Total difference between a cell from the DEM and its surrounding cells, averaged over the catchment
- Maximum ruggedness ( $Rugg_{max}$ )
- Average catchment slope percentage ( $Slope_{av}$ )
- Maximum catchment slope percentage ( $Slope_{max}$ )

### C.3. Discharge variables

The discharge variables considered in this study are summarised in this section. Whenever needed, a short parameter explanation is provided. No parameter description is given for variables that are explained in the main body of this study.

- Base Flow Index (BFI)
  - Ratio of base flow to total stream flow. Base flow was defined as the minimum flow using a 7-days rolling mean.
- Total number of days without flow (CZ)
- Duration of high flow event ( $D_{high}$ )
  - Average duration of flow events that are larger than 3 times median flow
- Frequency of occurrence of high flow event ( $f_{high}$ )
- Duration of low flow event ( $D_{low}$ )
  - Average duration of flow events that are smaller than  $\frac{1}{3}$  of the median flow
- Frequency of occurrence of low flow event ( $f_{low}$ )
- Rising limb density (RLD)
  - Ratio between the number of peaks and the cumulative time of the rising limbs
- Falling limb density (DLD)
  - Ratio between the number of peaks and the cumulative time of the falling limbs
- Average rising rate of the discharge signal (RR)
- Average rising rate of the discharge signal (FR)
- 90-percentile discharge ( $Q_{perc}$ )

- Normalised 90-percentile discharge ( $Q_{norm}$ )
  - The 90-percentile discharge has been normalised using the mean liquid input to identify how much high flow deviates from mean flow.
- Peak distribution ( $PD$ )
  - Ratio between high peaks (90-percentile peaks) and median peaks (50-percentile peak flows)
- Phase difference maximum liquid input and discharge ( $\phi_{liq,Q}$ )
- Phase difference maximum melt input and discharge ( $\phi_{melt,Q}$ )
- Phase difference maximum precipitation and discharge ( $\phi_{P,Q}$ )
- Phase difference maximum potential evaporation and discharge ( $\phi_{E_p,Q}$ )
- Yearly average discharge ( $Q$ )
- Average yearly maximum discharge ( $Q_{max}$ )
- Average yearly minimum discharge ( $Q_{min}$ )
- Interannual variability discharge ( $Q_{inter}$ )
  - Coefficient of variation of yearly discharge totals
- Interannual variability maximum flow ( $Q_{inter,max}$ )
  - Coefficient of variation of yearly discharge maxima
- Interannual variability minimum flow ( $Q_{inter,min}$ )
  - Coefficient of variation of yearly discharge minima
- Seasonality index discharge ( $SI_Q$ )

# D

## Python code

The most relevant code that has been used in this study is published in an online repository, to enable reproducibility. The Python scripts can be acquired on <https://github.com/lvanvoorst/Thesis> or can be accessed using the following QR-code:





# E

## Overview root zone storage capacities

Table E.1: Root zone storage capacity magnitude for every study catchment

<b>catch.</b>	$S_r$ [mm]								
<b>1</b>	142	<b>138</b>	90	<b>298</b>	129	<b>422</b>	7	<b>575</b>	110
<b>22</b>	128	<b>143</b>	127	<b>301</b>	109	<b>426</b>	193	<b>579</b>	132
<b>23</b>	87	<b>145</b>	203	<b>306</b>	105	<b>432</b>	225	<b>580</b>	130
<b>27</b>	141	<b>150</b>	226	<b>311</b>	94	<b>435</b>	196	<b>586</b>	263
<b>28</b>	89	<b>151</b>	150	<b>319</b>	118	<b>436</b>	118	<b>588</b>	185
<b>31</b>	105	<b>155</b>	235	<b>325</b>	190	<b>438</b>	252	<b>596</b>	166
<b>32</b>	236	<b>164</b>	39	<b>328</b>	273	<b>441</b>	141	<b>610</b>	335
<b>36</b>	127	<b>167</b>	159	<b>335</b>	324	<b>449</b>	171	<b>615</b>	228
<b>40</b>	137	<b>169</b>	294	<b>338</b>	132	<b>454</b>	74	<b>619</b>	349
<b>42</b>	141	<b>171</b>	188	<b>343</b>	207	<b>455</b>	145	<b>628</b>	264
<b>46</b>	185	<b>173</b>	130	<b>344</b>	214	<b>458</b>	121	<b>630</b>	290
<b>49</b>	193	<b>174</b>	264	<b>345</b>	202	<b>459</b>	176	<b>631</b>	202
<b>51</b>	186	<b>175</b>	280	<b>347</b>	333	<b>460</b>	230	<b>634</b>	191
<b>52</b>	109	<b>178</b>	165	<b>348</b>	204	<b>462</b>	235	<b>643</b>	202
<b>54</b>	47	<b>179</b>	122	<b>350</b>	200	<b>463</b>	134	<b>644</b>	215
<b>57</b>	136	<b>181</b>	219	<b>352</b>	225	<b>465</b>	129	<b>646</b>	68
<b>62</b>	143	<b>183</b>	108	<b>353</b>	173	<b>466</b>	257	<b>651</b>	217
<b>63</b>	166	<b>195</b>	122	<b>354</b>	219	<b>469</b>	96	<b>652</b>	112
<b>66</b>	170	<b>204</b>	122	<b>355</b>	177	<b>470</b>	178	<b>653</b>	234
<b>68</b>	56	<b>208</b>	72	<b>356</b>	161	<b>472</b>	261	<b>654</b>	170
<b>69</b>	164	<b>210</b>	295	<b>357</b>	182	<b>473</b>	134	<b>655</b>	115
<b>71</b>	114	<b>213</b>	222	<b>362</b>	271	<b>474</b>	235	<b>657</b>	177
<b>73</b>	145	<b>215</b>	181	<b>365</b>	258	<b>475</b>	59	<b>658</b>	148
<b>74</b>	227	<b>217</b>	102	<b>366</b>	233	<b>477</b>	195	<b>662</b>	180
<b>76</b>	122	<b>218</b>	302	<b>367</b>	192	<b>484</b>	143	<b>663</b>	389
<b>77</b>	241	<b>219</b>	147	<b>368</b>	151	<b>486</b>	139	<b>664</b>	234
<b>78</b>	172	<b>226</b>	153	<b>369</b>	288	<b>490</b>	80	<b>666</b>	208
<b>80</b>	263	<b>227</b>	200	<b>373</b>	238	<b>497</b>	102	<b>667</b>	293
<b>82</b>	241	<b>229</b>	257	<b>374</b>	360	<b>498</b>	163	<b>668</b>	164
<b>85</b>	187	<b>230</b>	178	<b>375</b>	205	<b>502</b>	155	<b>669</b>	363
<b>86</b>	164	<b>232</b>	281	<b>377</b>	256	<b>504</b>	81	<b>670</b>	170
<b>96</b>	197	<b>233</b>	70	<b>378</b>	309	<b>506</b>	122	<b>671</b>	192
<b>98</b>	206	<b>238</b>	232	<b>383</b>	143	<b>507</b>	166	<b>674</b>	342
<b>99</b>	233	<b>241</b>	174	<b>384</b>	143	<b>514</b>	224	<b>675</b>	189
<b>100</b>	148	<b>243</b>	261	<b>385</b>	75	<b>516</b>	60	<b>676</b>	224
<b>101</b>	130	<b>255</b>	169	<b>386</b>	166	<b>521</b>	44	<b>677</b>	188
<b>104</b>	173	<b>259</b>	73	<b>387</b>	250	<b>525</b>	301	<b>678</b>	215
<b>105</b>	71	<b>260</b>	227	<b>390</b>	143	<b>533</b>	140	<b>680</b>	238
<b>106</b>	246	<b>274</b>	106	<b>393</b>	194	<b>534</b>	206	<b>681</b>	277
<b>107</b>	216	<b>283</b>	216	<b>394</b>	163	<b>535</b>	161	<b>686</b>	317
<b>113</b>	145	<b>286</b>	180	<b>395</b>	162	<b>542</b>	226	<b>688</b>	113
<b>114</b>	335	<b>290</b>	87	<b>397</b>	291	<b>546</b>	215	<b>692</b>	266
<b>116</b>	207	<b>293</b>	199	<b>416</b>	148	<b>554</b>	120	<b>694</b>	269
<b>129</b>	168	<b>294</b>	133	<b>417</b>	139	<b>560</b>	61	<b>695</b>	231
<b>134</b>	97	<b>296</b>	146	<b>418</b>	235	<b>562</b>	144	<b>697</b>	255
<b>137</b>	155	<b>297</b>	202	<b>420</b>	271	<b>573</b>	251	<b>698</b>	248

# F

## Correlation of all test variables and $S_r$

### **F.1. Climate variables**

This section provides an overview of climate variables in respectively Figure E1, E2 and E3. The numbers in the figure refer back to Appendix C.1, where the variables are explained.

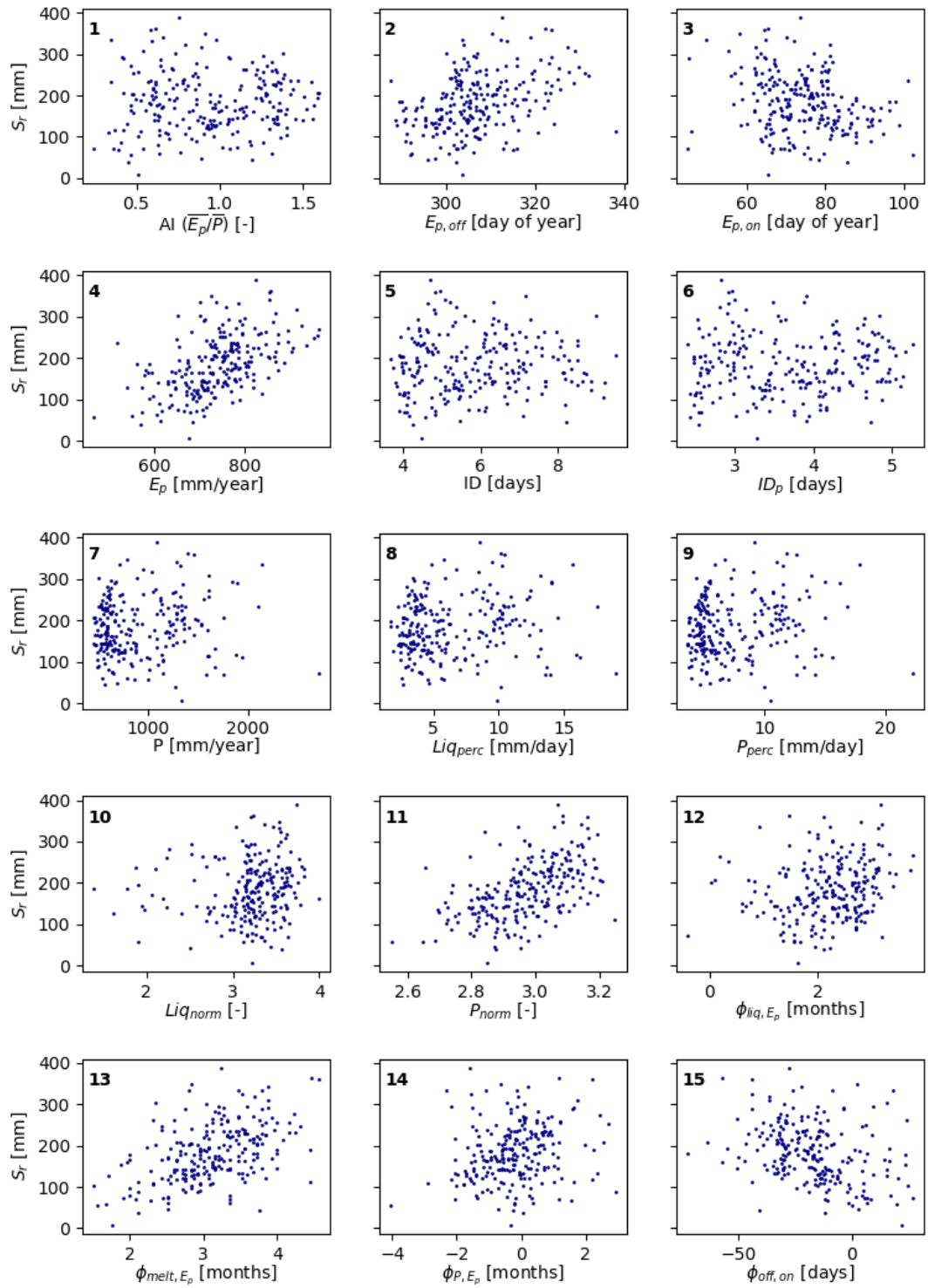


Figure E.1: Relationship between  $S_r$  and the first 15 climate variables. The numbers in the plot refer to the numbers in Appendix C.1.

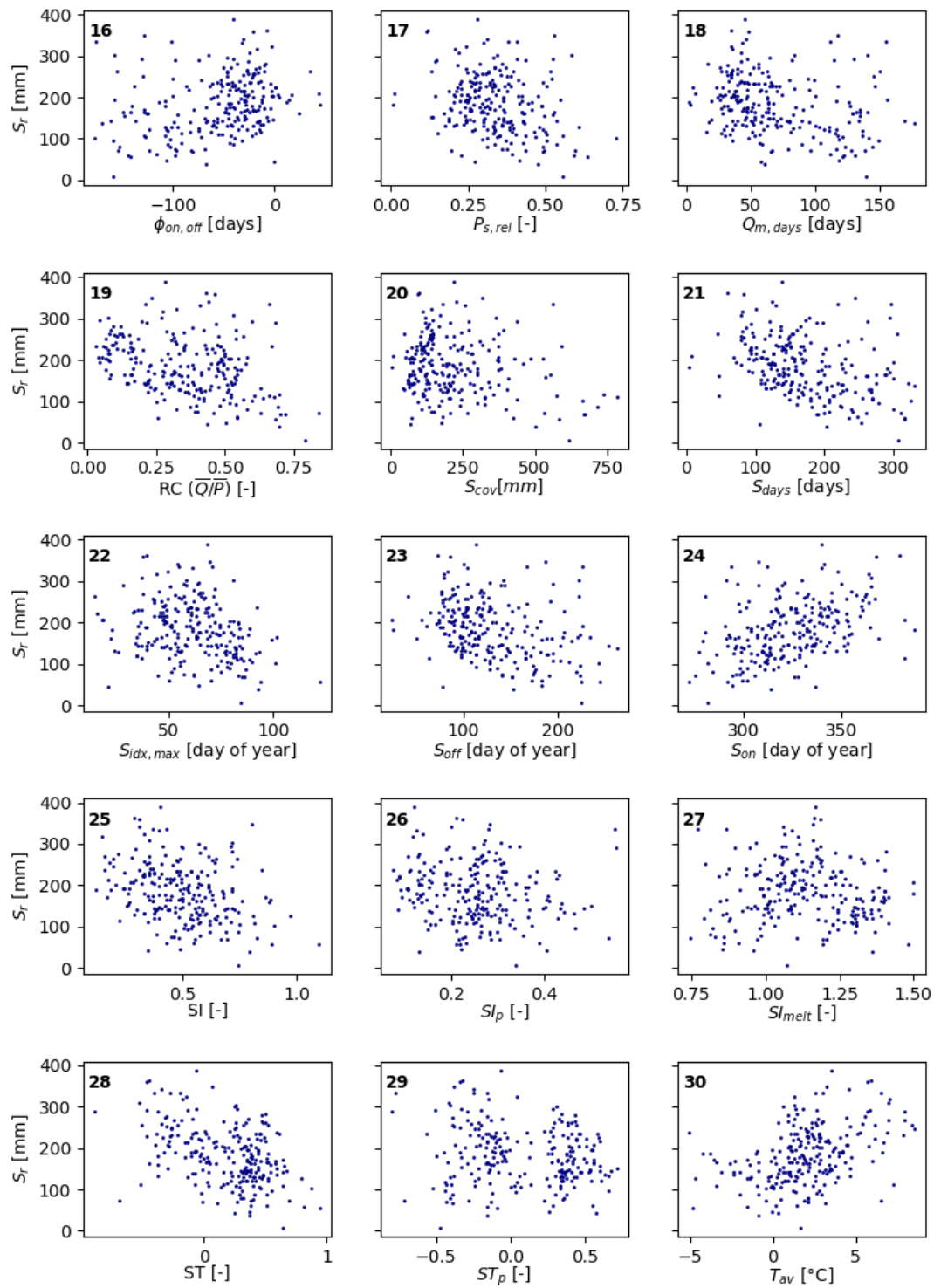


Figure E2: Relationship between  $S_r$  and the second 15 climate variables. The numbers in the plot refer to the numbers in Appendix C.1.

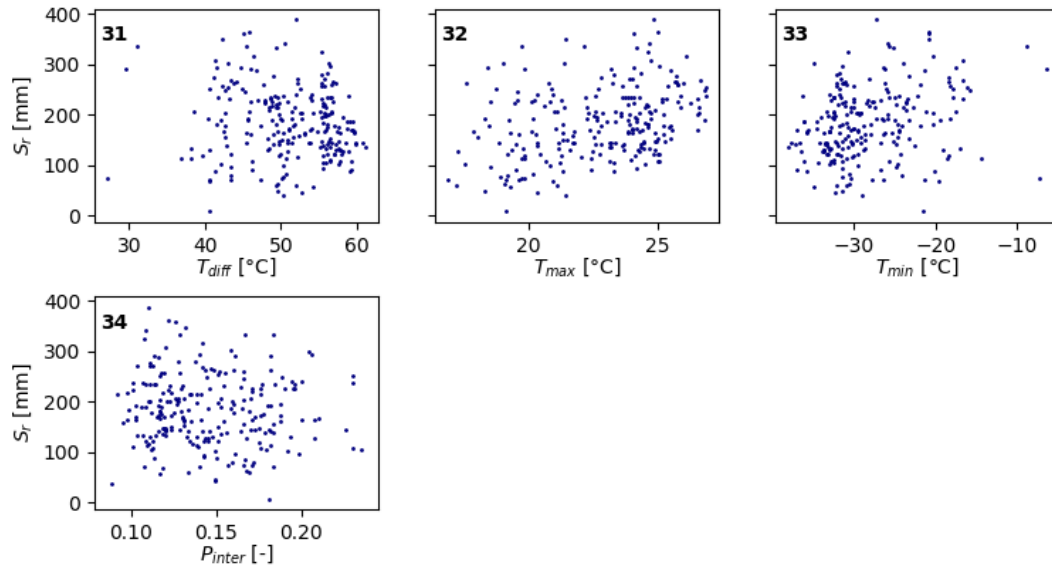


Figure E.3: Relationship between  $S_r$  and the last climate variables. The numbers in the plot refer to the numbers in Appendix C.1.

## F2. Landscape variables

This section provides an overview of climate variables in respectively Figure F4 and F5. The numbers in the figure refer back to Appendix C.2, where the variables are explained.

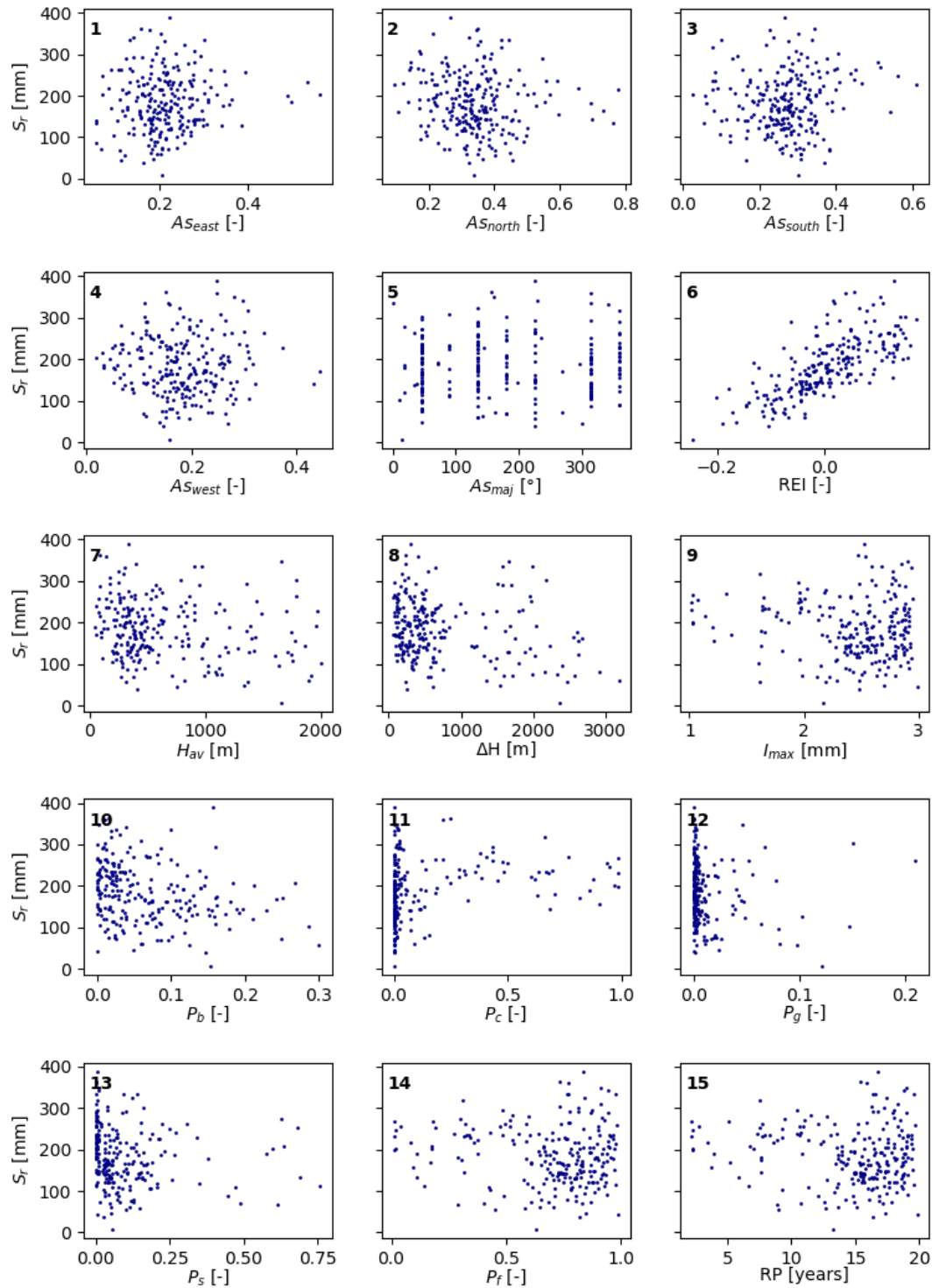


Figure F4: Relationship between  $S_r$  and the first 15 landscape variables. The numbers in the plot refer to the numbers in Appendix C.2.

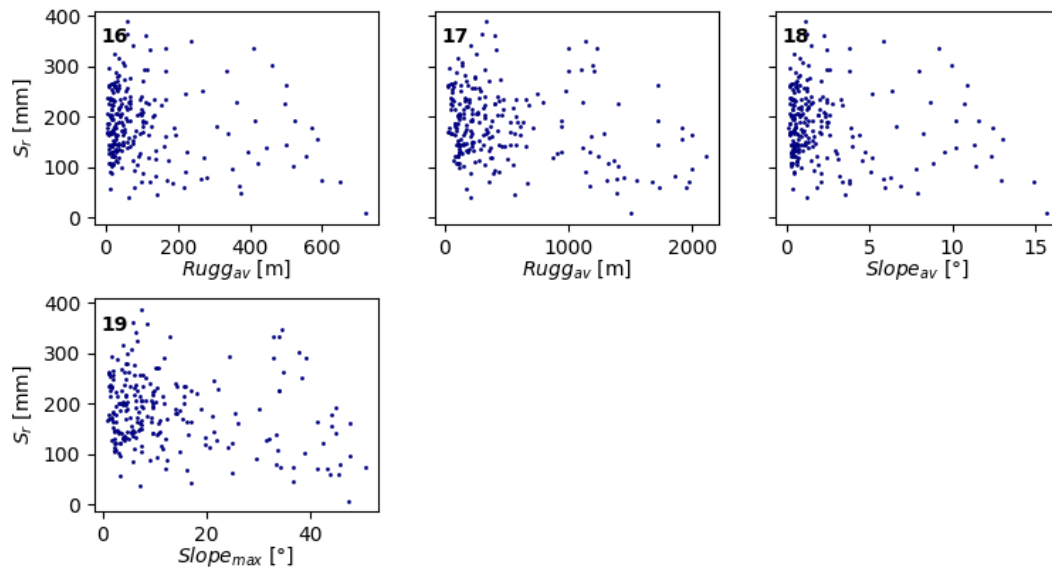


Figure E.5: Relationship between  $S_r$  and the last landscape variables. The numbers in the plot refer to the numbers in Appendix C.2.

### E.3. Discharge variables

This section provides an overview of climate variables in respectively Figure E6 and E7. The numbers in the figure refer back to Appendix C.3, where the variables are explained.

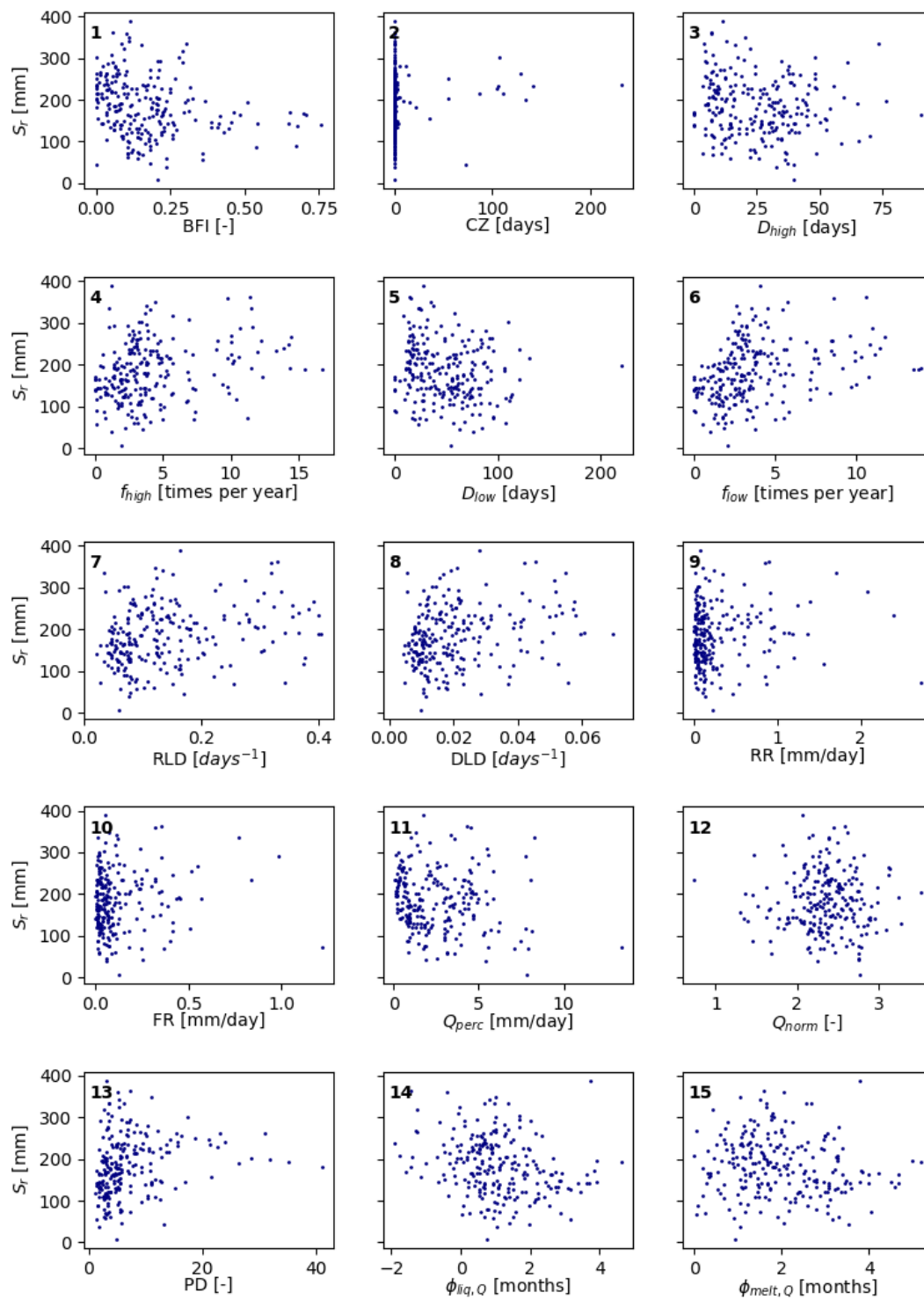


Figure E6: Relationship between  $S_r$  and the first 15 discharge variables. The numbers in the plot refer to the numbers in Appendix C.3.

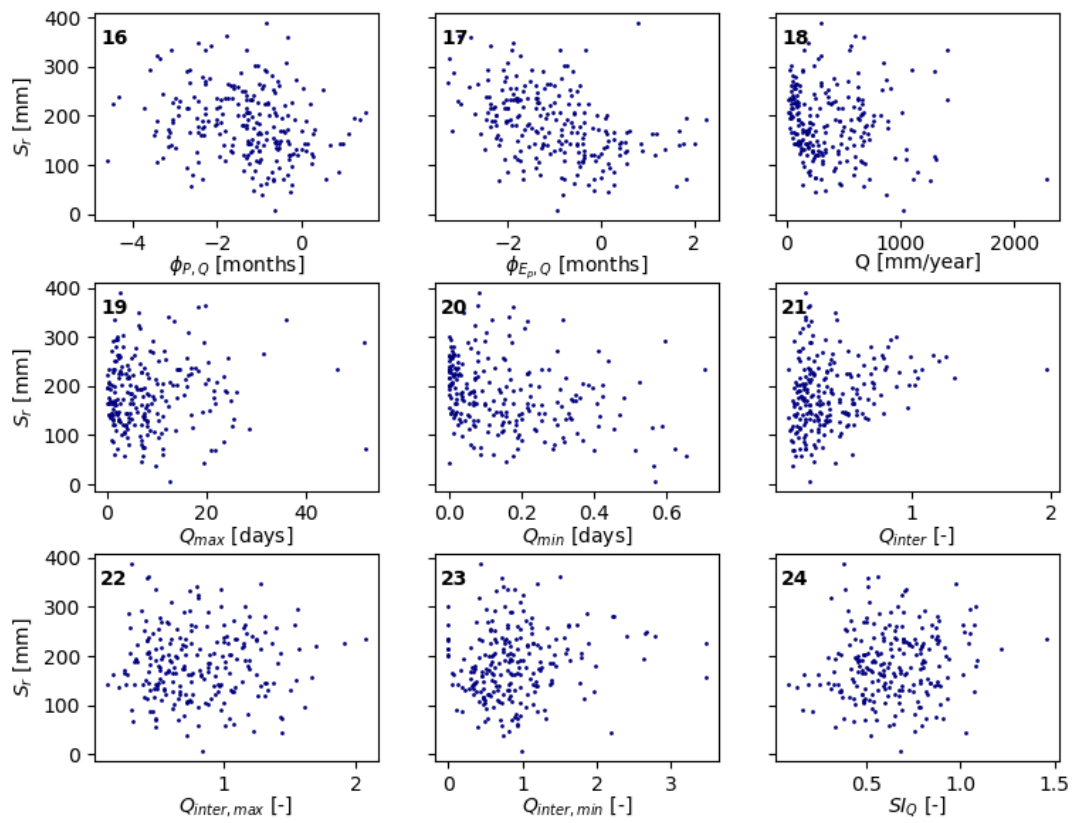


Figure E.7: Relationship between  $S_r$  and the last discharge variables. The numbers in the plot refer to the numbers in Appendix C.3.

# G

## Feature selection parameter set

The forward and backward feature selection in this study are applied using the following parameter set. All individual parameters are also stated in Appendix C.

*[Aridity index, Runoff coefficient, Average yearly precipitation, Average temperature, Minimum temperature, Maximum temperature, Temperature difference, Average maximum snow water equivalent, Fractional forest cover, Fractional shrubland/herbaceous cover, Fractional crop cover, Fractional bare cover, Fractional solid precipitation input, Inter-annual variability of precipitation, Number of snow days, Duration of snow melt, Seasonality of snow melt, Average catchment elevation, Elevation difference in a catchment, Interstorm duration, Average yearly potential evaporation, Seasonality timing index, Normalised 90-percentile liquid input, Slope direction (majority), Northern aspect, Eastern aspect, Southern aspect, Western aspect, Return period, Seasonality index discharge, Normalised 90-percentile discharge, Phase difference precipitation and discharge, Phase difference liquid input and discharge, Phase difference melt input and discharge, Phase difference potential evaporation and discharge, Inter-annual variability discharge, Yearly average discharge, Frequency of occurrence of high flow event, Duration of high flow event, Frequency of occurrence of low flow event, Duration of low flow event, Rising limb density, Peak distribution, Base Flow Index, Inter-annual variability maximum flow, Inter-annual variability minimum flow, Average yearly maximum discharge, Average yearly minimum discharge, Total number of days without flow, Average rising rate of discharge signal]*



# H

## Snow influence on change in $S_r$

The influence of all tested snow parameters on change in  $S_r$  between the two model runs is shown in Figure H.1. The numbers in the plot refer to the numbers that are used in Appendix C to explain the climate variables.

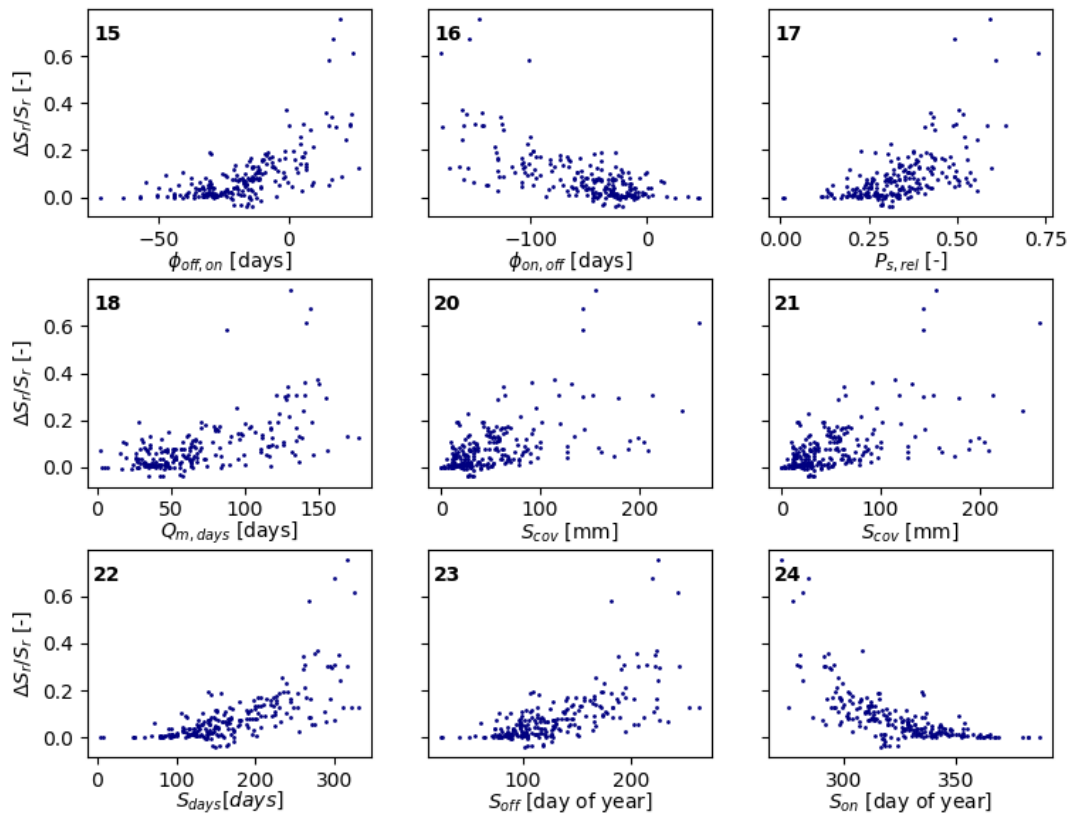


Figure H.1: Relationship between several snow parameters and the change in  $S_r$ . The numbers in the plot refer to the numbers in Appendix C.